

PERFORMANCE ANALYSIS OF RAIN FADES ON TERRESTRIAL OPTICAL AND MICROWAVE EARTH-TO-SATELLITE LINKS

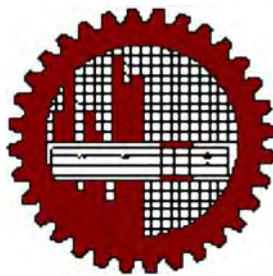
A Thesis submitted to the Department of Electrical and Electronic Engineering in
partial fulfillment of the requirements for the degree of
Master of Science in Electrical and Electronic Engineering (EEE)

By

Mohammad Mahfujur Rashid

Under the supervision of

Professor Dr. Satya Prasad Majumder



**DEPARTMENT OF ELECTRICAL AND ELECTRONIC ENGINEERING (EEE)
BANGLADESH UNIVERSITY OF ENGINEERING AND TECHNOLOGY
DHAKA, BANGLADESH.**

JUNE 2010

The thesis titled **“Performance analysis of rain fades on terrestrial optical and microwave earth-to-satellite links”** submitted by Mohammad Mahfujur Rashid, Roll No. 040406203P, session - April 2004 has been accepted as satisfactory in partial fulfillment of the requirements for the degree of **Master of Science in Electrical and Electronic Engineering** on June 2010.

Board of Examiners

1. _____
(Dr. Satya Prasad Majumder) Chairman
Professor
Department of Electrical and Electronic Engineering
Bangladesh University of Engineering and Technology
Dhaka – 1000, Bangladesh.

2. _____
(Dr. Md. Saifur Rahman) Member (Ex-Officio)
Professor and Head
Department of Electrical and Electronic Engineering
Bangladesh University of Engineering and Technology
Dhaka – 1000, Bangladesh.

3. _____
(Dr. Md. Shah Alam) Member
Associate Professor
Department of Electrical and Electronic Engineering
Bangladesh University of Engineering and Technology
Dhaka – 1000, Bangladesh.

4. _____
(Dr. Jugal Krishna Das) Member (External)
Professor
Department of Computer Science and Engineering
Jahangirnagar University
Savar, Bangladesh.

DECLARATION

It is hereby declared that neither this thesis “**Performance analysis of rain fades on terrestrial optical and microwave Earth-to-Satellite links**” nor any part of this has been submitted elsewhere for the award of any degree or diploma.

Signature of the candidate

(Mohammad Mahfujur Rashid)
Roll No. 040406203P

DEDICATION

To my beloved wife MOMII

ACKNOWLEDGEMENT

This thesis is accomplished under the supervision of Dr. Satya Prasad Majumder, Professor and Ex-Head, Department of Electrical and Electronic Engineering, Bangladesh University of Science and Technology (BUET), Dhaka. It is a great pleasure to express the author's indebtedness gratitude and profound respect to his supervisor for the supervisor's consistent guidance, relentless encouragement, helpful suggestions, constructive criticism and endless patience throughout the progress of this research. Without his generous support, participation and persistent motivation this thesis would not have been a success.

The author is also grateful to Dr. Md. Saifur Rahman, Professor and Head, Department of Electrical and Electronic Engineering, Bangladesh University of Science and Technology (BUET), Dhaka for his support, valuable advice and providing all the facilities to complete this thesis work successfully.

The author is also indebted to the librarian and other staffs of the Department of EEE for their help and co-operation in completing the thesis.

Finally, all praises to Allah, the most gracious benevolent, without Whose help this work would not have been possible.

TABLE OF CONTENT

CONTENT	PAGE NO.
Declaration	ii
Dedication	iii
Acknowledgement	iv
Table of Content	v-viii
List of figures	ix-xi
List of tables	xii-xiii
Abstract	xiv
CHAPTER 1 INTRODUCTION	1-14
1.1 General Perspective	2
1.2 Introduction to Microwave Communication System	4
1.2.1 Microwaves	4
1.2.2 Microwave Sources	5
1.2.3 Uses of Microwave	5
1.2.3.1 Communication	5
1.2.3.2 Remote Sensing	7
1.2.3.3 Navigation	7
1.2.3.4 Power	7
1.2.3.5 Spectroscopy	7
1.2.4 Microwave Frequency Bands	7
1.3 Definition of Attenuation	8
1.3.1 Types	8
1.3.2 Causes of Attenuation	9
1.3.3 Impacts of Attenuation on Communication System	11
1.4 Review of Some Previous Works	12
1.5 Objectives with Specific Aims and Possible Outcome	13
1.6 Outline of Methodology	13
1.7 Organization of this thesis	14
CHAPTER 2 EFFECT OF RAIN ON MICROWAVE PROPAGATION	15-29
2.1 Introduction	16

2.2	Satellite Rain Fade	17
2.2.1	What Is Fading	17
2.2.2	What Is Rain Fade	17
2.2.3	The Causes of Rain Fade	17
2.2.4	How Rain Affect The Higher Frequencies	18
2.2.5	The Impact of Satellite Rain Fade	19
2.2.6	Effect of Rainfall in Tropical Area	19
2.3	The Method for the Prediction of Rain Attenuation	20
2.4	Overview of Some Existing Models for Rain-Attenuation and Rain-Rate	21
2.4.1.	Rain-rate Prediction Models	21
2.4.2	How 1-minute Rain Rate fall data can be achieved by Conversion where measurement is not done	23
2.4.3	Why 1-minute Rain Rate fall data is important	24
2.4.4	Rain-attenuation Prediction Model	24
CHAPTER 3	STATISTICAL DATA AND PERFORMANCE ANALYSIS	30-69
3.1	Introduction	31
3.2	Earth Stations in Bangladesh	31
3.3	Rainfall Data Collection	32
3.3.1	Locations of Rain Gauge Stations	32
3.3.2	Rain Gauge Specifications and Sample Data	33
3.3.3	Annual Distribution	34
3.3.4	Availability Calculations	35
3.4	Conversion from Annual Avg. to 1-minute Integration	36
3.5	Rain Intensities Distribution	37
3.6	Rain Attenuation Statistics from Rainfall Rate for Earth to Satellite Link	39
3.6.1	Determination of Rain Attenuation from ITU-R Predicted Rainfall Rate	46
3.7	Link Budget Calculation for Earth-to-Satellite Downlink at Three Bands using ITU-R Proposed and Measured Rain Rate for Bangladesh at Horizontal Polarization	47
3.8	Rain Attenuation Statistics from Rainfall Rate for Terrestrial Link	56

3.8.1	Determination of Rain Attenuation from ITU-R Predicted Rainfall Rate	59
3.9	Link Budget Calculation for Terrestrial Downlink at Three Bands using ITU-R Proposed and Measured Rain Rate for Bangladesh at Horizontal Polarization	61
CHAPTER 4 COMPARISON OF PREDICTED RAIN ATTENUATION AND ITS EFFECTS ON LINK'S PERFORMANCE		69-101
4.1	Introduction	70
4.2	Results and Discussion	70
4.3	Comparison Study for Earth to Satellite Link	71
4.3.1	Comparison between Predicted Attenuation at Measured Maximum $R_{0.01}$ and ITU-R Predicted Attenuation for C/Ku/Ka- Band at Horizontal Polarization	71
4.3.2	Comparison between Predicted Attenuation at Measured Minimum $R_{0.01}$ and ITU-R Predicted Attenuation for C/Ku/Ka- Band at Horizontal Polarization	73
4.3.3	Comparison between Predicted Attenuation at Measured Maximum $R_{0.01}$ and ITU-R Predicted Attenuation for C/Ku/Ka- Band at Vertical Polarization	75
4.3.4	Comparison between Predicted Attenuation at Measured Minimum $R_{0.01}$ and ITU-R Predicted Attenuation for C/Ku/Ka- Band at Vertical Polarization	77
4.3.5	Comparison between Predicted Attenuation at Measured Maximum $R_{0.01}$ and ITU-R Predicted Attenuation for C/Ku/Ka- Band at Circular Polarization	79
4.3.6	Comparison between Predicted Attenuation at Measured Minimum $R_{0.01}$ and ITU-R Predicted Attenuation for C/Ku/Ka- Band at Circular Polarization	81
4.4	Deviation Calculation for Earth to Satellite Link	83
4.5	Comparison Study for Terrestrial Link	85
4.5.1	Comparison between Predicted Attenuation at Measured Maximum $R_{0.01}$ and ITU-R Predicted Attenuation for C/Ku/Ka- Band at Horizontal Polarization	85

4.5.2	Comparison between Predicted Attenuation at Measured Minimum $R_{0.01}$ and ITU-R Predicted Attenuation for C/Ku/Ka-Band at Horizontal Polarization	87
4.5.3	Comparison between Predicted Attenuation at Measured Maximum $R_{0.01}$ and ITU-R Predicted Attenuation for C/Ku/Ka-Band at Vertical Polarization	89
4.5.4	Comparison between Predicted Attenuation at Measured Minimum $R_{0.01}$ and ITU-R Predicted Attenuation for C/Ku/Ka-Band at Vertical Polarization	91
4.5.5	Comparison between Predicted Attenuation at Measured Maximum $R_{0.01}$ and ITU-R Predicted Attenuation for C/Ku/Ka-Band at Circular Polarization	93
4.5.6	Comparison between Predicted Attenuation at Measured Minimum $R_{0.01}$ and ITU-R Predicted Attenuation for C/Ku/Ka-Band at Circular Polarization	95
4.6	Deviation Calculation for Terrestrial Link	97
4.7	Link Budget Analysis for Earth-to-Satellite Downlink at C/Ku/Ka-Bands using ITU-R Proposed and Measured Rain Rate at horizontal Polarization for Bangladesh	99
4.8	Link Budget Analysis for Terrestrial Downlink at C/Ku/Ka- Bands using ITU-R Proposed and Measured Rain Rate at horizontal Polarization for Bangladesh	100
4.9	The measurements and deviations in different Countries	102
CHAPTER 5 CONCLUSION		106-109
5.1	Further scope of improvement	109
REFERENCES		110-112
APPENDICES		113-134

LIST OF FIGURES

FIGURE NO.	NAME OF FIGURE	PAGE NO.
Fig. 1.1	Frequency Spectrum	4
Fig. 1.2	Microwave atmospheric propagation environments	9
Fig. 1.3	Attenuation of wanted signal due to rain	10
Fig. 1.4	Attenuation due to rain at various frequency and polarization	11
Fig. 2.1	Satellite communications system	16
Fig. 2.2	Schematic presentation of an earth-space path given the parameters to be input to the attenuation prediction process	26
Fig. 3.1	Rain Gauge Stations in Bangladesh	32
Fig. 3.2	Annual rainfall rate at Teknaf station for the period of 13 years	34
Fig. 3.3	Annual rainfall rate at Ishurdi station for the period of 13 years	34
Fig. 3.4	Average Annual accumulation, M (mm/year) for 34 rain stations in Bangladesh	38
Fig. 3.5	1- min rain rate cumulative distribution, $R_{0.01}$ (mm/hr) for 34 rain stations in Bangladesh	38
Fig. 3.6	Schematic presentation of an earth-space path given the parameters to be input to the attenuation prediction process.	39
Fig. 4.1	Comparison Curves between Predicted Attenuation at Measured Maximum $R_{0.01}$ and ITU-R Predicted Attenuation for C/Ku/Ka-Band at Horizontal Polarization	71
Fig. 4.2	Attenuation vs. System Reliability Curves at Horizontal Polarization for Measured Maximum $R_{0.01}$	72
Fig. 4.3	Comparison Curves between Predicted Attenuation at Measured Minimum $R_{0.01}$ and ITU-R Predicted Attenuation for C/Ku/Ka-Band at Horizontal Polarization	73
Fig. 4.4	Attenuation vs. System Reliability Curves at Horizontal Polarization for Measured Minimum $R_{0.01}$	74
Fig. 4.5	Comparison Curves between Predicted Attenuation at Measured Maximum $R_{0.01}$ and ITU-R Predicted Attenuation for C/Ku/Ka-Band at Vertical Polarization	75
Fig. 4.6	Attenuation vs. System Reliability Curves at Vertical Polarization for Measured Maximum $R_{0.01}$	76
Fig. 4.7	Comparison Curves between Predicted Attenuation at Measured	

	Minimum $R_{0.01}$ and ITU-R Predicted Attenuation for C/Ku/Ka-Band at Vertical Polarization	77
Fig. 4.8	Attenuation vs. System Reliability Curves at Vertical Polarization for Measured Minimum $R_{0.01}$	78
Fig. 4.9	Comparison Curves between Predicted Attenuation at Measured Maximum $R_{0.01}$ and ITU-R Predicted Attenuation for C/Ku/Ka-Band at Circular Polarization	79
Fig. 4.10	Attenuation vs. System Reliability Curves at Circular Polarization for Measured Maximum $R_{0.01}$	80
Fig. 4.11	Comparison Curves between Predicted Attenuation at Measured Minimum $R_{0.01}$ and ITU-R Predicted Attenuation for C/Ku/Ka-Band at Circular Polarization	81
Fig. 4.12	Attenuation vs. System Reliability Curves at Circular Polarization for Measured Minimum $R_{0.01}$	82
Fig. 4.13	Deviation vs. System Reliability Curves for Measured Maximum $R_{0.01}$	84
Fig. 4.14	Deviation vs. System Reliability Curves for Measured Minimum $R_{0.01}$	84
Fig. 4.15	Comparison Curves between Predicted Attenuation at Measured Maximum $R_{0.01}$ and ITU-R Predicted Attenuation for C/Ku/Ka-Band at Horizontal Polarization	85
Fig. 4.16	Attenuation vs. System Reliability Curves at Horizontal Polarization for Measured Maximum $R_{0.01}$	86
Fig. 4.17	Comparison Curves between Predicted Attenuation at Measured Minimum $R_{0.01}$ and ITU-R Predicted Attenuation for C/Ku/Ka-Band at Horizontal Polarization	87
Fig. 4.18	Attenuation vs. System Reliability Curves at Horizontal Polarization for Measured Minimum $R_{0.01}$	88
Fig. 4.19	Comparison Curves between Predicted Attenuation at Measured Maximum $R_{0.01}$ and ITU-R Predicted Attenuation for C/Ku/Ka-Band at Vertical Polarization	89
Fig. 4.20	Attenuation vs. System Reliability Curves at Vertical Polarization for Measured Maximum $R_{0.01}$	90
Fig. 4.21	Comparison Curves between Predicted Attenuation at Measured Minimum $R_{0.01}$ and ITU-R Predicted Attenuation for C/Ku/Ka-Band at Vertical Polarization	91

Fig. 4.22	Attenuation vs. System Reliability Curves at Vertical Polarization for Measured Minimum $R_{0.01}$	92
Fig. 4.23	Comparison Curves between Predicted Attenuation at Measured Maximum $R_{0.01}$ and ITU-R Predicted Attenuation for C/Ku/Ka-Band at Circular Polarization	93
Fig. 4.24	Attenuation vs. System Reliability Curves at Circular Polarization for Measured Maximum $R_{0.01}$	94
Fig. 4.25	Comparison Curves between Predicted Attenuation at Measured Minimum $R_{0.01}$ and ITU-R Predicted Attenuation for C/Ku/Ka-Band at Circular Polarization	95
Fig. 4.26	Attenuation vs. System Reliability Curves at Circular Polarization for Measured Minimum $R_{0.01}$	96
Fig. 4.27	Deviation vs. System Reliability Curves for Measured Maximum $R_{0.01}$	98
Fig. 4.28	Deviation vs. System Reliability Curves for Measured Minimum $R_{0.01}$	98
Fig. 4.29	Rain attenuation distribution measured at 15 GHz frequency over microwave links at Kuala Lumpur-1, Taiping, Alor star and Kuantan and those predicted by ITU-R.	102
Fig. 4.30	Rain attenuation distribution measured at 23 GHz frequency over microwave links at Kuala Lumpur -2 and those predicted by ITU-R.	103
Fig. 4.31	Rain attenuation distribution measured at 15 GHz frequency over microwave links at Johor Bahru, Penang and Temerloh and those predicted by ITU-R.	103
Fig.4.32	Measured vs. Predicted Rain Attenuation at Bandung, Indonesia for 12.24 GHz at Horizontal Polarization.	104
Fig.4.33	Measured vs. Predicted Rain Attenuation at Cibinong, Indonesia for 11.2 GHz at Circular Polarization.	104
Fig.4.34	Measured and predicted attenuation distributions at Belim in Brazil for 11.45 GHz at Circular Polarization.	105
Fig.4.35	Measured and predicted attenuation distributions at Rio de Janeiro in Brazil for 11.45 GHz at Circular Polarization.	105

LIST OF TABLES

TABLE NO.	NAME OF THE TABLE	PAGE NO.
Table 1.1	Microwave frequency bands	8
Table 3.1	Rain gauge stations with longitude and latitude situated in Bangladesh	33
Table 3.2	Availability calculation for Chittagong station	35
Table 3.3	Availability calculation for Sandwip station	35
Table 3.4	Rain Intensities Distribution for 34 rain stations	37
Table 3.5	Table from Recommendation ITU-R P.838-3	41
Table 3.6	Frequency-dependent coefficients for estimating specific rain attenuation using equations (7), (8) and (6)	41
Table 3.7	Specific attenuation, γ_R (dB/km)	41
Table 3.8	Predicted Attenuation, $A_{0.01}$ at different percentages of time for measured maximum $R_{0.01}$ at horizontal polarization	45
Table 3.9	Predicted Attenuation, $A_{0.01}$ at different percentages of time for measured minimum. $R_{0.01}$ at horizontal polarization	45
Table 3.10	Specific attenuation, γ_R (dB/km) for ITU-R predicted value	46
Table 3.11	Predicted Attenuation, $A_{0.01}$ for ITU-R predicted value	46
Table 3.12	Predicted Attenuation, $A_{0.01}$ at different percentages of time for ITU-R predicted value of $R_{0.01}$ at horizontal polarization	47
Table 3.13	Receiving Antenna Gain	48
Table 3.14	Free Space Path Loss	48
Table 3.15	Clear air atmospheric loss	48
Table 3.16	Received power due to rain	49
Table 3.17	Predicted Attenuation, $A_{0.01}$ for measured max. and min. $R_{0.01}$	57
Table 3.18	Predicted Attenuation, $A_{0.01}$ at different percentages of time for measured maximum $R_{0.01}$ at horizontal polarization	58
Table 3.19	Predicted Attenuation, $A_{0.01}$ at different percentages of time for measured minimum $R_{0.01}$ at horizontal polarization	58
Table 3.20	Predicted attenuation, $A_{0.01}$ for ITU-R predicted value of $R_{0.01}$ for Terrestrial Link	59
Table 3.21	Predicted attenuation, $A_{0.01}$ at different percentages of time for ITU-R predicted value of $R_{0.01}$	59

Table 3.22	Receiving Antenna Gain	60
Table 3.23	Free Space Path Loss	61
Table 3.24	Clear air atmospheric loss	61
Table 3.16	Received power due to rain	62
Table 4.1	Comparison among predicted attenuations for measured maximum $R_{0.01}$, minimum $R_{0.01}$ and ITU-R predicted $R_{0.01}$ at horizontal polarization	71
Table 4.2	Comparison among predicted attenuations for measured maximum $R_{0.01}$, minimum $R_{0.01}$ and ITU-R predicted $R_{0.01}$ at vertical polarization	75
Table 4.3	Comparison among predicted attenuations for measured maximum $R_{0.01}$, minimum $R_{0.01}$ and ITU-R predicted $R_{0.01}$ at circular polarization	79
Table 4.4	Deviation between predicted attenuation for measured maximum $R_{0.01}$ and ITU-R predicted attenuation at horizontal polarization	83
Table 4.5	Deviation between predicted attenuation for measured minimum $R_{0.01}$ and ITU-R predicted attenuation at horizontal polarization	83
Table 4.6	Comparison among predicted attenuations for measured maximum $R_{0.01}$, minimum $R_{0.01}$ and ITU-R predicted $R_{0.01}$ at horizontal polarization	85
Table 4.7	Comparison among predicted attenuations for measured maximum $R_{0.01}$, minimum $R_{0.01}$ and ITU-R predicted $R_{0.01}$ at vertical polarization	89
Table 4.8	Comparison among predicted attenuations for measured maximum $R_{0.01}$, minimum $R_{0.01}$ and ITU-R predicted $R_{0.01}$ at circular polarization	93
Table 4.9	Deviation between predicted attenuation for measured maximum $R_{0.01}$ and ITU-R predicted attenuation	97
Table 4.10	Deviation between predicted attenuation for measured minimum $R_{0.01}$ and ITU-R predicted attenuation	97
Table 4.11	Link Budget Analysis for Earth-To-Satellite downlink	99
Table 4.12	Link Budget Analysis for Terrestrial downlink	100

ABSTRACT

Rain is a dominant source of attenuation at higher frequencies and consequently it degrades the system performance of microwave satellite and terrestrial links in tropical and subtropical regions. Bangladesh has a subtropical monsoon climate characterized by wide seasonal variations in rainfall and most parts of the country receive at least 2000 mm of rainfall per year. The knowledge of rain fade and its performance is essential in order to optimize system capacity and meet quality and reliability. The rain intensity data for Bangladesh is not available since it has not been measured so far. In this thesis, investigations have been carried out to find the rain fade and intensity data and their effect on the performance of terrestrial and satellite microwave links in Bangladesh. In this regard, long term rainfall data are collected from 34 meteorological stations of Bangladesh for thirteen years. The collected data are converted to 1-minute integration time rain intensity which can be used to design microwave systems in any parts of Bangladesh. The converted rain intensity data are used to estimate rain fades at C, Ku and Ka bands for both terrestrial and earth to satellite microwave links. The converted rain intensity data and ITU-R recommended rain intensity are used to estimate the deviation of rain fades at C, Ku and Ka-bands for comparison. The deviations are found to be small at lower frequency bands and are significantly higher at higher frequency bands. Performance of terrestrial and earth-to-satellite links in terms of Carrier-to-Noise (CNR) are also evaluated considering the predicted rain fades at different frequency bands operating in Bangladesh.

CHAPTER 5
CONCLUSION

CONCLUSION

Rain is a dominant source of attenuation at higher frequencies in tropical and subtropical regions. Therefore accurate estimation of rain fade is very essential in order to design reliable microwave links in such regions. Rain attenuation prediction methods require 1-min rain rate data, which is scarce in the tropical and subtropical regions. However, yearly rainfall data are available at many meteorological stations in almost every country. A method for converting the available rainfall data to the equivalent 1-min rain rate cumulative distribution (CD) would be very useful for radio wave engineers. For this reason 1 min rain rate CD can be estimated by the use of conversion models and long-term mean annual rainfall data.

This research has conducted a campaign to collect long term rainfall statistics in a subtropical country Bangladesh. Data has been collected from 34 Meteorological stations for thirteen years period. Using conversion model proposed by Chebil for tropical region, mean annual rainfall data measured in Bangladesh has been converted to 1-min rain rate data. The highest rain intensity is observed at Teknaf of Bangladesh at 148.4576 mm/hr and lowest at Ishurdi is 109.4259 mm/hr. The rain intensity recommended by ITU-R map is found 95 mm/hr for Bangladesh which is far lower than converted rain intensity from measured thirteen years annual rainfall.

All three bands, rain attenuation are estimated based on ITU-R recommended rain rate as well as converted rain rate from long term measured data. It is observed that ITU-R recommendation underestimates the rain rate measured in Bangladesh and consequently the rain attenuation estimation introduces significant errors especially at Ku and Ka-bands. It is observed that rain fade is not significant at C-band, but is very critical at Ku and Ka-bands. It is also observed that horizontally polarized wave suffers the most and the vertically polarized wave is the least. The circularly polarized wave is middle.

Rain fade and corresponding Carrier-to-noise ratio (CNR) have been estimated using terrestrial and earth-to-satellite links for all three bands. From observation, it is found

that C/N ratio is 2.6-3.65 dB higher in Ku and Ka-bands than C-band during clear air condition. But during the rains C/N ratios falls to 22.95 dB at C-band and -23.21 dB and -74.78 dB at Ku and at Ka-band respectively. These estimations are based on ITU-R recommended rain rates. But the C/N ratio falls to -54.38 dB at Ku-band and -131.95 dB at Ka-band based on converted measured rain rate. These prediction shows that use of Ku and Ka-bands is very challenging and critical in Bangladesh. From various studies it has been observed that not only for Bangladesh but also for some others countries ITU-R underestimate the value of rainfall rate, $R_{0.01}$ (mm/hr) and sometimes overestimates. For example in Malaysia the value of ITU-R predicted $R_{0.01}$ is 145 mm/hr at any locations where measured $R_{0.01}$ varies from 80-150 mm/hr. So for areas with lower rainfall such as Chuping, Temerloh, Kuala Lumpur and Senai $R_{0.01}$ is lower than the ITU-R value. It is observed that for areas with higher rainfall rate such as Taiping, Jerangau and Tapah, $R_{0.01}$ is 145mm/h where the ITU-R value is quite acceptable. Also ITU-R rain zoning overestimated rain rate values in Nigeria and in Brazil for different locations ITU-R underestimated rain rate values. However in this thesis the measured rain rate data is converted from measured long term annual rainfall data, it is too preliminary to comment correctly. Therefore it is highly recommended to measure rain intensity and rain drop size distribution urgently for the design of reliable microwave link operating at Ku and Ka-bands in Bangladesh.

5.1 Further scope of improvement

Rain attenuation modeling on satellite paths have been done by many researchers. Several empirical and non-empirical rain attenuation prediction models that have been developed are based on the measurement data obtained from temperate regions. Most of these existing rain attenuation prediction models, like the Excell model and the Crane model do not appear to perform well in high rainfall regions. The ITU-R model is currently being widely used. Cumulative distribution empirical evidence shows that the ITU-R model underestimates the measured rain attenuation when applied to tropical and sub tropical regions. A modified ITU-R model can be developed using the complete rainfall rate cumulative distribution and the horizontal path length to calculate the cumulative distribution of rain attenuation for tropical and sub tropical regions [34].

In this thesis the measured rain rate data is converted from measured long term annual rainfall data using J. Chebil's model. But real time rain gauge measurement can be performed for better accuracy for example - An experimental setup include a tipping bucket rain gauge with 0.1 mm capacity and a data acquisition unit that samples the AGC voltage of each receiver once per second, storing the data in digital form together with the date and time of each rain gauge tip. The data files will be then processed to convert AGV voltage into received power levels and to provide cumulative distributions of point rainfall rate with one-minute integration time and rain attenuation [35].

Not only rain intensity affects the link performance but rain drop size distribution also affects the performance. So, further research work can be carried out on the measurement of real time rain drop size distribution.

CHAPTER 1

INTRODUCTION

INTRODUCTION

1.1 GENERAL PERSPECTIVE

The intensity and distribution of rainfall greatly affects transmission quality and limits system's availability. Rain effects on microwave systems are more critical in tropical and equatorial zones, where rainfall is higher than in temperate zones. In temperate regions the rain effects becomes significant above 10 GHz, while in tropical climates in general and in equatorial climate particularly, since the rain drops are larger than in temperate climates, the incidence of rainfall on radio links becomes important for frequencies as low as about 7 GHz . When designing microwave links operating above such frequencies, the major problem in link design is to determine the excess attenuation due to rainfall.

In the design of a radio communication system, one of the major concerns is to assess system unavailability also called outage time. Unavailability or outage time is the amount of time during which the system's performance will be below some threshold value or that it will not be usable. For designing a reliable system, the amount of outage time has to be kept below some objective. In microwave systems, outages can occur either due to equipment failure or it can be propagation outage. In modern systems, the equipment outage time can be made negligibly small by using standby equipment and automatic protection switching systems. However, at higher frequencies, attenuation by rain can cause an outage, which can not be easily protected. Therefore the practical way of achieving a reliable radio system at those frequencies where there is substantial rain attenuation is to design the system in such a way that the expected amount of rain outage is below some objective. For a reliable communication system, unavailability time during a year has to be kept at 0.01 percent. This corresponds to availability time of 99.99 percent during a year. Therefore rainfall with one-minute integration time is very important parameter to predict attenuation at 0.01% of time availability. The long term cumulative annual rainfall data are available for most of the countries of the world. This thesis will present the cumulative rainfall data collected for fifty years in four different parts of Bangladesh. Using appropriate conversion model, the long-term annual rainfall data has been converted to rain intensity data. The rain intensity proposed by International Telecommunication Union (ITU-R) as well as converted data

are used to predict the rain fade for earth-to-satellite at C, Ku and Ka-Bands. This thesis will predict the rain fade for earth-to-satellite links at different frequency bands operating in Bangladesh. It will also investigate the performance of Ku and Ka-Bands during rains in a subtropical region.

Atmospheric effects play a major role in the design of microwave links operating at frequencies above 10 GHz. Raindrops absorb and scatter radio waves, leading to signal attenuation and reduction of the system availability and reliability. The severity of rain impairment increases with frequency and varies with regional locations. Hence the incidence of rainfall on radio links becomes even more important for frequencies as low as about 7 GHz particularly in the tropical and equatorial climates, where intense rainfall events are common. It is therefore very important when planning both microwave and terrestrial line-of-sight system links; to make an accurate prediction of rain induced attenuation on propagation paths. Initially, attenuation prediction attempts involved extrapolation of measurements to other locations, frequencies, and elevation angles; however, the complex nature and regional variability of rain make this approach highly inaccurate. The method for the prediction of rain attenuation on microwave paths has been grouped into two classes: the empirical method which is based on measurement databases from stations in different climatic zones within a given region and the physical method which make an attempt to reproduce the physical behavior involved in the attenuation process. However, when a physical approach is used not all the input parameters needed for the analysis is available. Empirical method is therefore the most used methodologies. For the empirical methodology, an appropriate distribution of rainfall rate at 1-minute integration time is needed for the site under studied in order to predict accurate rain attenuation for the location. This input is sometime provided by meteorological and environmental agencies, universities, and independent researchers. Study has revealed that daily rainfall accumulations are universally recorded and hourly data are fairly available by national weather bureaus/environmental agencies. The critical role of the propagation impairment on communication systems cum lack of rain measurement data from tropical regions for verification for modeling purposes has been the concern of many organizations like, the International Telecommunication Union (ITU), European Space Agency (ESA), and European cooperative program (COST) among others [1]. This has become necessary because of the peculiarity of the tropical regions, which are characterized by high

intensity rainfall, enhanced frequency of rain occurrence and the increased presence of large raindrops when compared with temperate climates [2].

1.2 INTRODUCTION TO MICROWAVE COMMUNICATION SYSTEM

1.2.1 MICROWAVES

Microwaves are electromagnetic waves with wavelengths ranging from as long as one meter to as short as one millimeter, or equivalently, with frequencies between 300 MHz (0.3 GHz) and 300 GHz [3]. This broad definition includes both UHF and EHF (millimeter waves), and various sources use different boundaries. In all cases, microwave includes the entire SHF band (3 to 30 GHz, or 10 to 1 cm) at minimum, with RF engineering often putting the lower boundary at 1 GHz (30 cm), and the upper around 100 GHz (3mm). The fig.1.1 shows electromagnetic spectrum [4].

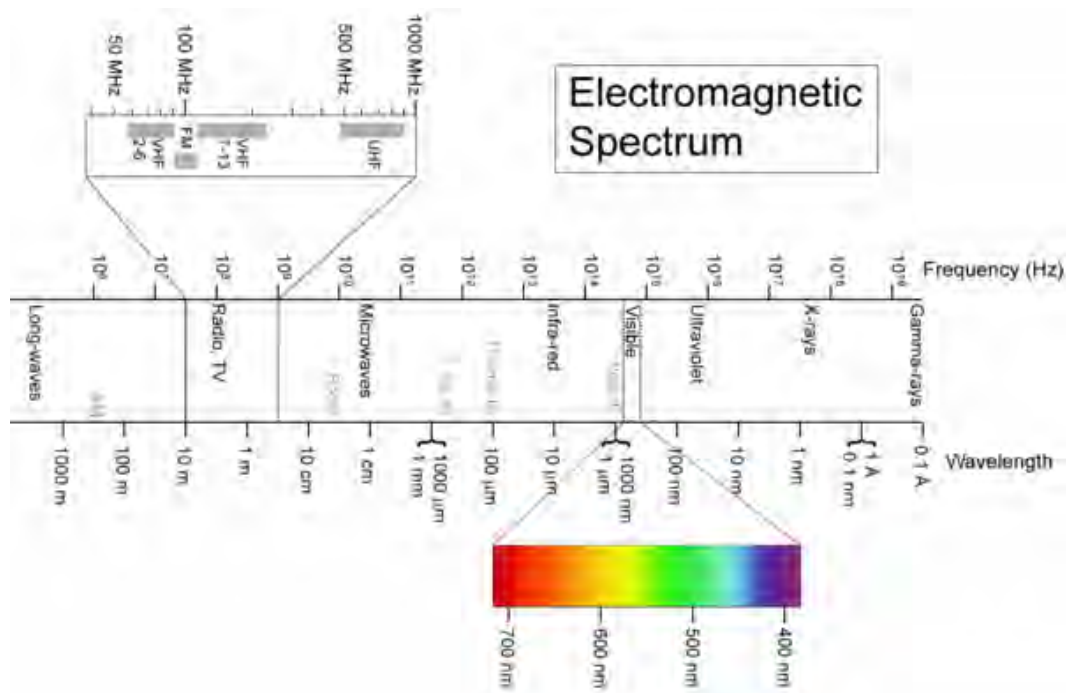


Fig. 1.1: Frequency Spectrum

While the name may suggest a micrometer wavelength, it is better understood as indicating wavelengths very much smaller than those used in radio broadcasting. The boundaries between far infrared light, terahertz radiation, microwaves, and ultra-high frequency radio waves are fairly arbitrary and are used variously between different fields of study. Electromagnetic waves longer (lower frequency) than microwaves are

called "radio waves". Electromagnetic radiation with shorter wavelengths may be called "millimeter waves", terahertz radiation or even T-rays. Definitions differ for millimeter wave band, which the IEEE defines as 110 GHz to 300 GHz. Above 300 GHz, the absorption of electromagnetic radiation by Earth's atmosphere is so great that it is effectively opaque, until the atmosphere becomes transparent again in the so-called infrared and optical frequency ranges.

1.2.2 MICROWAVE SOURCES

Vacuum tube devices operate on the ballistic motion of electrons in a vacuum under the influence of controlling electric or magnetic fields, and include the magnetron, klystron, traveling-wave tube (TWT), and gyrotron. These devices work in the density modulated mode, rather than the current modulated mode. This means that they work on the basis of clumps of electrons flying ballistically through them, rather than using a continuous stream. A maser is a device similar to a laser, except that it works at microwave frequencies. Solid-state sources include the field-effect transistor (at least at lower frequencies), tunnel diodes, Gunn, and IMPATT diodes. The sun also emits microwave radiation; most of it is blocked by the atmosphere.

1.2.3 USES OF MICROWAVE

1.2.3.1 COMMUNICATION

Most long distance telephone calls were carried via microwave point-to-point links through sites like the AT&T Long Lines. Starting in the early 1950s, frequency division multiplex was used to send up to 5,400 telephone channels on each microwave radio channel, with as many as ten radio channels combined into one antenna for the hop to the next site, up to 70 km away.

Wireless LAN protocols, such as Bluetooth and the IEEE 802.11 specifications, also use microwaves in the 2.4 GHz ISM band, although 802.11a uses ISM band and UNII frequencies in the 5 GHz range. Licensed long-range (up to about 25 km) Wireless Internet Access services have been used for almost a decade in many countries in the 3.5–4.0 GHz range. The FCC recently carved out spectrum for carriers that wish to offer services in this range in the U.S. — with emphasis on 3.65 GHz. Dozens of service providers across the country are securing or have already received licenses from the

FCC to operate in this band. The WIMAX service offerings that can be carried on the 3.65 GHz band will give business customers another option for connectivity.

Metropolitan-area networks: MAN protocols, such as WiMAX (Worldwide Interoperability for Microwave Access) based in the IEEE 802.16 specification. The IEEE 802.16 specification was designed to operate between 2 to 11 GHz. The commercial implementations are in the 2.3 GHz, 2.5 GHz, 3.5 GHz and 5.8 GHz ranges.

Wide Area Mobile Broadband Wireless Access: MBWA protocols based on standards specifications such as IEEE 802.20 or ATIS/ANSI HC-SDMA (e.g. iBurst) are designed to operate between 1.6 and 2.3 GHz to give mobility and in-building penetration characteristics similar to mobile phones but with vastly greater spectral efficiency.

Some mobile phone networks, like GSM, use the low-microwave/high-UHF frequencies around 1.8 and 1.9 GHz in the Americas and elsewhere, respectively. DVB-SH and S-DMB use 1.452 to 1.492 GHz, while proprietary/incompatible satellite radio in the U.S. uses around 2.3 GHz for DARS.

Microwave radio is used in broadcasting and telecommunication transmissions because, due to their short wavelength, highly directional antennas are smaller and therefore more practical than they would be at longer wavelengths (lower frequencies). There is also more bandwidth in the microwave spectrum than in the rest of the radio spectrum; the usable bandwidth below 300 MHz is less than 300 MHz while many GHz can be used above 300 MHz. Typically, microwaves are used in television news to transmit a signal from a remote location to a television station from a specially equipped van. Most satellite communications systems operate in the C, X, Ka, or Ku bands of the microwave spectrum. These frequencies allow large bandwidth while avoiding the crowded UHF frequencies and staying below the atmospheric absorption of EHF frequencies. Satellite TV either operates in the C band for the traditional large dish fixed satellite service or Ku band for direct-broadcast satellite. Military communications run primarily over X or Ku-band links, with Ka band being used for Milstar.

1.2.3.2 REMOTE SENSING

Radar uses microwave radiation to detect the range, speed, and other characteristics of remote objects. Development of radar was accelerated during World War II due to its

great military utility. Now radar is widely used for applications such as air traffic control, weather forecasting, navigation of ships, and speed limit enforcement.

1.2.3.3 NAVIGATION

Global Navigation Satellite Systems (GNSS) including the Chinese Beidou, the American Global Positioning System (GPS) and the Russian GLONASS broadcast navigational signals in various bands between about 1.2 GHz and 1.6 GHz.

1.2.3.4 POWER

Microwave heating is used in industrial processes for drying and curing products. Many semiconductor processing techniques use microwaves to generate plasma for such purposes as reactive ion etching and plasma-enhanced chemical vapor deposition (PECVD).

Microwaves can be used to transmit power over long distances, and post-World War II research was done to examine possibilities. NASA worked in the 1970s and early 1980s to research the possibilities of using solar power satellite (SPS) systems with large solar arrays that would beam power down to the Earth's surface via microwaves [5].

1.2.3.5 SPECTROSCOPY

Microwave radiation is used in electron paramagnetic resonance (EPR or ESR) spectroscopy, typically in the X-band region (~9 GHz) in conjunction typically with magnetic fields of 0.3 T. This technique provides information on unpaired electrons in chemical systems, such as free radicals or transition metal ions such as Cu (II).

1.2.4 MICROWAVE FREQUENCY BANDS

The microwave spectrum is usually defined as electromagnetic energy ranging from approximately 1 GHz to 100 GHz in frequency, but older usage includes lower frequencies. Most common applications are within the 1 to 40 GHz range. Microwave frequency bands, as defined by the Radio Society of Great Britain (RSGB), are shown in the table below [6]:

Table 1.1: Microwave frequency bands

Letter Designation	Frequency Range	Wavelength
L band	1 to 2 GHz	30 - 15 cm
S band	2 to 4 GHz	15 - 7.5 cm
C band	4 to 8 GHz	7.5 - 3.75 cm
X band	8 to 12 GHz	3.75 - 2.50 cm
Ku band	12 to 18 GHz	2.5 - 1.67 cm
K band	18 to 26 GHz	1.67 - 1.15 cm
Ka band	26 to 40 GHz	11.5 - 7.5 mm

1.3 DEFINITION OF ATTENUATION

Attenuation is the reduction of signal strength during transmission. Greater signal loss equals higher attenuation [7]. A signal can lose intensity, or experience increased attenuation, with each surface or medium it traverses. Optical signal strength is measured in decibels (dB) and is based on a logarithmic scale. If a signal attenuates too much, the destination device cannot identify it, or worse, it may not even reach the destination.

In physics, attenuation (in some contexts also called extinction) is the gradual loss in intensity of any kind of flux through a medium. For instance, sunlight is attenuated by dark glasses, X-rays are attenuated by lead, and light and sound are attenuated while passing through seawater. In electrical engineering and telecommunications, attenuation affects the propagation of waves and signals in electrical circuits, in optical fibers, as well as in air (radio waves).

1.3.1 TYPES

There are mainly two types of attenuations that will affect the power margin at higher frequencies. One is the atmospheric gaseous absorption, while another is the rain attenuation when microwave signals pass through the rain. Additional environmental phenomena, such as, cloud, fog, ice, snow, aerosol, dust, etc., can also cause severer signals impairment as increasing operating frequency. Several anomalous propagation

modes (such as ducting and tropospheric scatter) also play major roles in trans-horizon interference for a very small percent time. At low elevation angle, the atmospheric scintillation and multipath fading become significant. A microwave propagation scenario [8] through the atmospheric medium is shown in Fig. 1.2

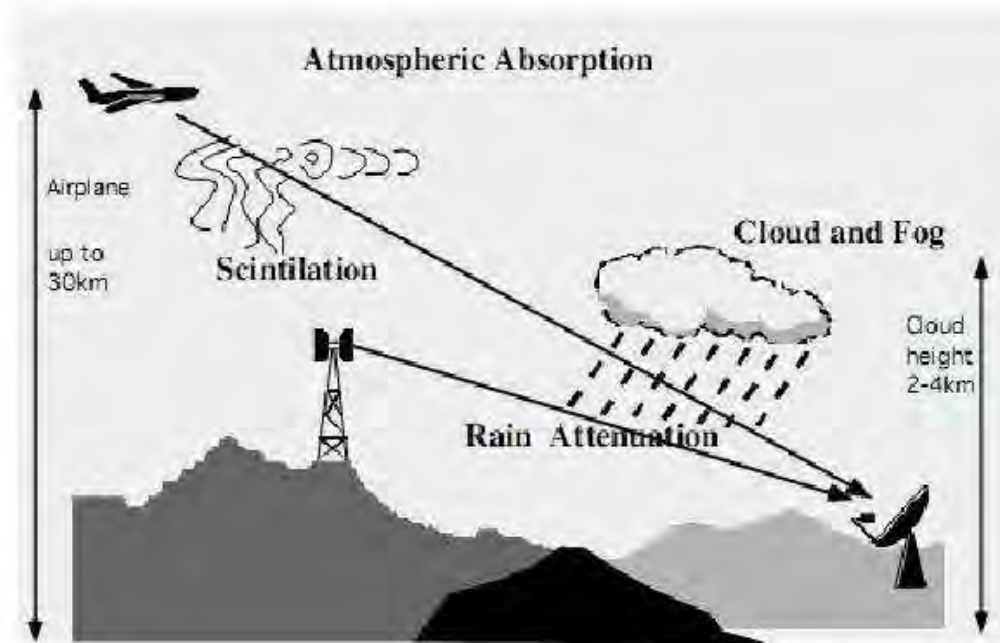


Fig. 1.2: Microwave atmospheric propagation environments.

In fig.1.2 some typical radio paths linking aircraft to the ground and ground to ground are shown. There are mainly 4 types of attenuations at SHF band: Atmospheric gaseous attenuation from O_2 and condensed H_2O , rain attenuation, cloud and fog absorption and scintillation.

1.3.2 CAUSES OF ATTENUATION

LONG DISTANCE ATTENUATION

The signal gets attenuated as it propagates through the medium and longer the distance it travels the more it gets attenuated and finally after propagating through a long distance, the signal get vanished completely. So, as the signal travels, it gets attenuated exponentially. In general, the maximum transmission distance between two stations is 50 km but when the signal propagates through the reflected surfaces such as rivers, oceans, lakes, sea etc., then the maximum distance it can propagate is only about 35 km.

ATMOSPHERIC ATTENUATION

RAIN ATTENUATION

Another important source of microwave signal attenuation is rain. When the rain rate intensity is high, then the microwave signal gets significantly attenuated. For example, it is observed that at high rain intensity (150 mm/hr), the fading of RF signal at 2.4 GHz reached the value 0.02 dB/km. So even if the transmission distance is near and the transmitted power is large enough, the signal will be attenuated in a very significant amount due to heavy rain that the link between the two stations may break down. At higher frequencies, the signal can get attenuated up to 1 dBm/km due to heavy rain fall.

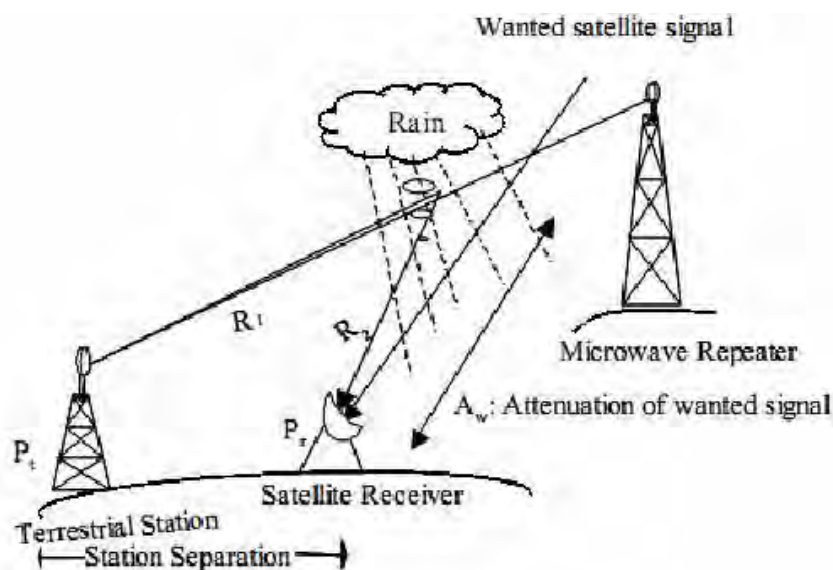


Fig. 1.3: Attenuation of wanted signal due to rain

Rainfall attenuates a microwave signal. The level of attenuation is dependent upon factors such as the frequency of operation, the polarization of the signal, the path length, and the rainfall rate. Other rain factors that influence attenuation include drop size, shape and distribution, terminal velocity and temperature. Rain starts having an impact at frequencies above 10 GHz, and the attenuation becomes critical beyond 15 GHz. The higher the frequency of operation, the more significant the attenuation due to rain. For links working at 12-15 GHz the attenuation may reach 10-12 dB/km, which is significantly high. Transmission planning or microwave link planning engineers should remember that the rainfall rate varies with time and location. Thus, the accuracy of the calculations depends upon how the rainfall was recorded and how stable the cumulative distribution remains over a given period. In general, it has been seen that one year of data has 0.1% of error, while two years of data contains 0.01% of error; if the data are

collected for a period of 10-15 years, the error rate reduces to 0.001%. In the absence of any data, it is recommended that the ITU maps be used instead [9]. The attenuation (A) due to rain is given by:

$$A = \alpha R^\beta \quad (1)$$

Where R is the rainfall rate and α and β are constants. Both the parameters α and β are defined for spherical drops and they are independent of polarization. The value of these constants depends upon the drop size distribution, canting angle, terminal velocity and the properties of water. During network design these values are not easily available, so transmission planning engineers are recommended to use the ITU recommendation 838 as it gives the values for these parameters for both horizontal and vertical polarizations. Attenuation also increases with distance and frequency (see Fig.1.4). Thus, in summary, attenuation increases with distance, frequency and rain rate.

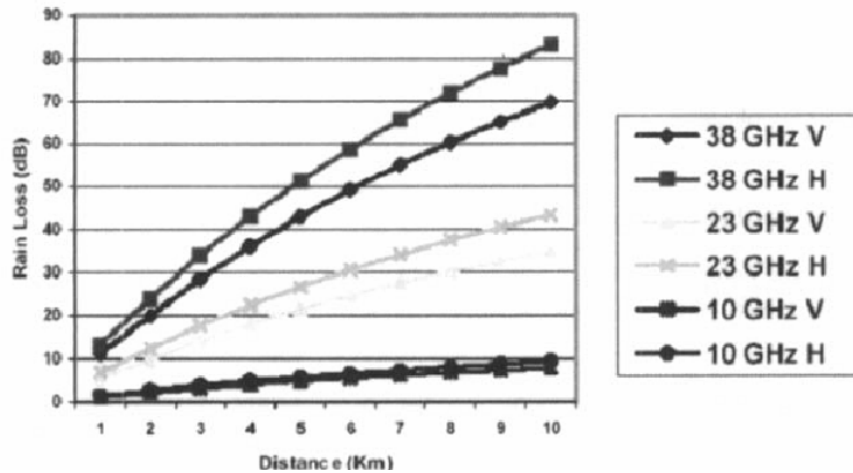


Fig. 1.4: Attenuation due to rain at various frequency and polarization

1.3.3 IMPACTS OF ATTENUATION ON COMMUNICATION SYSTEM

There are several impacts of signal attenuation on communication system [10]. They are discussed below:

POSSIBILITY OF BREAKDOWN OF RADIO LINK

The significant amount of signal attenuation can result in breakdown of the radio link between the two stations. If there is a significant attenuation and the RSL (Receive Signal Level) or received power exceeds the fade Margin, then the radio link will break down and hence the communication system is completely interrupted.

COST OF USE OF NUMEROUS REPEATERS USED FOR SIGNAL ENHANCEMENT

For very long distance communication, the signal has to propagate carrying enough power level for the receiver to receive the signal. But as already discussed, the microwave signal can propagate only up to 50 km. So if one has to establish the microwave link at a greater distance than 50 km, there comes the need of power amplifier or repeater which regenerates the signal and the signal can again propagate 50 km further. So if the transmission distance is so far, a number of repeaters will be needed which makes the communication system costly.

1.4 REVIEW OF SOME PREVIOUS WORKS

To estimate the rain attenuation ITU-R has proposed [11] the following model which has been accepted globally as follows:

$$\text{Specific Attenuation due to Rain, } \gamma_R = kR_{0.01}^\alpha \quad \text{dB/km} \quad (2)$$

Where $R_{0.01}$ is point rainfall rate for 0.01% of an average year in mm/h, Values for the coefficients k and α are determined as functions of frequency, f (GHz), polarization of microwave and drop size distribution rainfall. $R_{0.01}$ (mm/h) is the rainfall rate which can be determined from Moupfouma's [12] rain rate distribution models. Recent analysis suggests that the rain rate distribution is better described by a model which approximates a log-normal distribution at the low rates, and a gamma distribution at high rain rate. This kind of model was developed by Moupfouma and Martins [12]. The model is good for both tropical and temperate climate.

The Moupfouma model requires three parameters; λ , γ and $R_{0.01}$. The first two parameters have been provided but $R_{0.01}$ (mm/h) data is not available for many countries. To estimate $R_{0.01}$, the use of J. Chebil's model [13] appears suitable, it allow the usage of long-time mean annual accumulation, M , at the location of interest. Chebil has made a comparison between some models based on measured values of $R_{0.01}$ and M in Malaysia, Indonesia, Brazil, Singapore and Vietnam. He showed that his model is the best estimate of the measured data.

Many rain attenuation prediction models have been developed including the ITU-R methods in order to permit the design of effect microwave communication systems [14]. It is therefore very important when planning both microwave and terrestrial line-of-sight

system links; to make an accurate prediction of rain induced attenuation on propagation paths.

1.5 OBJECTIVES WITH SPECIFIC AIMS AND POSSIBLE OUTCOME

- i)** To collect long term rainfall data (Hourly, Daily and Yearly) from 34 available meteorological stations in Bangladesh. Then to process the collected data and calculate availability.
- ii)** To convert the collected data to 1-minute integration time rain intensity data for microwave link design using the J. Chebil's model.
- iii)** To develop 1-minute integration time rain data for the use of any locations in Bangladesh.
- iv)** To carryout the performance analysis of terrestrial free space optical link and microwave link considering the rainfall model.
- v)** To investigate the rain fades for both terrestrial optical and earth-to-satellite microwave links operating at the Ku and Ka bands.
- vi)** To evaluate the performance of the links in terms of Carrier-to-Noise Ratio (CNR) for various fade margins and reliability objectives.

1.6 OUTLINE OF METHODOLOGY

In this research annual measured rainfall data will be collected and will be used to estimate $R_{0.01}$ (mm/h) for Bangladesh. The hourly and annual rain fall data will be collected from Meteorological Department of Bangladesh from 34 different locations for the period of 13 years. All these data will be used for availability calculation and then 1-minute integration rainfall data will be derived using J. Chebil's conversion model. Contour map will be developed along with a data bank of 1-min rainfall rate for all latitude and longitude in Bangladesh. Rain fade margin at any location will be estimated by using the contour map. The performance analysis for both terrestrial optical and earth-to-satellite microwave links operating at Ku and Ka bands will be carried out to find the carrier-to-noise ratio (CNR) performance considering the effect of rain fade model. The converted rain intensity data and ITU-R recommended rain intensity will be used to estimate the deviation of rain fades at C, Ku and Ka-bands for comparison.

1.7 ORGANIZATION OF THIS THESIS

Chapter 1 gives a brief overview of microwave communications system, description of different microwave frequency bands, microwave sources and various uses of microwave communication system. Attenuation, its' type, causes and impacts of attenuation on communication system are also described briefly. The review of previous work, objectives and possible outcomes are also presented in this chapter.

In Chapter 2, rain fades, the causes and impact of Satellite rain fades, effects of rain fades on higher frequencies, effect of rainfall on tropical area are described briefly. Overview of some methods for the prediction of rain attenuation and rain-rate fall, the conversion process of 1-min rain rate fall data and the importance of 1-min rain rate fall data are discussed. ITU-R recommended rain attenuation prediction model for earth to satellite link and terrestrial link are also presented in this chapter.

In Chapter 3 statistical long-term rainfall data for 34 rain gauge stations of Bangladesh collected from Meteorological Department are processed for availability calculations. After performing availability calculations, the annual rainfall data for the period of 13 years of 34 rain stations are converted into average annual accumulation, M (mm/year) and converted to 1-minute rain rate cumulative distribution data for microwave link design. Analysis of predicted rain attenuation, $A_{0.01}$ for earth to satellite and terrestrial link is also carried out. The analysis is extended for Link budget analysis and C/N ratio for clear air and due to rain fade.

In Chapter 4 attenuation vs. different percentage of time curves for C/Ku/Ka band at three polarizations are plotted and briefly described. Comparison curves between predicted attenuation for measured $R_{0.01}$ and ITU-R predicted attenuation are plotted and also deviation curves between predicted attenuation for measured $R_{0.01}$ and ITU-R predicted attenuation at different system reliability are compared and briefly illustrated. Link performance investigations for earth-to-satellite and terrestrial link for three bands in clear air and during raining condition are performed also.

Chapter 5 concludes the thesis by discussing the contribution of this work and scope for further research.

CHAPTER 2
EFFECT OF RAIN ON
MICROWAVE PROPAGATION

EFFECT OF RAIN ON MICROWAVE PROPAGATION**2.1 INTRODUCTION**

A satellite communications system uses satellites to relay radio transmissions between earth terminals. The two types of communications satellites [15] are ACTIVE and PASSIVE. A passive satellite only reflects received radio signals back to earth. An active satellite acts as a REPEATER; it amplifies signals received and then retransmits them back to earth. This increases signal strength at the receiving terminal to a higher level than would be available from a passive satellite.

A typical operational link involves an active satellite and two or more earth terminals. One station transmits to the satellite [16] on a frequency called the UP-LINK frequency. The satellite then amplifies the signal, converts it to the DOWN-LINK frequency, and transmits it back to earth [17]. The signal is next picked up by the receiving terminal. Fig.2.1 shows a satellite handling several combinations of links simultaneously.

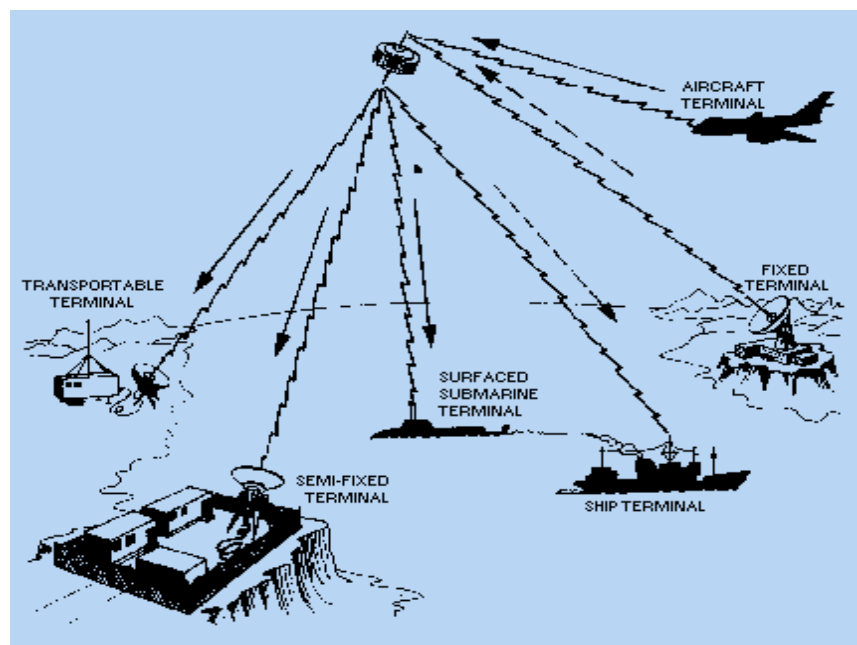


Fig. 2.1: Satellite communications system.

2.2 SATELLITE RAIN FADE

The most reliable satellite communications technology can sometimes be out-matched by the forces of nature. It's a phenomenon known as "rain fade" or "rain attenuation" – a weakening of the satellite signal as it passes through raindrops. Rain fade is one of the most common, and often most misunderstood, phenomena to affect satellite signals.

2.2.1 WHAT IS FADING

In wireless communications, fading [18] is deviation of the attenuation that a carrier-modulated telecommunication signal experiences over certain propagation media. The fading may vary with time, geographical position and/or radio frequency, and is often modeled as a random process. A fading channel is a communication channel that experiences fading. In wireless systems, fading may either be due to multipath propagation, referred to as multipath induced fading, or due to shadowing from obstacles affecting the wave propagation, sometimes referred to as shadow fading.

2.2.2 WHAT IS RAIN FADE

Rain fade [19] refers primarily to the absorption of a microwave Radio Frequency (RF) signal by atmospheric rain, snow or ice, and losses are especially prevalent at frequencies above 11 GHz. It also refers to the degradation of a signal caused by the electromagnetic interference of the leading edge of a storm front. Rain fade can be caused by precipitation at the uplink or downlink location [20]. However, it does not need to be raining at a location for it to be affected by rain fade, as the signal may pass through precipitation many miles away, especially if the satellite dish has a low look angle. From 5 to 20 percent of rain fade or satellite signal attenuation may also be caused by rain, snow or ice on the uplink or downlink antenna reflector, radome or feed horn.

2.2.3 THE CAUSES OF RAIN FADE

Any satellite communications system network operator using a Ku-Band system (12/14 GHz or higher frequencies) will face the effects of rain fade at some time. But to understand why this weakening occurs with Ku-Band transmissions, one must first

understand the causes of rain fade. Two of the most common causes [21] are listed below:

- i. Absorption – Part or all of the energy generated when a radio wave strikes a rain droplet. The droplet is converted to heat energy and absorbed by the droplet.
- ii. Scattering – A non-uniform transmission medium (the raindrops in the atmosphere) causes energy to be dispersed from its initial travel direction.

Scattering can be caused by either refraction or diffraction:

- Refraction – The refractive index of the water droplets encountered by the radio wave.
- Diffraction – the travel direction of the radio wave also changes as it propagates around the obstacle in its path (a water droplet).

These different reactions ultimately have the same effect – they cause any satellite system to lose some of its normal signal level.

2.2.4 HOW RAIN AFFECT THE HIGHER FREQUENCIES

Several frequencies are used to carry satellite transmissions. The most popular today are C-band and Ku band, with Ka-band deployments increasing. At the higher operating frequencies of Ku and Ka-band, the satellite signal strength may be affected by heavy rain conditions. Earth stations located in regions of heavy rain compensate through the use of more transmit power. C-band is almost totally immune to poor weather conditions.

A problem arises when microwave and satellite transmissions have their signals attenuated, or weakened as a result of interference caused by raindrops. The raindrops weaken the transmission by absorbing and scattering the electromagnetic signals.

Rain can be a problem at either end of the link – whether it is raining over the remote site or over the teleport – or both. In either event the signal strength can be degraded resulting in higher error rates, and slower throughput due to retransmissions – or complete loss of service in very heavy rain conditions. Rain attenuation increases with higher signal frequencies. At the lower frequencies used by C-band, attenuation is

insignificant and will require exceptional downpour conditions before the service is affected. At higher frequencies such as Ku and Ka-band however, less severe storms will result in earlier degradation of the signal strength. This occurs because of the frequency wavelength and the size of the raindrop which the signal must pass. The longer wavelengths of C-band are less susceptible to rain attenuation than the shorter Ku and Ka wavelengths.

2.2.5 THE IMPACT OF SATELLITE RAIN FADE

Rain rate is the most common factor used to determine rain fade. Rain fade seems to correlate very closely with the volume of raindrops (expressed in cubic wavelengths) along the path of propagation. This is opposed to the common misconception that the degree of attenuation is proportional to the quantity or individual size of the raindrops falling near the receive site. Pinpointing the specific factor that lead to attenuation is essential to accurately predicting the problem. Models can be developed from this data to chart the effects of rain fade on a regional or individual site basis.

2.2.6 EFFECT OF RAINFALL IN TROPICAL AREA

The amount of rainfall determines the affect of attenuation and the period of disruption or degraded service. In some tropical/equatorial regions one can expect short outages almost every day during the rainy season for Ku and Ka systems [22]. In more temperate climates, outages may be very rare and of very short duration. The elevation of the satellite is also a factor, as the more atmospheres the signal has to traverse, the more rain it may potentially have to pass through.

Tropical rainfall is most often convective, is characterized by large raindrop sizes, is of high intensity and often times accompanied by severe lightning and thunderstorm. If a convective rain cell passes over the common volume formed by the intersecting beams of a satellite downlink antenna and a terrestrial microwave relay system, interference will be received in the satellite system so long as the frequencies are the same. Further, the satellite signal suffers additional rain attenuation on its path hence, the statistics of the transmission loss alone will not be sufficient to predict the interference received by the wanted satellite channel. This additional attenuation has the potential to further reduce the signal-to-noise ratio at the satellite terminal. Thus the additional attenuation is the basis of the evaluation of the effective transmission loss on the path, and whenever it becomes larger than the link margin may result in

the total outage of the satellite channel no matter the interference levels received from the terrestrial system. It is therefore important to consider this extra attenuation of the wanted signal in the analysis of intersystem interference, if the correct interference levels are to be determined for the purpose of better planning and design of microwave communication systems in these locations.

2.3 THE METHOD FOR THE PREDICTION OF RAIN ATTENUATION

Rain rate and rain attenuation predictions are one of the vital steps to be considered when analyzing a microwave satellite communication links at the Ku and Ka bands. Atmospheric effects play a major role in the design of satellite-to-earth links operating at frequencies above 10 GHz. Raindrops absorb and scatter radio waves, leading to signal attenuation and reduction of the system availability and reliability. The severity of rain impairment increases with frequency and varies with regional locations. Hence the incidence of rainfall on radio links becomes even more important for frequencies as low as about 7 GHz particularly in the tropical and equatorial climates, where intense rainfall events are common. It is therefore very important when planning both microwave and terrestrial line-of-sight system links; to make an accurate prediction of rain induced attenuation on propagation paths. Initially, attenuation prediction attempts involved extrapolation of measurements to other locations, frequencies, and elevation angles; however, the complex nature and regional variability of rain make this approach highly inaccurate.

The method for the prediction of rain attenuation on microwave paths has been grouped into two classes:

- The empirical method which is based on measurement databases from stations in different climatic zones within a given region and
- The physical method which makes an attempt to reproduce the physical behavior involved in the attenuation process.

However, when a physical approach is used not all the input parameters needed for the analysis is available. Empirical method is therefore the most used methodologies. For the empirical methodology, an appropriate distribution of rainfall rate at 1-minute integration time is needed for the site under studied in order to predict accurate rain

attenuation for the location. This input is sometime provided by meteorological and environmental agencies, universities, and independent researchers. Study has revealed that daily rainfall accumulations are universally recorded and hourly data are fairly available by national weather bureaus/environmental agencies. There is still dearth of rainfall rate of 1-minute integration time necessary for the study of rain induced impairment to telecommunication especially in the tropical region (Bangladesh). This is because global national weather services are established to satisfy more traditional requirements such as those for agriculture, hydrology and forest management. A method for converting the available rain rate data to the equivalent 1-minute rain rate cumulative distribution is therefore necessary.

2.4 OVERVIEW OF SOME EXISTING MODELS FOR RAIN-ATTENUATION AND RAIN-RATE

A lot of methodologies exist for the prediction of rain-rate and rain-attenuation. In this section an overview of some of the important models and their results are considered.

2.4.1. RAIN-RATE PREDICTION MODELS

Rainfall of high intensity is difficult to record and measure experimentally, as well as being highly variable from year to year. However, in system design it is the highest rainfall rates which are frequently of great interest. Short integration-time rainfall rate is the most essential input parameter in the prediction models for rain attenuation.

Several models exist for the prediction of point rainfall-rate cumulative distribution; this include the work of Crane which has considerably influenced the zonal models of the ITU-R and have been used extensively in the United States, although to a lesser extent in other parts of the world, the limit of the model being the number of station-years of measurements available and not all stations fulfilled the one minute integration time requirement. The results reported by Segal [23] also influenced the ITU-R zonal models, and provided a systematic approach for obtaining a specified number of rain zones in country such as Canada. Watson et al. [24] later mapped rain rates exceeded for 0.1% and 0.01% of an average year based on data for 400 locations within Europe. This approach has been excellent in providing high quality estimates of rain intensity and was used to update the ITU-R rain zones in Europe. The

drawback of this approach is that it requires a relatively high density of short integration-time point precipitation measurements or measurements from which these can be derived. The topography is also not explicitly taken into account, therefore requiring a high spatial resolution for the measurement data.

This approach cannot be easily used on global data due to the low spatial resolution of point measurements on a global scale and the errors that would arise from the spatial interpolation of precipitation rates for fixed annual probability levels.

Holmberg and Rice [25] also developed a model for obtaining rain rate values for use in fading calculations known as Rice-Holmberg's model. The model requires certain parameters like; highest monthly rainfall accumulation observed in a set of 30-year period, number of thunderstorm days expected in an average year and the average annual accumulation. The thunderstorm ratio is not always readily available from local weather agencies. The model was later modified by Dutton and Dougherty [26] to make it depend on four parameters, two of which are used to estimate the fraction of thunderstorm rain. However, it has been acknowledged that the Rice-Holmberg method overestimates rain rates in the high-availability range (0.01%), and underestimates in the range between 0.1% and 1% [27].

Recent analysis suggests that the rain rate distribution is better described by a model which approximates a log-normal distribution at the low rates, and a gamma distribution at high rain rate. This kind of model was developed by Moupfouma and Martins. The model is good for both tropical and temperate climate and can be expressed as:

$$P(R = r) = 10^{-4} \left(\frac{R_{0.01}}{r+1} \right)^b \exp(u[R_{0.01} - r]) \quad (1)$$

Where r (mm/h) represents the rain rate exceeded for a fraction of the time, $R_{0.01}$ is the rain intensity exceeded during 0.01 percent of time in an average year (mm/h) and b is approximated by the following expression:

$$b = \left(\frac{r - R_{0.01}}{R_{0.01}} \right) \ln \left(1 + \frac{r}{R_{0.01}} \right) \quad (2)$$

The parameter u in Equation (1) governs the slope of rain rate cumulative distribution and depends on the local climatic conditions and geographical features. For tropical and sub-tropical localities

$$u = \frac{4 \ln 10}{R_{0.01}} \exp \left(-\lambda \left[\frac{r}{R_{0.01}} \right]^\gamma \right) \quad (3)$$

Where $\lambda = 1.066$ and $\gamma = 0.214$.

Thus, the Moupfouma model requires three parameters; λ , γ and $R_{0.01}$. The first two parameters have been provided.

2.4.2 HOW 1-MINUTE RAIN RATE FALL DATA CAN BE ACHIEVED BY CONVERSION WHERE MEASUREMENT IS NOT DONE

Common rain attenuation prediction methods require 1- min rain rate data, which is scarce in the tropical and subtropical region. However, yearly rainfall data are available at many meteorological stations. A method for converting the available rainfall data to the equivalent 1 min rain rate cumulative distribution (CD) would be very useful for radio wave engineers. For this reason 1 min rain rate CD can be estimated by the use of Chebil model and long-term mean annual rainfall data. J. Chebil's model allows the usage of long-time mean annual accumulation, M , at the location of interest.

The power law relationship of the model is given by

$$R_{0.01} = \alpha M^\beta \quad (4)$$

Where α and β are regression coefficients. Chebil has made a comparison between some models based on measured values of $R_{0.01}$ and M in Malaysia, Indonesia, Brazil, Singapore and Vietnam. He showed that his model is the best estimate of the measured data. The regression coefficient α and β are defined as

$$\alpha = 12.2903 \text{ and } \beta = 0.2973 \quad (5)$$

Thus, using the refined Moupfouma model and Chebil model, the 1 min rain-rate cumulative distribution is fully determined from the long-term mean annual rainfall data.

2.4.3 WHY 1-MINUTE RAIN RATE FALL DATA IS IMPORTANT

For a reliable communication system, unavailability time during a year has to be kept at 0.01 percent. This corresponds to availability time of 99.99 percent during a year. Therefore rainfall with one-minute integration time is very important parameter to predict attenuation at 0.01% of time availability. The long term cumulative annual rainfall data are available for most of the countries of the world.

This thesis has presented the cumulative rainfall data collected for 13 years in 34 different stations of Bangladesh. Using appropriate conversion model, the long-term annual rainfall data has been converted to rain intensity data. The rain intensity proposed by International Telecommunication Union (ITU-R) as well as converted data are used to predict the rain fade for earth-to-satellite and terrestrial at C, Ku and Ka-Bands. This paper has investigated performance of earth-to-satellite link due to rain fades at different frequency bands operating in Bangladesh.

2.4.4 RAIN-ATTENUATION PREDICTION MODEL

A number of rain attenuation prediction models have been published which claim global applicability. Attenuation predictions require first the estimation of a surface rain rate distribution and second the prediction of the radio wave attenuation value distribution, given by the rain rate distribution. Several workers have proposed different models for calculation of attenuation along a path.

Way back in 1946, Ryde presented a rain attenuation model. After three decades, Crane looked afresh at the model predictions and compared them with the measured values taking the data available and new data published after that. He found an average matching between model predictions and measurements [28-29]. He later proposed another model called, two-component model, followed by the revised version [30]. Several other models also include: simple attenuation model by Stutzman and Dishman, Dutton et al. model, Excell model, Misme Waldteufel, Garcia model, ITU-R model, Bryant model, Flavin model, DHA model, Moupfouma Model among others.

To calculate long-term rain attenuation statistics from point rainfall rate ITU rain attenuation model was used. It has been reported that the ITU rain attenuation

prediction model result were close to the average prediction of a set of results obtained from the application of eight different methodologies [31]. The input parameters needed for the model are:

$R_{0.01}$: point rainfall rate for the location for 0.01% of an average year (mm/h)

h_s : height above mean sea level of the earth station (km),

θ : elevation angle (degrees)

ϕ : latitude of the earth station (degrees),

f : frequency (GHz)

R_e : effective radius of the Earth (8500 km).

The geometry is illustrated in Fig. 2.2; where

A = frozen precipitation,

B = rain height,

C = liquid precipitation and

D = Earth-space path

Step 1: Determine the rain height, h_R , as given in Recommendation ITU-R P.839.

Step 2: For $\theta \geq 5^\circ$ compute the slant-path length, L_s , below the rain height from:

$$L_s = \frac{(h_R - h_s)}{\sin \theta} \quad \text{km} \quad (6)$$

For $\theta < 5^\circ$, the following formula is used:

$$L_s = \frac{2(h_R - h_s)}{\left(\sin^2 \theta + \frac{2(h_R - h_s)}{R_e} \right)^{1/2} + \sin \theta} \quad \text{km} \quad (7)$$

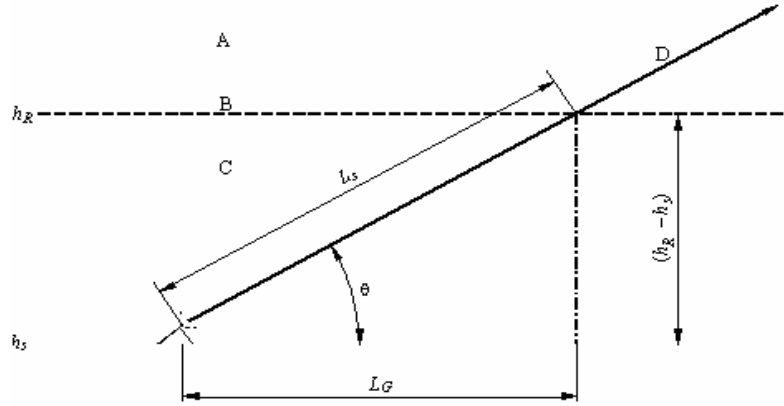


Fig. 2.2: Schematic presentation of an earth-space path given the parameters to be input to the attenuation prediction process.

If $h_R - h_s$ is less than or equal to zero, the predicted rain attenuation for any time percentage is zero and the following steps are not required.

Step 3: Calculate the horizontal projection, L_G , of the slant-path length from:

$$L_G = L_s \cos \theta \quad \text{km} \quad (8)$$

Step 4: Obtain the rainfall rate, $R_{0.01}$, exceeded for 0.01% of an average year (with an integration time of 1 min). If this long-term statistic cannot be obtained from local data sources, an estimate can be obtained from the maps of rainfall rate given in Recommendation ITU-R P.837. If $R_{0.01}$ is equal to zero, the predicted rain attenuation is zero for any time percentage and the following steps are not required.

Step 5: Obtain the specific attenuation, γ_R , using the frequency-dependent coefficients given in Recommendation ITU-R P.838 and the rainfall rate, $R_{0.01}$, determined from Step 4, by using:

$$\gamma_R = k (R_{0.01})^\alpha \quad \text{dB/km} \quad (9)$$

Step 6: Calculate the horizontal reduction factor, $r_{0.01}$, for 0.01% of the time:

$$r_{0.01} = \frac{1}{1 + 0.78 \sqrt{\frac{L_G \gamma_R}{f}} - 0.38 (1 - e^{-2L_G})} \quad (10)$$

Step 7: Calculate the vertical adjustment factor, $v_{0.01}$, for 0.01% of the time:

$$\zeta = \tan^{-1} \left(\frac{h_R - h_s}{L_G r_{0.01}} \right) \quad \text{degrees}$$

For $\zeta > \theta$, $L_R = \frac{L_G r_{0.01}}{\cos \theta} \quad \text{km}$

Else, $L_R = \frac{(h_R - h_s)}{\sin \theta} \quad \text{km}$

If $|\varphi| < 36^\circ$, $\chi = 36 - |\varphi| \quad \text{degrees}$

Else, $\chi = 0 \quad \text{degrees}$

$$v_{0.01} = \frac{1}{1 + \sqrt{\sin \theta} \left(31 (1 - e^{-(\theta/(1+\chi))}) \sqrt{\frac{L_R \gamma_R}{f^2}} - 0.45 \right)} \quad (11)$$

Step 8: The effective path length is:

$$L_E = L_R v_{0.01} \quad \text{km} \quad (12)$$

Step 9: The predicted attenuation exceeded for 0.01% of an average year is obtained from:

$$A_{0.01} = \gamma_R L_E \quad \text{dB} \quad (13)$$

Step 10: The estimated attenuation to be exceeded for other percentages of an average year, in the range 0.001% to 5%, is determined from the attenuation to be exceeded for 0.01% for an average year:

If $p \geq 1\%$ or $|\varphi| \geq 36^\circ$: $\beta = 0$

If $p < 1\%$ and $|\varphi| < 36^\circ$ and $\theta \geq 25^\circ$: $\beta = -0.005(|\varphi| - 36)$

Otherwise: $\beta = -0.005(|\varphi| - 36) + 1.8 - 4.25 \sin \theta$

$$A_p = A_{0.01} \left(\frac{p}{0.01} \right)^{-(0.655 + 0.033 \ln(p) - 0.045 \ln(A_{0.01}) - \beta(1-p) \sin \theta)} \quad \text{dB} \quad (14)$$

This method provides an estimate of the long-term statistics of attenuation due to rain for earth-to-satellite link. For the terrestrial link for estimating the long-term statistics of rain attenuation the following method has been proposed by ITU-R:

Step 1: Obtain the rain rate $R_{0.01}$ exceeded for 0.01% of the time (with an integration time of 1 min). If this information is not available from local sources of long-term measurements, an estimate can be obtained from the information given in Recommendation ITU-R P.837.

Step 2: Compute the specific attenuation, γ_R (dB/km) for the frequency, polarization and rain rate of interest using Recommendation ITU-R P.838.

Step 3: Compute the effective path length, d_{eff} , of the link by multiplying the actual path length d by a distance factor r . An estimate of this factor is given by:

$$r = \frac{1}{1 + \frac{d}{d_0}} \quad (15)$$

where, for $R_{0.01} \leq 100$ mm/h:

$$d_0 = 35 e^{-0.015 R_{0.01}} \quad (16)$$

For $R_{0.01} > 100$ mm/h, use the value 100 mm/h in place of $R_{0.01}$.

Step 4: An estimate of the path attenuation exceeded for 0.01% of the time is given by:

$$A_{0.01} = \gamma_R d_{\text{eff}} = \gamma_R dr \quad \text{dB} \quad (17)$$

Step 5: For radio links located in latitudes equal to or greater than 30° (North or South), the attenuation exceeded for other percentages of time p in the range 0.001% to 1% may be deduced from the following power law:

$$\frac{A_p}{A_{0.01}} = 0.12 p^{-(0.546 + 0.043 \log_{10} p)} \quad (18)$$

Step 6: For radio links located at latitudes below 30° (North or South), the attenuation exceeded for other percentages of time p in the range 0.001% to 1% may be deduced from the following power law:

$$\frac{A_p}{A_{0.01}} = 0.07 p^{-(0.855 + 0.139 \log_{10} p)} \quad (19)$$

Step 7: If worst-month statistics are desired, calculate the annual time percentages p corresponding to the worst-month time percentages p_w using climate information specified in Recommendation ITU-R P.841. The values of A exceeded for percentages of the time p on an annual basis will be exceeded for the corresponding percentages of time p_w on a worst-month basis.

The prediction procedure outlined above is considered to be valid in all parts of the world at least for frequencies up to 40 GHz and path lengths up to 60 km.

CHAPTER 3
STATISTICAL DATA AND
PERFORMANCE ANALYSIS

3.1 INTRODUCTION

Bangladesh is a developing country in South Asia located between 20° 34 ' to 26° 38 ' north latitude and 88°01' to 92°42' east longitude [32]. It has a subtropical monsoon climate characterized by wide seasonal variations in rainfall, moderately warm temperatures, and high humidity. Monsoon rainfall is considered to be an atmospheric heat source that influences the global atmospheric circulation (Ose, 1998). It is known that a large amount of rainfall occurs in Bangladesh (88.05 ° – 92.74 ° E and 20.67 ° – 26.63 ° N). In and around Bangladesh, the rainy season is divided into the following periods: (1) pre-monsoon (March–May), (2) monsoon (June–September) and (3) post-monsoon (October–November). In this chapter we have collected daily rain fall data from 34 different rain gauge stations for the period of 13 years. The daily rainfall data are converted into annual rainfall data; availability calculation and average annual accumulation, M (mm/year) are also calculated. The Chebil model has been used to convert long term rain statistic to 1-minute rain intensity. The data has been used for the prediction of rain attenuation in order to design a reliable microwave link in Bangladesh. Comparing the ITU-R predicted rain attenuation with our measured rain attenuation it has been observed that ITU-R has underestimated the rain rate in Bangladesh.

3.2 EARTH STATIONS IN BANGLADESH

Advanced digital transmission technologies and radio frequency are in operation in Bangladesh for satellite transmission to facilitate tranception through satellite [33]. BTCL has established 4 earth stations till to date. They are situated in Betbunia (standard A), Talibabad (standard B), Mohakhali (Standard A), Sylhet (Standard F3). They all are working with INTELSAT at 61.8° E IOR and their carrier is IDR. 462 International Circuits (voice 457, VFT 2, data 3) with 8 countries are working through Betbunia earth station. 331 International Circuits (voice 328, VFT 3,) with 2 countries are working through Talibabad earth station. 2741 (voice, VFT 5, data 11) International Circuits with 20 countries are working through Mahakhali earth station. 128 International Circuits are working through Sylhet earth station. In addition to that 100 terrestrial International Circuits between 2

countries are working via microwave. These earth stations are operating with different INTELSAT. Till to date BTCL has five INMARSAT-A Terminals which are operating through one LES (Land Earth Station) located in Jeddah. Besides this according to IMN number allocated by BTCL, there are two numbers B type (Land Mobile), 34 numbers C type (Maritime Mobile) and 5 numbers Mini-M type Terminal working in commercial basis.

3.3 RAINFALL DATA COLLECTION

The daily rain fall data were collected from Meteorological Department of Bangladesh from 34 different rain stations for the period of 13 years

3.3.1 LOCATIONS OF RAIN GAUGE STATIONS

There are thirty-four rain gauge stations in Bangladesh. Each of them constructed at different times. All the Rain Gauge Stations are located in the map:

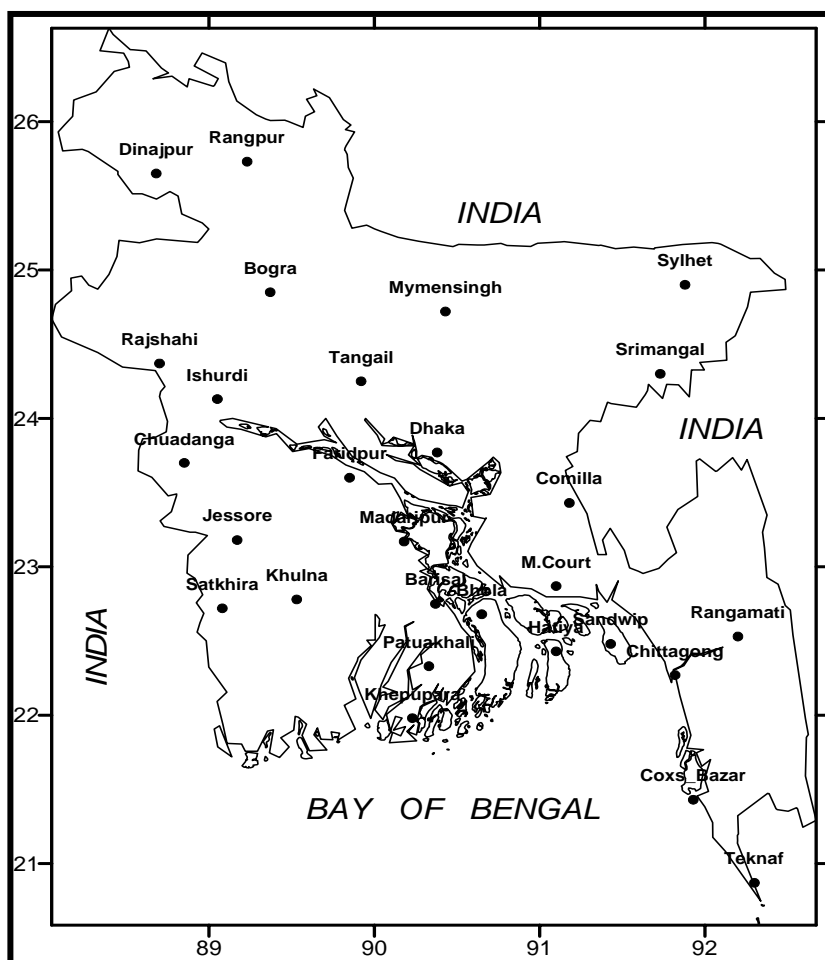


Fig. 3.1: Rain Gauge Stations in Bangladesh

3.3.2 RAIN GAUGE SPECIFICATIONS AND SAMPLE DATA

The rain gauge stations are specified according to their station ID, latitude and longitude as followed:

Table 3.1: Rain gauge stations with longitude and latitude situated in Bangladesh

Station Name	Station ID	Latitude (°)	Longitude (°)
Dhaka	41923	23.77	90.38
Mymensingh	41886	24.72	90.43
Tangail	41909	24.25	89.92
Faridpur	41929	23.6	89.85
Madaripur	41939	23.17	90.18
Chittagong	41978	22.27	91.82
Sandwip	41964	22.48	91.43
Sitakunda	41965	22.58	91.7
Rangamati	41966	22.53	92.2
Comilla	41933	23.43	91.18
Chandpur	41941	23.27	90.7
M.Court	41953	22.87	91.1
Feni	41943	23.03	91.42
Hatiya	41963	22.43	91.1
Coxs	41992	21.43	91.93
Kutubdia	41989	21.82	91.85
Teknaf	41998	20.87	92.3
Sylhet	41891	24.9	91.88
Srimangal	41915	24.3	91.73
Rajshahi	41895	24.37	88.7
Ishurdi	41907	24.13	89.05
Bogra	41883	24.85	89.37
Rangpur	41859	25.73	89.23
Dinajpur	41863	25.65	88.68
Sayedpur	41858	25.8	88.95
Khulna	41947	22.78	89.53
Mongla	41958	22.35	89.75
Satkhira	41946	22.72	89.08
Jessore	41936	23.18	89.17
Chuadanga	41926	23.7	88.85
Barisal	41950	22.75	90.37
Patuakhali	41960	22.33	90.33
Khepupara	41984	21.98	90.23
Bhola	41951	22.68	90.65

The sample data collected from Meteorological Department of Bangladesh for Teknaf and Ishurdi rain station for the period of thirteen years are shown in appendix - A.

3.3.3 ANNUAL DISTRIBUTION

The raw data collected from Meteorological Department of Bangladesh was in WordPad. Then we converted it in Excel sheet. The daily rainfalls in mm for the period of 13 years of 34 different rain stations were converted into annual rainfall. The annual rainfall of Teknaf and Ishurdi between 34 stations for 13 years is shown below -

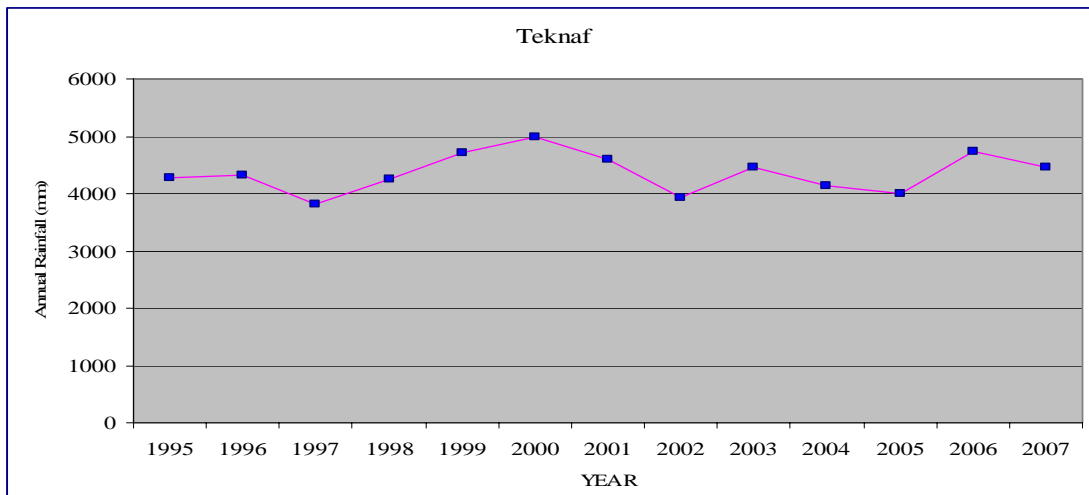


Fig. 3.2: Annual rainfall rate at Teknaf station for the period of 13 years.

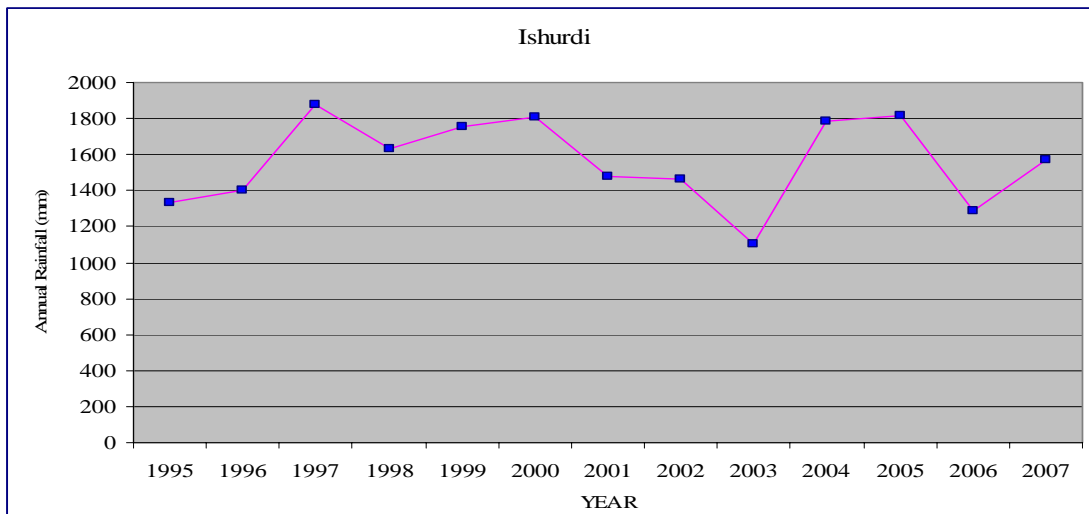


Fig. 3.3: Annual rainfall rate at Ishurdi station for the period of 13 years.

3.3.4 AVAILABILITY CALCULATIONS

All the rainfall data were not available for each day of different stations. So we performed availability calculations. It is performed as,

$$Availability = 100 - \frac{\text{No. of missing data among 365 days} \times 100}{365} \quad (\%)$$

Say, for Chittagong no. of missing data of year 2001 is 8. So, availability of data for year 2001 for this station is 97.808%. The availability calculations of Chittagong and Sandwip stations for each of 13 years are shown in tabular form as below:

Table 3.2: Availability calculation for Chittagong station

Year	Annual Rainfall (mm)	Availability (%)
1995	2444	100
1996	2904	100
1997	3015	100
1998	3833	100
1999	3194	100
2000	3503	100
2001	1647	97.808
2002	2745	100
2003	2769	100
2004	2924	100
2005	2331	100
2006	2375	100
2007	4340	100

Table 3.3: Availability calculation for Sandwip station

Year	Annual Rainfall (mm)	Availability (%)
1995	2234	100
1996	3307	100
1997	3143	100
1998	4254	100
1999	4099	100
2000	4252	100
2001	6095	100
2002	4325	66.575
2003	Data missing	0.0
2004	4670	100
2005	3067	100
2006	3111	100
2007	4305	100

After performing availability calculations, then annual rainfall data for the period of 13 years of 34 rain stations are converted into average annual accumulation, M (mm/year).

3.4 CONVERSION FROM ANNUAL AVG. TO 1-MINUTE INTEGRATION

Common rain attenuation prediction methods require 1- min rain rate data, which is scarce in the tropical and subtropical region. However, yearly rainfall data are available at many meteorological stations. A method for converting the available rainfall data to the equivalent 1 min rain rate cumulative distribution (CD) would be very useful for radio wave engineers. For this reason 1 min rain rate CD can be estimated by the use of Chebil model and long-term mean annual rainfall data. His model is as follows:

$$R_{0.01} = \alpha M^{\beta} \quad (1)$$

Where α and β are regression coefficients. In Chebil model the regression coefficients α and β are defined as

$$\alpha = 12.2903 \text{ and } \beta = 0.2973 \quad (2)$$

Chebil has developed his model based on measured values of M in Malaysia, Indonesia, Singapore, Brazil and Vietnam. He showed that his model is the best estimate of the measured data. Using Chebil model, long-term mean annual rainfall data has been converted to 1 min rain rate data and are presented in Table 3.4:

3.5 RAIN INTENSITIES DISTRIBUTION

Table 3.4: Rain Intensities Distribution for 34 rain stations

Station Name	Avg. Annual accumulation M (mm/year)	Max. Rainfall (mm/year)	Min. Rainfall (mm/year)	Avg. of 13 years availability of data	R _{0.01} (mm/hr)
Dhaka	2118.00			100	119.7734
Mymensingh	2316.307			100	123.0032
Tangail	1882.230			100	115.6439
Faridpur	1830.153			100	114.6832
Madaripur	2013.923			100	117.9925
Chittagong	2924.923			99.83	131.8373
Sandwip	3604.769			89.736	140.2885
Sitakunda	3054.00			99.705	133.5408
Rangamati	2713.461			100	128.9285
Comilla	2195.3076			100	121.0568
Chandpur	1981.769			99.85	117.4293
M.Court	3062.1538			99.178	133.6467
Feni	2935.4615			99.325	131.9783
Hatiya	2552.4615			69.209	126.6052
Cox's Bazar	3890.1538			100	143.5025
Kutubdia	2986.5384			100	132.6569
Teknaf	4360.6923	<i>4360.6923</i>		100	148.4576
Sylhet	3916.3846			99.978	143.7895
Srimangal	2442.5384			100	124.9591
Rajshahi	1572.923			100	109.6336
Ishurdi	1562.923		<i>1562.923</i>	100	109.4259
Bogra	1818.692			100	114.4693
Rangpur	2398.2307			100	124.2808
Dinajpur	2140.3076			100	120.1470
Sayedpur	2389.6153			100	124.1479
Khulna	1905.0769			100	116.0594
Mongla	2053.3846			100	118.6752
Satkhira	1846.3846			100	114.9847
Jessore	1767.0769			100	113.4936
Chuadanga	1602.00			100	110.2322
Barisal	2136.538			100	120.0841
Patuakhali	2695.923			100	128.6802
Khepupara	3027.0769			100	133.1897
Bhola	2368.00			100	123.8130

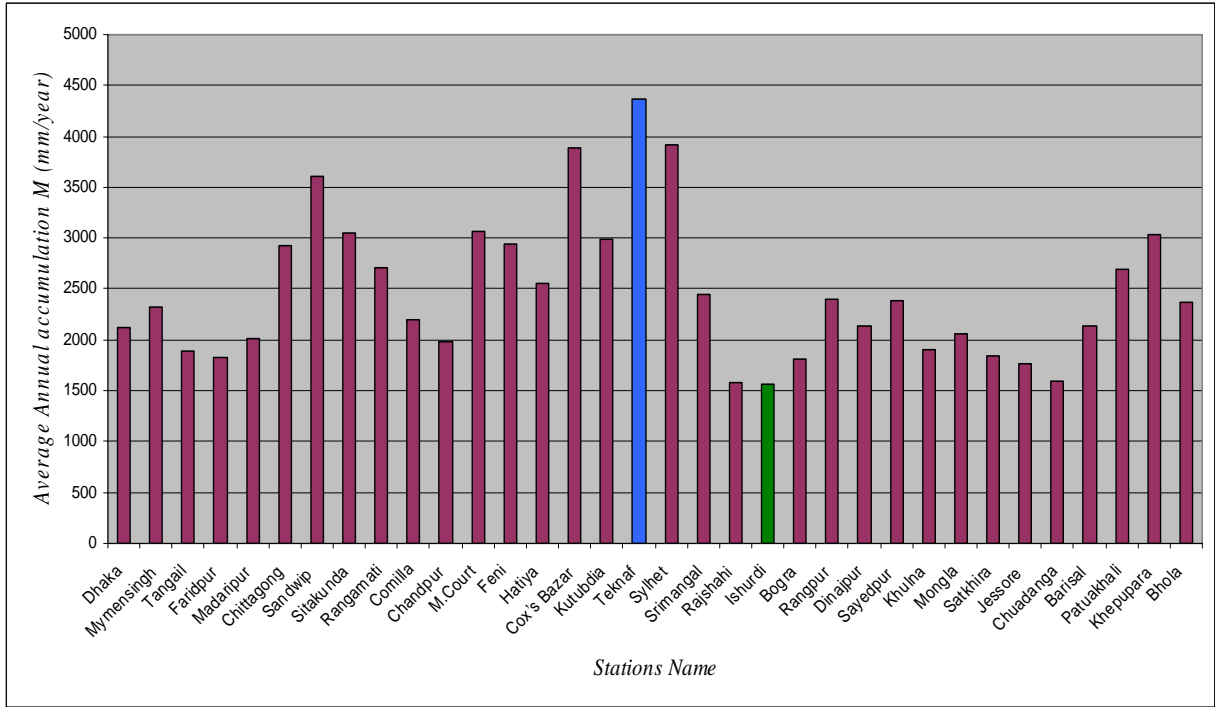


Fig. 3.4 Average Annual accumulation, M (mm/year) for 34 rain stations in Bangladesh

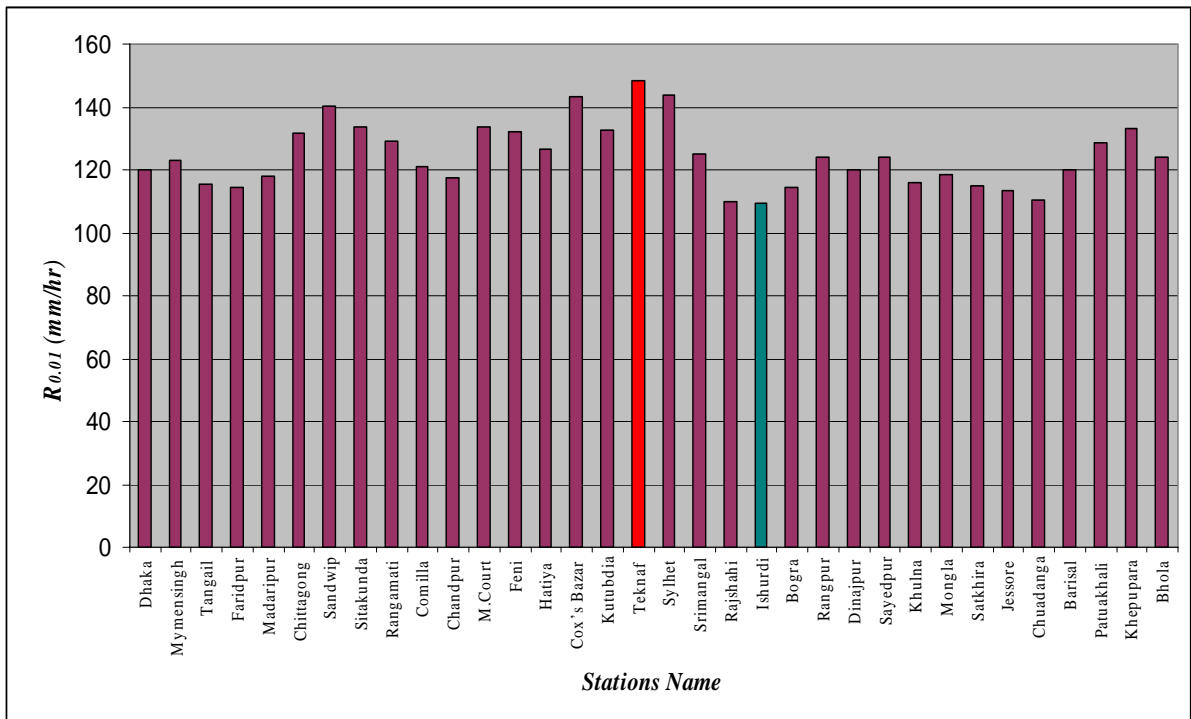


Fig. 3.5: 1- min rain rate cumulative distribution, $R_{0.01}$ (mm/hr) for 34 rain stations in Bangladesh

3.6 RAIN ATTENUATION STATISTICS FROM RAINFALL RATE FOR EARTH – SATELLITE LINK

The following procedure provides estimates of the long-term statistics of the slant-path rain attenuation at a given location for frequencies up to 55 GHz. The following parameters are required:

- $R_{0.01}$: point rainfall rate for the location for 0.01% of an average year (mm/h)
- h_s : height above mean sea level of the earth station (km) = 0.006 km
- θ : elevation angle (degrees) = 61.8°
- φ : latitude of the earth station (degrees) = 22.32° N
- f : frequency (GHz): C-Band (4 GHz), Ku-Band (12 GHz) and Ka-Band (20 GHz)
- R_e : effective radius of the Earth = 8500 km.

The geometry is illustrated in Fig. 3.6 where

A = frozen precipitation, B = rain height, C = liquid precipitation and D = Earth-space path

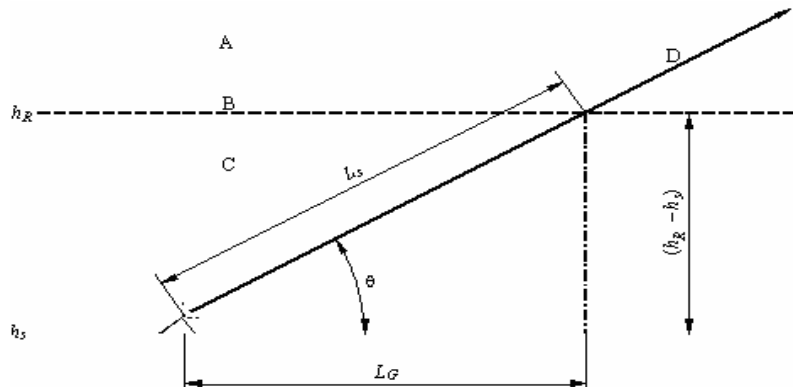


Fig. 3.6: Schematic presentation of an earth-space path given the parameters to be input to the attenuation prediction process.

Step 1: The rain height, h_R , as given in Recommendation ITU-R P.839 for Bangladesh is 5 km.

Step 2: As elevation angle, $\theta \geq 5^\circ$ the slant-path length, L_s is

$$L_s = \frac{(h_R - h_s)}{\sin \theta} \quad \text{km} \quad (3)$$

Where $h_R = 5$ km, $h_s = 0.006$ km and elevation angle, $\theta = 61.8^\circ$

$$L_s = \frac{(5 - 0.006)}{\sin(61.8^\circ)} \text{ km} = 5.666 \text{ km} \quad (4)$$

Step 3: The horizontal projection, L_G , of the slant-path length is

$$L_G = L_s \cos \theta \quad \text{km} \quad (5)$$

$$L_G = 5.666 \cos 61.8^\circ = 2.677 \text{ km}$$

Step 4: From the measured value of $R_{0.01}$ for 34 rain stations in Bangladesh as shown in Table 3.1 exceeded for 0.01% of an average year (with an integration time of 1 min) Measured Maximum $R_{0.01}$ is 148.4576 mm/hr at Teknaf and minimum $R_{0.01}$ is 109.4259 mm/hr at Ishurdi.

Step 5: The specific attenuation, γ_R , using the frequency-dependent coefficients given in Recommendation ITU-R P.838 as shown in Table 3.2 and the rainfall rate, $R_{0.01}$ determined from Step 4 is calculated as

$$\gamma_R = k (R_{0.01})^\alpha \quad (6)$$

$$k = \frac{[k_H + K_V + (k_H - k_V) \cos^2 \theta \cos 2\tau]}{2} \quad (7)$$

$$\alpha = \frac{[k_H \alpha_H + K_V \alpha_V + (k_H \alpha_H - k_V \alpha_V) \cos^2 \theta \cos 2\tau]}{2k} \quad (8)$$

Where θ is the path elevation angle and τ is the polarization tilt angle relative to the horizontal ($\tau = 45^\circ$ for circular polarization).

Table 3.5: Table from Recommendation ITU-R P.838-3

Frequency	k_H	α_H	k_V	α_V
4 GHz	0.0001071	1.6009	0.0002461	1.2476
12 GHz	0.02386	1.1825	0.02455	1.1216
20 GHz	0.09164	1.0568	0.09611	0.9847

Table 3.6: Frequency-dependent coefficients for estimating specific rain attenuation using equations (7), (8) and (6).

Frequency	Horizontal Polarization		Vertical Polarization		Circular Polarization	
	k	α	k	α	k	α
4 GHz	0.0001611	1.3912	0.0001921	1.3241	0.0001766	1.3547
12 GHz	0.0241	1.1584	0.0243	1.1448	0.0242	1.1516
20 GHz	0.0934	1.0280	0.0944	1.0119	0.0939	1.0199

Table 3.7: Specific attenuation, γ_R (dB/km)

Frequency	For maximum $R_{0.01}$ Specific attenuation, γ_R (dB/km)			For minimum $R_{0.01}$ Specific attenuation, γ_R (dB/km)		
	<i>Horizontal Polarization</i>	<i>Vertical Polarization</i>	<i>Circular Polarization</i>	<i>Horizontal Polarization</i>	<i>Vertical Polarization</i>	<i>Circular Polarization</i>
4 GHz	0.1692	0.1442	0.1545	0.1107	0.0963	0.1022
12 GHz	7.9098	7.4377	7.6693	5.5551	5.2453	5.3974
20 GHz	15.9433	14.8694	15.3939	11.6517	10.9203	11.2780

Step 6: The horizontal reduction factor, $r_{0.01}$, for 0.01% of the time:

$$r_{0.01} = \frac{1}{1 + 0.78 \sqrt{\frac{L_G \gamma_R}{f} - 0.38 (1 - e^{-2L_G})}} \quad (9)$$

For maximum $R_{0.01}$, Specific attenuation, $\gamma_R = 0.1692$ dB/km when $f = 4$ GHz
at Horizontal polarization:

$$r_{0.01} = \frac{1}{1 + 0.78 \sqrt{\frac{2.677 \times 0.1692}{4 \times 10^9} - 0.38 (1 - e^{-2 \times 2.677})}}$$

$$r_{0.01} = 1.6082$$

For maximum $R_{0.01}$, Specific attenuation, $\gamma_R = 0.1442$ dB/km when $f = 4$ GHz
At Vertical polarization

$$r_{0.01} = 1.6082$$

For maximum $R_{0.01}$, Specific attenuation, $\gamma_R = 0.1545$ dB/km when $f = 4$ GHz
At Circular polarization

$$r_{0.01} = 1.6082$$

The value of horizontal reduction factor, $r_{0.01}$, for 0.01% of the time remains constant for 12 GHz and 20 GHz at three different polarizations for maximum and minimum $R_{0.01}$.

Step 7: The vertical adjustment factor, $v_{0.01}$, for 0.01% of the time:

$$\zeta = \tan^{-1} \left(\frac{h_R - h_s}{L_G r_{0.01}} \right) \quad \text{degrees}$$

$$\zeta = \tan^{-1} \left(\frac{5 - 0.006}{2.677 \times 1.6082} \right) \quad \text{degrees}$$

$$\zeta = 49.236^\circ \quad \text{degrees}$$

Considering Singapore Satellite ST1 located at 88 degree East longitude and earth

station at Dhaka at 90° longitude (East) and 24° Latitude (North), the elevation angle is 61.8°.

Here, $\zeta > \theta$,

$$L_R = \frac{(h_R - h_s)}{\sin \theta} \quad \text{km}$$

$$L_R = \frac{(5 - 0.006)}{\sin (61.8^\circ)} \quad \text{km}$$

$$L_R = 5.666 \quad \text{km}$$

Latitude of Betunia earth station in Bangladesh is $\varphi = 22.32^\circ \text{ N}$

Here, $|\varphi| < 36^\circ$, So $\chi = 36^\circ - |\varphi|$ degrees

$$\chi = 36^\circ - |22.32^\circ| \quad \text{degrees}$$

$$\chi = 13.68^\circ$$

$$v_{0.01} = \frac{1}{1 + \sqrt{\sin \theta} \left(31 \left(1 - e^{-(\theta / (1 + 13.68^\circ))} \right) \frac{\sqrt{L_R \gamma_R}}{f^2} - 0.45 \right)} \quad (10)$$

For maximum $R_{0.01}$, Specific attenuation, $\gamma_R = 0.1692 \text{ dB/km}$ when $f = 4 \text{ GHz}$

At Horizontal polarization:

$$v_{0.01} = \frac{1}{1 + \sqrt{\sin (61.8^\circ)} \left(31 \left(1 - e^{-(61.8^\circ / (1 + 13.68^\circ))} \right) \frac{\sqrt{5.666 \times 0.1692}}{(4 \times 10^9)^2} - 0.45 \right)}$$

$$v_{0.01} = 1.7313$$

For maximum $R_{0.01}$, Specific attenuation, $\gamma_R = 0.1442 \text{ dB/km}$ when $f = 4 \text{ GHz}$

At Vertical polarization

$$v_{0.01} = 1.7313$$

For maximum $R_{0.01}$, Specific attenuation, $\gamma_R = 0.1545$ dB/km when $f = 4$ GHz
 At Circular polarization

$$v_{0.01} = 1.7313$$

The value of vertical adjustment factor factor, $v_{0.01}$, for 0.01% of the time remains constant for 12 GHz and 20 GHz at three different polarizations for maximum and minimum $R_{0.01}$.

Step 8: The effective path length is:

$$L_E = L_R v_{0.01} \quad \text{km} \quad (11)$$

$$L_E = 5.666 \times 1.7313 = 9.8095 \quad \text{km}$$

Step 9: The predicted attenuation exceeded for 0.01% of an average year is obtained in Table 3.8 and 3.9:

$$A_{0.01\%} = \gamma_R L_E \quad \text{dB} \quad (12)$$

Step 10: The estimated attenuation to be exceeded for other percentages of an average year, in the range 0.001% to 1%, is determined from the attenuation to be exceeded for 0.01% for an average year:

$$\text{Here } p < 1\% \text{ and } |\varphi| < 36^\circ \text{ and } \theta \geq 25^\circ: \beta = -0.005(|\varphi| - 36)$$

$$\beta = -0.005(22.32 - 36)$$

$$\beta = 0.0684$$

$$A_p = A_{0.01} \left(\frac{p}{0.01} \right)^{-(0.655 + 0.033 \ln(p) - 0.045 \ln(A_{0.01}) - \beta(1-p) \sin \theta)} \quad \text{dB} \quad (13)$$

Using MATLAB program the values of A_p for other percentages, p of an average year, in the range 0.001% to 1%, have been determined and shown in Table 3.8 and 3.9

Table 3.8: Predicted Attenuation, $A_{0.01}$ at different percentages of time for measured maximum $R_{0.01}$ at horizontal polarization

Percentage of Time, p(%)	System Reliability (%)	Predicted $A_{0.01}$ (dB)		
		4 GHz	12 GHz	20 GHz
0.001	99.999	3.6648	115.0322	215.6138
0.003	99.997	2.6238	99.5973	193.2650
0.005	99.995	2.1860	90.6464	178.7531
0.007	99.993	1.9201	84.3925	168.1961
0.01	99.99	1.6597	77.5910	156.3900
0.03	99.97	1.0035	56.7327	118.3805
0.05	99.95	0.7714	47.6412	101.0243
0.07	99.93	0.6416	42.0044	90.0217
0.1	99.90	0.5225	36.3802	78.8502
0.3	99.70	0.2554	21.5059	48.2552
0.5	99.50	0.1722	15.8394	36.1180
0.7	99.30	0.1284	12.5215	28.8568
1.0	99.00	0.0903	9.3636	21.8233

Table 3.9: Predicted Attenuation, $A_{0.01}$ at different percentages of time for measured minimum. $R_{0.01}$ at horizontal polarization

Percentage of Time, p(%)	System Reliability (%)	Predicted $A_{0.01}$ (dB)		
		4 GHz	12 GHz	20 GHz
0.001	99.999	2.5056	83.7972	162.7753
0.003	99.997	1.7566	71.2966	143.6586
0.005	99.995	1.4493	64.3641	131.9171
0.007	99.993	1.2649	59.6037	123.5382
0.01	99.99	1.0859	54.4900	114.2900
0.03	99.97	0.6429	39.1517	85.1816
0.05	99.95	0.4894	32.6115	72.1707
0.07	99.93	0.4045	28.5995	64.0059
0.1	99.90	0.3271	24.6301	55.7814
0.3	99.70	0.1566	14.3077	33.6122
0.5	99.50	0.1046	10.4526	24.9774
0.7	99.30	0.0775	8.2189	19.8613
1.0	99.00	0.0541	6.1114	14.9450

3.6.1 DETERMINATION OF RAIN ATTENUATION FROM ITU-R PREDICTED RAINFALL RATE

ITU-R has predicted rain fall rate $R_{0.01}$ for subtropical countries like Bangladesh as 95 mm/hr. Following the steps 1-10 for this ITU-R predicted value of $R_{0.01}$, the results are obtained as below -

Table 3.10: Specific attenuation, γ_R (dB/km) for ITU-R predicted value

Frequency	For ITU-R Predicted $R_{0.01} = 95$ mm/h Specific attenuation, γ_R (dB/km)		
	<i>Horizontal Polarization</i>	<i>Vertical Polarization</i>	<i>Circular Polarization</i>
4 GHz	0.0919	0.0794	0.0844
12 GHz	4.7319	4.4466	4.5865
20 GHz	10.1144	9.4294	9.7637

Table 3.11: Predicted Attenuation, $A_{0.01}$ for ITU-R predicted value

Frequency	For ITU-R Predicted $R_{0.01} = 95$ mm/hr Attenuation, $A_{0.01}$ (dB)		
	<i>Horizontal Polarization</i>	<i>Vertical Polarization</i>	<i>Circular Polarization</i>
4 GHz	0.9015	0.7788	0.8279
12 GHz	46.4175	43.618	44.99
20 GHz	99.2172	92.4976	95.777

Table 3.12: Predicted Attenuation, $A_{0.01}$ at different percentages of time for ITU-R predicted value of $R_{0.01}$ at horizontal polarization

Percentage of Time, p(%)	System Reliability (%)	ITU-R predicted value of $R_{0.01}$ predicted $A_{0.01}$ (dB)		
		4 GHz	12 GHz	20 GHz
0.001	99.999	2.1206	72.5781	143.3939
0.003	99.997	1.4731	61.2636	125.6716
0.005	99.995	1.2102	55.1031	115.0257
0.007	99.993	1.0532	50.9039	107.4892
0.01	99.99	0.9015	46.4170	99.2170
0.03	99.97	0.5289	33.0878	73.4323
0.05	99.95	0.4009	27.4592	62.0141
0.07	99.93	0.3304	24.0227	54.8806
0.1	99.90	0.2664	20.6353	47.7203
0.3	99.70	0.1264	11.8924	28.5545
0.5	99.50	0.0840	8.6562	21.1501
0.7	99.30	0.0621	6.7899	16.7820
1.0	99.00	0.0432	5.0358	12.5992

3.7 LINK BUDGET CALCULATION FOR EARTH-TO-SATELLITE DOWNLINK AT THREE BANDS USING ITU-R PROPOSED AND MEASURED RAIN RATE FOR BANGLADESH AT HORIZONTAL POLARIZATION

EIRP (Effective Isotropically Radiated Power)

It is the combination of transmitter power and gain in terms of an equivalent isotropic source with power $P_t G_t$ watts, radiating uniformly in all directions.

$$\text{EIRP} = 10 \log_{10}(P_t G_t) = 65 \quad \text{dBW} \quad (1)$$

Here, P_t is the output power of a transmitting antenna in watts and G_t is the gain of the transmitting antenna.

Transponder Output Back off = B_0

The value of Transponder Output Back off B_0 is typically 2 dB.

G_r = Receiving Antenna Gain:

In antenna theory the gain and area of an antenna are related by,

$$G = \frac{4\pi A_e}{\lambda^2} \quad (2)$$

$$\text{So, } G_r = 10 \log_{10} \left(\frac{4\pi A_e}{\lambda^2} \right) \quad \text{dB} \quad (3)$$

Here, A_e is the effective aperture area in $\text{m}^2 = 1.1064 \text{m}^2$

And λ is the wavelength at the frequency of operation in meters.

Table 3.13: Receiving Antenna Gain

Frequency	4GHz	12GHz	20GHz
Receiving Antenna Gain, G_r (dB)	33.93	43.47	47.91

Free Space Path Loss [FSL]

It accounts for the way energy spreads out as an electromagnetic wave travels away from a transmitting source in three-dimensional space.

$$[\text{FSL}] = 10 \log_{10} \left[\left(\frac{4\pi R}{\lambda} \right)^2 \right] = 20 \log_{10} \left(\frac{4\pi R}{\lambda} \right) \quad \text{dB} \quad (4)$$

Table 3.14: Free Space Path Loss

Frequency	4GHz	12GHz	20GHz
Free Space Path Loss (dB)	-199.7	-206.6	-209.7

L_{ant} = Edge of beam loss for Satellite Antenna

Edge of beam loss for Satellite Antenna is typically 3dB.

[AA] = Clear air atmospheric loss:

Table 3.15: Clear air atmospheric loss

Frequency	4GHz	12GHz	20GHz
Clear air atmospheric loss (dB)	0.075	0.11	0.4

Other losses (L_m)

Typically other losses are considered together as 0.5 dB.

Received power at receiver station P_r (Clear Air):

$$P_r = EIRP + G_r - FSL - L_{ant} - AA - L_m - B_0 \quad \text{dBW} \quad (5)$$

For 4GHz

$$P_r = 65 + 33.93 - 199.7 - 3 - 0.075 - 0.5 - 2 = -106.345 \quad \text{dBW} \quad (6)$$

For 12GHz

$$P_r = 65 + 43.47 - 206.6 - 3 - 0.11 - 0.5 - 2 = -103.74 \quad \text{dBW} \quad (7)$$

For 20GHz

$$P_r = 65 + 47.91 - 209.7 - 3 - 0.4 - 0.5 - 2 = -102.69 \quad \text{dBW} \quad (8)$$

P_r (due to rain):

$$P_r = P_r \text{ (due to rain)} - \text{Rain Attenuation, } A_{rain}$$

Table 3.16: Received power due to rain

Frequency	For ITU-R predicted $R_{0.01}$			For maximum $R_{0.01}$ (Worst Case)		
	4 GHz	12 GHz	20 GHz	4 GHz	12 GHz	20 GHz
P_r = Received power at receiver station (Clear Air)	-106.345	-103.74	-102.69	-106.345	-119.74	-102.69
Rain Attenuation, A_{rain}	0.9015	46.4175	99.2172	1.659	77.591	156.395
P_r (due to rain)	-107.25	-150.16	-201.91	-108.0	-181.33	-259.08

Boltzmann's constant, k in dBW/K/Hz

$$\text{The value in dBW/K/Hz is } = 10 \log_{10} (1.3806 \times 10^{-23}) = -228.6$$

System noise temperature, T_s :

$$\text{It is assumed as 140K and in dBK it is } = 10 \log_{10} (140) = 21.46$$

Noise bandwidth, B_n :

$$\text{It is assumed as 36MHz and in dBHz it is } = 10 \log_{10} (36 \times 10^6) = 75.56$$

Receiver Noise Power, N in clear air:

The receiver noise power, N in clear air in dBW is calculated as,

$$N = k + T_s + B_n = -228.6 + 21.46 + 75.56 = -131.58 \quad \text{dBW} \quad (9)$$

Attenuation:

The total path attenuation, A is the sum of the clear sky path attenuation due to atmospheric gaseous absorption, A_{ca} and attenuation due to rain, A_{rain} .

$$A = A_{ca} + A_{rain} \quad \text{dB} \quad (10)$$

$$T_{sky} = T_p (1 - G); \quad (11)$$

Here, G is the linear gain and less than unity.

$$G = 10^{-A/10}$$

And T_p is the physical temperature of the device = 273 K.

For ITU-R Predicted $R_{0.01}$

For 4GHz

$$A = 0.075 + 0.9015 = 0.9765 \text{ dB};$$

$$G = 10^{-A/10},$$

So, $G = 0.7986$;

$$T_{skyrain} = 273(1 - 0.7986) = 54.972 \text{ K}$$

$$T_{ca} = 0.95 \times 273(1 - 10^{-0.075/10}) = 4.44 \text{ K}$$

$$T_{srain} = T_{LNA} + T_{skyrain} = 140 - 4.44 + 54.972 = 190.532 \text{ K}$$

$$\Delta N_{rain} = 10 \log_{10} \left[\frac{T_{srain}}{T_{sca}} \right] = 10 \log_{10} \left[\frac{190.532}{140} \right] = 1.34 \text{ dB}$$

C/N in clear air

$C/N = P_r$ [Received power at receiver station in clear air] – N [Receiver Noise Power in clear air]

$$= -106.345 + 131.58 = 25.235$$

C/N due to rain

N= Receiver Noise Power (due to rain)

= Receiver Noise Power (Clear Air) + Increased due to rain (ΔN)

$$= -131.58 + 1.34$$

$$= -130.2$$

C/N = P_r [Received power at receiver station due to rain] – N [Receiver Noise Power due to rain]

$$= -107.25 - (-130.2) = 22.95$$

For 12GHz

$$A = 0.11 + 46.4175 = 46.5275 \text{ dB};$$

$$G = 10^{-A/10}$$

$$\text{So, } G = 0.00002245;$$

$$T_{\text{skyrain}} = 273(1 - 0.00002245) = 272.994 \text{ K}$$

$$T_{\text{ca}} = 0.95 \times 273(1 - 10^{-0.11/10}) = 6.486 \text{ K}$$

$$T_{\text{srain}} = T_{\text{LNA}} + T_{\text{skyrain}} = 140 - 6.486 + 272.994 = 406.508 \text{ K}$$

$$\Delta N_{\text{rain}} = 10 \log_{10} \left[\frac{T_{\text{srain}}}{T_{\text{sca}}} \right] = 10 \log_{10} \left[\frac{406.508}{140} \right] = 4.63 \text{ dB}$$

C/N in clear air

C/N = P_r [Received power at receiver station in clear air] – N [Receiver Noise Power in clear air]

$$= -103.74 + 131.58 = 27.84$$

C/N due to rain

N= Receiver Noise Power (due to rain)

= Receiver Noise Power (Clear Air) + Increased due to rain (ΔN)

$$= -131.58 + 4.63$$

$$= - 126.95$$

$C/N = P_r$ [Received power at receiver station due to rain] – N [Receiver Noise Power due to rain]

$$= - 150.16 - (-) 126.95 = - 23.21$$

For 20GHz

$$A = 0.4 + 99.2172 = 99.6172 \text{ dB};$$

$$G = 10^{-A/10} = 1.092 \times 10^{-10}$$

$$T_{\text{skyrain}} = 273(1 - 1.092 \times 10^{-10}) = 273 \text{ K}$$

$$T_{ca} = 0.95 \times 273(1 - 10^{-0.4/10}) = 22.82 \text{ K}$$

$$T_{\text{srain}} = T_{LNA} + T_{\text{skyrain}} = 140 - 22.82 + 273 = 390.18 \text{ K}$$

$$\Delta N_{\text{rain}} = 10 \log_{10} \left[\frac{T_{\text{srain}}}{T_{\text{sca}}} \right] = 10 \log_{10} \left[\frac{390.18}{140} \right] = 4.45 \text{ dB}$$

C/N in clear air

$C/N = P_r$ [Received power at receiver station in clear air] – N [Receiver Noise Power in clear air]

$$= - 102.69 + 131.58 = 28.89$$

C/N due to rain

$N =$ Receiver Noise Power (due to rain)

$=$ Receiver Noise Power (Clear Air) + Increased due to rain (ΔN)

$$= - 131.58 + 4.45$$

$$= - 127.13$$

$C/N = P_r$ [Received power at receiver station due to rain] – N [Receiver Noise Power due to rain]

$$= -201.91 - (-) 127.13 = -74.78$$

For measured maximum $R_{0.01}$ (Worst Case)

For 4GHz

$$A=0.075+1.659=1.734 \text{ dB};$$

$$G = 10^{-A/10},$$

$$\text{So, } G = 0.6708;$$

$$T_{\text{skyrain}} = 273(1 - 0.6708) = 89.87 \text{ K}$$

$$T_{\text{ca}} = 0.95 \times 273(1 - 10^{-0.075/10}) = 4.44 \text{ K}$$

$$T_{\text{srain}} = T_{\text{LNA}} + T_{\text{skyrain}} = 140 - 4.44 + 89.87 = 225.43 \text{ K}$$

$$\Delta N_{\text{rain}} = 10 \log_{10} \left[\frac{T_{\text{srain}}}{T_{\text{sca}}} \right] = 10 \log_{10} \left[\frac{225.43}{140} \right] = 2.068 \text{ dB}$$

C/N in clear air

$$\text{C/N} = P_r [\text{Received power at receiver station in clear air}] - N [\text{Receiver Noise Power in clear air}]$$

$$= -106.345 + 131.58 = 25.235$$

C/N due to rain

$$N = \text{Receiver Noise Power (due to rain)}$$

$$= \text{Receiver Noise Power (Clear Air)} + \text{Increased due to rain } (\Delta N)$$

$$= -131.58 + 2.068$$

$$= -129.512$$

$$\text{C/N} = P_r [\text{Received power at receiver station due to rain}] - N [\text{Receiver Noise Power due to rain}]$$

$$= -108.0 - (-) 129.512 = 21.512$$

For 12GHz

$$A=0.11+77.591=77.701 \text{ dB};$$

$$G = 10^{-A/10} = 1.697 \times 10^{-8}$$

$$T_{\text{skyrain}} = 273(1 - 1.697 \times 10^{-8}) = 272.999 \text{ K}$$

$$T_{ca} = 0.95 \times 273(1 - 10^{-0.11/10}) = 6.486 \text{ K}$$

$$T_{\text{srain}} = T_{LNA} + T_{\text{skyrain}} = 140 - 6.486 + 272.999 = 406.513 \text{ K}$$

$$\Delta N_{\text{rain}} = 10 \log_{10} \left[\frac{T_{\text{srain}}}{T_{\text{sca}}} \right] = 10 \log_{10} \left[\frac{406.513}{140} \right] = 4.629 \text{ dB}$$

C/N in clear air

$$\begin{aligned} C/N &= P_r \text{ [Received power at receiver station in clear air]} - N \text{ [Receiver Noise Power in} \\ &\quad \text{clear air]} \\ &= -103.74 + 131.58 = 27.84 \end{aligned}$$

C/N due to rain

$$\begin{aligned} N &= \text{Receiver Noise Power (due to rain)} \\ &= \text{Receiver Noise Power (Clear Air)} + \text{Increased due to rain } (\Delta N) \\ &= -131.58 + 4.629 \\ &= -126.951 \end{aligned}$$

$$\begin{aligned} C/N &= P_r \text{ [Received power at receiver station due to rain]} - N \text{ [Receiver Noise Power due to} \\ &\quad \text{rain]} \\ &= -181.33 - (-126.951) = -54.38 \end{aligned}$$

For 20GHz

$$A=0.4+156.3958=156.7958\text{dB};$$

$$G = 10^{-A/10} = 2.091 \times 10^{-16}$$

$$T_{\text{skyrain}} = 273(1 - 2.091 \times 10^{-16}) = 273 \text{ K}$$

$$T_{ca} = 0.95 \times 273(1 - 10^{-0.4/10}) = 22.82 \text{ K}$$

$$T_{\text{srain}} = T_{LNA} + T_{\text{skyrain}} = 140 - 22.82 + 273 = 390.18 \text{ K}$$

$$\Delta N_{\text{rain}} = 10 \log_{10} \left[\frac{T_{\text{srain}}}{T_{\text{sca}}} \right] = 10 \log_{10} \left[\frac{390.18}{140} \right] = 4.45 \text{ dB}$$

C/N in clear air

$$C/N = P_r \text{ [Received power at receiver station in clear air]} - N \text{ [Receiver Noise Power in clear air]}$$

$$= -102.69 + 131.58 = 28.89$$

C/N due to rain

$$N = \text{Receiver Noise Power (due to rain)}$$

$$= \text{Receiver Noise Power (Clear Air)} + \text{Increased due to rain } (\Delta N)$$

$$= -131.58 + 4.45$$

$$= -127.13$$

$$C/N = P_r \text{ [Received power at receiver station due to rain]} - N \text{ [Receiver Noise Power due to rain]}$$

$$= -259.08 - (-127.13) = -131.95$$

3.8 RAIN ATTENUATION STATISTICS FROM RAINFALL RATE FOR TERRESTRIAL LINK

The following techniques are used for estimating the long-term statistics of rain attenuation for terrestrial link:

Step 1: From the measured value of $R_{0.01}$ for 34 rain stations in Bangladesh as shown in Table 3.1 exceeded for 0.01% of an average year (with an integration time of 1 min) Measured Maximum $R_{0.01}$ is 148.4576 mm/hr at Teknaf and minimum $R_{0.01}$ is 109.4259 mm/hr at Ishurdi.

Step 2: The specific attenuation, γ_R , using the frequency-dependent coefficients given in Recommendation ITU-R P.838 as shown in Table 3.2 and the rainfall rate, $R_{0.01}$ determined from Step 1 is calculated as shown in Table – 3.3 and 3.4.

Step 3: For $R_{0.01} \leq 100$ mm/h:

$$d_0 = 35 e^{-0.015 R_{0.01}} \quad (1)$$

For $R_{0.01} > 100$ mm/h, use the value 100 mm/h in place of $R_{0.01}$.

Distance factor r ,

$$r = \frac{1}{1 + \frac{d}{d_0}} \quad (2)$$

The actual path length $d=20$ km;

For both $R_{0.01}$ maximum and minimum we have $R_{0.01} > 100$ mm/h. so, we use the value 100 mm/h in place of $R_{0.01}$ in the equation (1).

$$\begin{aligned} d_0 &= 35 e^{-0.015 R_{0.01}} \\ &= 35 e^{-0.015 \times 100} \\ &= 7.80955 \quad \text{km} \end{aligned}$$

$$\begin{aligned} d_{eff} &= d \times r \\ &= \frac{d}{1 + \frac{d}{d_0}} = \frac{dd_0}{d_0 + d} = \frac{20 \times 7.80955}{20 + 7.80955} = 5.61645 \end{aligned}$$

Step 4: The measured attenuation exceeded for 0.01% of an average year is obtained in Table 3.5:

$$A_{0.01} = \gamma_R d_{eff} = \gamma_R dr \quad \text{dB} \quad (3)$$

Table 3.17: Predicted Attenuation, $A_{0.01}$ for measured maximum and minimum $R_{0.01}$

Frequency	For measured maximum $R_{0.01}$ predicted attenuation, $A_{0.01}$ (dB)			For measured minimum $R_{0.01}$ predicted attenuation, $A_{0.01}$ (dB)		
	<i>Horizontal Polarization</i>	<i>Vertical Polarization</i>	<i>Circular Polarization</i>	<i>Horizontal Polarization</i>	<i>Vertical Polarization</i>	<i>Circular Polarization</i>
4 GHz	0.9503	0.8099	0.8677	0.6217	0.5409	0.5740
12 GHz	44.425	41.7735	43.0743	31.200	29.460	30.3143
20 GHz	89.5448	83.5133	86.4591	65.4412	61.3334	63.3424

Step 5: For radio links located at latitudes below 30° (North or South), the attenuation exceeded for other percentages of time p in the range 0.001% to 1% has been deduced from the following power law:

$$\frac{A_p}{A_{0.01}} = 0.07 p^{-(0.855 + 0.139 \log_{10} p)} \quad (4)$$

Using MATLAB program the values of A_p for other percentages, p of an average year, in the range 0.001% to 1%, have been determined and shown in Table – 3.10 and 3.11

Table 3.18: Predicted Attenuation, $A_{0.01}$ at different percentages of time for measured maximum $R_{0.01}$ at horizontal polarization

Percentage of Time, p(%)	System Reliability (%)	For measured maximum $R_{0.01}$ predicted $A_{0.01}$ (dB)		
		4 GHz	12 GHz	20 GHz
0.001	99.999	1.3708	64.0804	129.1631
0.003	99.997	1.2454	58.2188	117.3482
0.005	99.995	1.1334	52.9831	106.7949
0.007	99.993	1.0470	48.9447	98.6549
0.01	99.99	0.9483	44.3328	89.3590
0.03	99.97	0.6348	29.6772	59.8186
0.05	99.95	0.5013	23.4328	47.2320
0.07	99.93	0.4217	19.7137	39.7358
0.1	99.90	0.3459	16.1706	32.5941
0.3	99.70	0.1706	7.9760	16.0767
0.5	99.50	0.1169	5.4640	11.0134
0.7	99.30	0.0895	4.1863	8.4381
1.0	99.00	0.0665	3.109	6.2681

Table 3.19: Predicted Attenuation, $A_{0.01}$ at different percentages of time for measured minimum $R_{0.01}$ at horizontal polarization

Percentage of Time, p(%)	System Reliability (%)	For measured minimum $R_{0.01}$ predicted $A_{0.01}$ (dB)		
		4 GHz	12 GHz	20 GHz
0.001	99.999	0.8968	45.0042	94.3951
0.003	99.997	0.8147	40.8875	85.7605
0.005	99.995	0.7415	37.2104	78.0479
0.007	99.993	0.6850	34.3742	72.0991
0.01	99.99	0.6204	31.1353	65.3054
0.03	99.97	0.4153	20.8425	43.7167
0.05	99.95	0.3279	16.4570	34.5182
0.07	99.93	0.2759	13.8451	29.0397
0.1	99.90	0.2263	11.3567	23.8204
0.3	99.70	0.1116	5.6016	11.7492
0.5	99.50	0.0765	3.8374	8.0489
0.7	99.30	0.0586	2.9401	6.1667
1.0	99.00	0.0435	2.1840	4.5809

3.8.1 DETERMINATION OF RAIN ATTENUATION FROM ITU-R PREDICTED RAINFALL RATE

ITU-R has predicted rain fall rate $R_{0.01}$ for subtropical countries like Bangladesh as 95 mm/hr. Following the steps 1- 4 for this ITU-R predicted value of $R_{0.01}$, the results are obtained as below -

Table 3.20: Predicted attenuation, $A_{0.01}$ for ITU-R predicted value of $R_{0.01}$ for Terrestrial Link

Frequency	ITU-R Predicted $R_{0.01} = 95$ mm/h predicted attenuation, $A_{0.01}$ (dB)		
	<i>Horizontal Polarization</i>	<i>Vertical Polarization</i>	<i>Circular Polarization</i>
4 GHz	0.5444	0.4704	0.500
12 GHz	28.033	26.343	27.172
20 GHz	59.9210	55.8624	57.8430

Table 3.21: Predicted attenuation, $A_{0.01}$ at different percentages of time for ITU-R predicted value of $R_{0.01}$ at horizontal polarization

Percentage of Time, $p(\%)$	System Reliability (%)	ITU-R predicted value of $R_{0.01}$ predicted attenuation $A_{0.01}$ (dB)		
		4 GHz	12 GHz	20 GHz
0.001	99.999	0.7853	40.4359	86.4325
0.003	99.997	0.7134	36.7371	78.5263
0.005	99.995	0.6493	33.4333	71.4643
0.007	99.993	0.5998	30.8850	66.0173
0.01	99.99	0.5433	27.9748	59.7967
0.03	99.97	0.3637	18.7269	40.0290
0.05	99.95	0.2872	14.7865	31.6064
0.07	99.93	0.2416	12.4397	26.5901
0.1	99.90	0.1982	10.2039	21.8111
0.3	99.70	0.0977	5.0330	10.7581
0.5	99.50	0.0670	3.4479	7.3699
0.7	99.30	0.0513	2.6416	5.6465
1.0	99.00	0.0381	1.9623	4.1945

3.9 LINK BUDGET CALCULATION FOR TERRESTRIAL DOWNLINK AT THREE BANDS USING

EIRP (Effective Isotropically Radiated Power)

It is the combination of transmitter power and gain in terms of an equivalent isotropic source with power $P_t G_t$ watts, radiating uniformly in all directions.

$$\text{EIRP} = 10 \log_{10}(P_t G_t) = 65 \quad \text{dBW} \quad (1)$$

Here, P_t is the output power of a transmitting antenna in watts and G_t is the gain of the transmitting antenna.

Transponder Output Back off = B_0 :

The value of Transponder Output Back off B_0 is typically 2 dB.

G_r = Receiving Antenna Gain:

In antenna theory the gain and area of an antenna are related by,

$$G = \frac{4\pi A_e}{\lambda^2} \quad (2)$$

$$\text{So, } G_r = 10 \log_{10}\left(\frac{4\pi A_e}{\lambda^2}\right) \quad \text{dB} \quad (3)$$

Here, A_e is the effective aperture area in $\text{m}^2 = 1.1064 \text{m}^2$

And λ is the wavelength at the frequency of operation in meters.

Table 3.22: Receiving Antenna Gain

Frequency	4 GHz	12 GHz	20 GHz
Receiving Antenna Gain, G_r (dB)	33.93	43.47	47.91

Free Space Path Loss [FSL]:

It accounts for the way energy spreads out as an electromagnetic wave travels away from a transmitting source in three-dimensional space.

$$[FSL] = 10 \log_{10} \left[\left(\frac{4\pi R}{\lambda} \right)^2 \right] = 20 \log_{10} \left(\frac{4\pi R}{\lambda} \right) \quad \text{dB} \quad (4)$$

Table 3.23: Free Space Path Loss

Frequency	4 GHz	12 GHz	20 GHz
Free Space Path Loss (dB)	-199.7	-206.6	-209.7

L_{ant} =Edge of beam loss for Satellite Antenna:

Edge of beam loss for Satellite Antenna is typically 3dB.

[AA]=Clear air atmospheric loss:

Table 3.24: Clear air atmospheric loss

Frequency	4 GHz	12 GHz	20 GHz
Clear air atmospheric loss (dB)	0.075	0.11	0.4

Other losses (L_m)

Typically other losses are considered together as 0.5 dB.

Received power at receiver station P_r (Clear Air):

$$P_r = EIRP + G_r - FSL - L_{ant} - AA - L_m - B_0 \quad \text{dBW} \quad (5)$$

For 4GHz

$$P_r = 65 + 33.93 - 199.7 - 3 - 0.075 - 0.5 - 2 = -106.345 \quad \text{dBW} \quad (6)$$

For 12GHz

$$P_r = 65 + 43.47 - 206.6 - 3 - 0.11 - 0.5 - 2 = -103.74 \quad \text{dBW} \quad (7)$$

For 20GHz

$$P_r = 65 + 47.91 - 209.7 - 3 - 0.4 - 0.5 - 2 = -102.69 \quad \text{dBW} \quad (8)$$

P_r (due to rain)

$$P_r = P_r(\text{due to rain}) - \text{Rain Attenuation, } A_{rain}$$

Table 3.25: Received power due to rain

Boltzmann's constant, k in dBW/K/Hz:

The value in dBW/K/Hz is $=10\log_{10}(1.3806 \times 10^{-23}) = -228.6$

Frequency	For ITU-R predicted $R_{0.01}$			For maximum $R_{0.01}$ (Worst Case)		
	4 GHz	12 GHz	20 GHz	4 GHz	12 GHz	20 GHz
P_r = Received power at receiver station (Clear Air)	-106.345	-103.74	-102.69	-106.345	-119.74	-102.69
Rain Attenuation, A_{rain}	0.54	28.03	59.92	0.95	44.42	89.54
P_r (due to rain)	-106.89	-131.77	-162.61	-107.29	-148.16	-192.23

System noise temperature, T_s :

It is assumed as 140K and in dBK it is $=10\log_{10}(140) = 21.46$

Noise bandwidth, B_n :

It is assumed as 36MHz and in dBHz it is $=10\log_{10}(36 \times 10^6) = 75.56$

Receiver Noise Power, N in clear air:

The receiver noise power, N in clear air in dBW is calculated as,

$$N = k + T_s + B_n = -228.6 + 21.46 + 75.56 = -131.58 \quad \text{dBW} \quad (9)$$

Attenuation:

The total path attenuation, A is the sum of the clear sky path attenuation due to atmospheric gaseous absorption, A_{ca} and attenuation due to rain, A_{rain} .

$$A = A_{ca} + A_{rain} \quad \text{dB} \quad (10)$$

$$T_{sky} = T_p(1 - G); \quad (11)$$

Here, G is the linear gain and less than unity.

$$G = 10^{-A/10}$$

And T_p is the physical temperature of the device = 273 K.

For ITU-R Predicted $R_{0.01}$

For 4GHz

$$A=0.075+0.9015=0.9765 \text{ dB};$$

$$G = 10^{-A/10},$$

$$\text{So, } G=0.7986;$$

$$T_{\text{skyrain}} = 273(1 - 0.7986) = 54.972 \text{ K}$$

$$T_{\text{ca}} = 0.95 \times 273(1 - 10^{-0.075/10}) = 4.44 \text{ K}$$

$$T_{\text{srain}} = T_{\text{LNA}} + T_{\text{skyrain}} = 140 - 4.44 + 54.972 = 190.532 \text{ K}$$

$$\Delta N_{\text{rain}} = 10 \log_{10} \left[\frac{T_{\text{srain}}}{T_{\text{sca}}} \right] = 10 \log_{10} \left[\frac{190.532}{140} \right] = 1.34 \text{ dB}$$

C/N in clear air

$$\begin{aligned} \text{C/N} &= P_r \text{ [Received power at receiver station in clear air]} - N \text{ [Receiver Noise Power in} \\ &\text{clear air]} \end{aligned}$$

$$= -106.345 + 131.58 = 25.235$$

C/N due to rain

$$N = \text{Receiver Noise Power (due to rain)}$$

$$= \text{Receiver Noise Power (Clear Air)} + \text{Increased due to rain } (\Delta N)$$

$$= -131.58 + 1.34$$

$$= -130.2$$

$$\begin{aligned} \text{C/N} &= P_r \text{ [Received power at receiver station due to rain]} - N \text{ [Receiver Noise Power due to} \\ &\text{rain]} \end{aligned}$$

$$= -106.89 - (-130.2)$$

$$= 23.31$$

For 12GHz

$$A = 0.11 + 46.4175 = 46.5275 \text{ dB};$$

$$G = 10^{-A/10}$$

$$\text{So, } G = 0.00002245;$$

$$T_{\text{skyrain}} = 273(1 - 0.00002245) = 272.994 \text{ K}$$

$$T_{\text{ca}} = 0.95 \times 273(1 - 10^{-0.11/10}) = 6.486 \text{ K}$$

$$T_{\text{srain}} = T_{\text{LNA}} + T_{\text{skyrain}} = 140 - 6.486 + 272.994 = 406.508 \text{ K}$$

$$\Delta N_{\text{rain}} = 10 \log_{10} \left[\frac{T_{\text{srain}}}{T_{\text{sca}}} \right] = 10 \log_{10} \left[\frac{406.508}{140} \right] = 4.63 \text{ dB}$$

C/N in clear air

$$\begin{aligned} \text{C/N} &= P_r [\text{Received power at receiver station in clear air}] - N [\text{Receiver Noise Power in clear air}] \\ &= -103.74 + 131.58 = 27.84 \end{aligned}$$

C/N due to rain

$$\begin{aligned} N &= \text{Receiver Noise Power (due to rain)} \\ &= \text{Receiver Noise Power (Clear Air)} + \text{Increased due to rain } (\Delta N) \\ &= -131.58 + 4.63 \\ &= -126.95 \end{aligned}$$

$$\begin{aligned} \text{C/N} &= P_r [\text{Received power at receiver station due to rain}] - N [\text{Receiver Noise Power due to rain}] \\ &= -131.77 - (-126.95) \\ &= -4.82 \end{aligned}$$

For 20GHz

$$A = 0.4 + 99.2172 = 99.6172 \text{ dB};$$

$$G = 10^{-A/10} = 1.092 \times 10^{-10}$$

$$T_{\text{skyrain}} = 273(1 - 1.092 \times 10^{-10}) = 273 \text{ K}$$

$$T_{\text{ca}} = 0.95 \times 273(1 - 10^{-0.4/10}) = 22.82 \text{ K}$$

$$T_{\text{srain}} = T_{\text{LNA}} + T_{\text{skyrain}} = 140 - 22.82 + 273 = 390.18 \text{ K}$$

$$\Delta N_{\text{rain}} = 10 \log_{10} \left[\frac{T_{\text{srain}}}{T_{\text{sca}}} \right] = 10 \log_{10} \left[\frac{390.18}{140} \right] = 4.45 \text{ dB}$$

C/N in clear air

$$\begin{aligned} \text{C/N} &= P_r \text{ [Received power at receiver station in clear air]} - N \text{ [Receiver Noise Power in} \\ &\quad \text{clear air]} \\ &= -102.69 + 131.58 = 28.89 \end{aligned}$$

C/N due to rain

$$\begin{aligned} N &= \text{Receiver Noise Power (due to rain)} \\ &= \text{Receiver Noise Power (Clear Air)} + \text{Increased due to rain } (\Delta N) \\ &= -131.58 + 4.45 \\ &= -127.13 \end{aligned}$$

$$\begin{aligned} \text{C/N} &= P_r \text{ [Received power at receiver station due to rain]} - N \text{ [Receiver Noise Power due to} \\ &\quad \text{rain]} \\ &= -162.61 - (-127.13) \\ &= -35.48 \end{aligned}$$

For measured maximum $R_{0.01}$ (Worst Case)

For 4GHz

$$A=0.075+1.659=1.734 \text{ dB};$$

$$G = 10^{-A/10},$$

$$\text{So, } G = 0.6708;$$

$$T_{\text{skyrain}} = 273(1 - 0.6708) = 89.87 \text{ K}$$

$$T_{\text{ca}} = 0.95 \times 273(1 - 10^{-0.075/10}) = 4.44 \text{ K}$$

$$T_{\text{srain}} = T_{\text{LNA}} + T_{\text{skyrain}} = 140 - 4.44 + 89.87 = 225.43 \text{ K}$$

$$\Delta N_{\text{rain}} = 10 \log_{10} \left[\frac{T_{\text{srain}}}{T_{\text{sca}}} \right] = 10 \log_{10} \left[\frac{225.43}{140} \right] = 2.068 \text{ dB}$$

C/N in clear air

$$\text{C/N} = P_r \text{ [Received power at receiver station in clear air]} - N \text{ [Receiver Noise Power in clear air]}$$

$$= -106.345 + 131.58 = 25.235$$

C/N due to rain

$$N = \text{Receiver Noise Power (due to rain)}$$

$$= \text{Receiver Noise Power (Clear Air)} + \text{Increased due to rain } (\Delta N)$$

$$= -131.58 + 2.068$$

$$= -129.512$$

$$\text{C/N} = P_r \text{ [Received power at receiver station due to rain]} - N \text{ [Receiver Noise Power due to rain]}$$

$$= -107.29 - (-129.512)$$

$$= 22.22$$

For 12GHz

$$A=0.11+77.591=77.701 \text{ dB}$$

$$G = 10^{-A/10} = 1.697 \times 10^{-8}$$

$$T_{\text{skyrain}} = 273(1 - 1.697 \times 10^{-8}) = 272.999 \text{ K}$$

$$T_{\text{ca}} = 0.95 \times 273(1 - 10^{-0.11/10}) = 6.486 \text{ K}$$

$$T_{\text{srain}} = T_{\text{LNA}} + T_{\text{skyrain}} = 140 - 6.486 + 272.999 = 406.513 \text{ K}$$

$$\Delta N_{\text{rain}} = 10 \log_{10} \left[\frac{T_{\text{srain}}}{T_{\text{sca}}} \right] = 10 \log_{10} \left[\frac{406.513}{140} \right] = 4.629 \quad \text{dB}$$

C/N in clear air

$$\begin{aligned} \text{C/N} &= P_r \text{ [Received power at receiver station in clear air]} - N \text{ [Receiver Noise Power in} \\ &\quad \text{clear air]} \\ &= -103.74 + 131.58 = 27.84 \end{aligned}$$

C/N due to rain

$$\begin{aligned} N &= \text{Receiver Noise Power (due to rain)} \\ &= \text{Receiver Noise Power (Clear Air)} + \text{Increased due to rain } (\Delta N) \\ &= -131.58 + 4.629 \\ &= -126.951 \end{aligned}$$

$$\begin{aligned} \text{C/N} &= P_r \text{ [Received power at receiver station due to rain]} - N \text{ [Receiver Noise Power due to} \\ &\quad \text{rain]} \\ &= -148.165 - (-126.951) \\ &= -21.21 \end{aligned}$$

For 20GHz

$$A = 0.4 + 156.3958 = 156.7958 \text{ dB}$$

$$G = 10^{-A/10} = 2.091 \times 10^{-16}$$

$$T_{\text{skyrain}} = 273(1 - 2.091 \times 10^{-16}) = 273 \text{ K}$$

$$T_{\text{ca}} = 0.95 \times 273(1 - 10^{-0.4/10}) = 22.82 \text{ K}$$

$$T_{\text{srain}} = T_{\text{LNA}} + T_{\text{skyrain}} = 140 - 22.82 + 273 = 390.18 \text{ K}$$

$$\Delta N_{\text{rain}} = 10 \log_{10} \left[\frac{T_{\text{srain}}}{T_{\text{sca}}} \right] = 10 \log_{10} \left[\frac{390.18}{140} \right] = 4.45 \text{ dB}$$

C/N in clear air

$$\begin{aligned} \text{C/N} &= P_r \text{ [Received power at receiver station in clear air]} - N \text{ [Receiver Noise Power in} \\ &\quad \text{clear air]} \\ &= -102.69 + 131.58 = 28.89 \end{aligned}$$

C/N due to rain

$$\begin{aligned} N &= \text{Receiver Noise Power (due to rain)} \\ &= \text{Receiver Noise Power (Clear Air)} + \text{Increased due to rain } (\Delta N) \\ &= -131.58 + 4.45 \\ &= -127.13 \end{aligned}$$

$$\begin{aligned} \text{C/N} &= P_r \text{ [Received power at receiver station due to rain]} - N \text{ [Receiver Noise Power due to} \\ &\quad \text{rain]} \\ &= -192.23 - (-127.13) \\ &= -65.1 \end{aligned}$$

CHAPTER 4
COMPARISON OF PREDICTED
RAIN ATTENUATION AND ITS
EFFECTS ON LINK'S
PERFORMANCE

COMPARISON OF PREDICTED RAIN ATTENUATION AND ITS EFFECTS ON LINK'S PERFORMANCE

4.1 INTRODUCTION

The simulation results of measured Attenuation and ITU-R predicted attenuation of Bangladesh are presented and described in this chapter. The various comparison curves between measured attenuation and ITU-R predicted attenuation at different percentages of time are shown for C, Ku and Ka band. The results of investigating the rain fades for both terrestrial and earth-satellite microwave links operating at the C, Ku and Ka bands are shown graphically. The outcome of evaluating the performance of the links in terms of Carrier-to-Noise ratio for various fade margins and reliability objects as well as Link Budget Analysis for both Earth-to-satellite and terrestrial downlink are also presented in this chapter.

4.2 RESULTS AND DISCUSSION

Rain is a dominant source of attenuation at higher frequencies in tropical and subtropical regions. Therefore accurate estimation of rain fade is very essential in order to design reliable microwave links in such regions like Bangladesh. In this thesis, rain fades have been predicted using rain intensity data derived from 13 years long term measured annual rainfall data. From all these analysis, it has been observed that rain fade is not significant at C-band but is very critical at Ku and Ka-bands. The performance of Earth-to-satellite and terrestrial links has also been investigated due to rain fades in all three frequency bands. In all three bands, rain attenuation are estimated based on ITU-R recommended rain rate as well as converted rain rate from long term measured data. It is obvious that ITU-R predicted rain attenuation are lower than those predicted using measured rain rate in both terrestrial and earth-satellite microwave links. Hence to design reliable earth-to-satellite and terrestrial microwave links it is necessary to modify the ITU-R recommended rainfall rate in Bangladesh.

4.3 COMPARISON STUDY FOR EARTH TO SATELLITE LINK

4.3.1 COMPARISON BETWEEN PREDICTED ATTENUATION AT MEASURED MAXIMUM $R_{0.01}$ AND ITU-R PREDICTED ATTENUATION FOR C/KU/KA-BAND AT HORIZONTAL POLARIZATION

Table 4.1: Comparison among predicted attenuations for measured maximum $R_{0.01}$, minimum $R_{0.01}$ and ITU-R predicted $R_{0.01}$ at horizontal polarization

Frequency	For Measured Max. $R_{0.01}$ ($R_{0.01} = 148.4576$ mm/h) Attenuation, $A_{0.01}$ (dB)	For Measured Min. $R_{0.01}$ ($R_{0.01} = 109.4259$ mm/h) Attenuation, $A_{0.01}$ (dB)	For ITU-R Predicted $R_{0.01}$ ($R_{0.01} = 95$ mm/h) Attenuation, $A_{0.01}$ (dB)
	Horizontal polarization	Horizontal polarization	Horizontal polarization
4 GHz	1.6597	1.0859	0.9015
12 GHz	77.591	54.4927	46.4175
20 GHz	156.3958	114.2973	99.2172

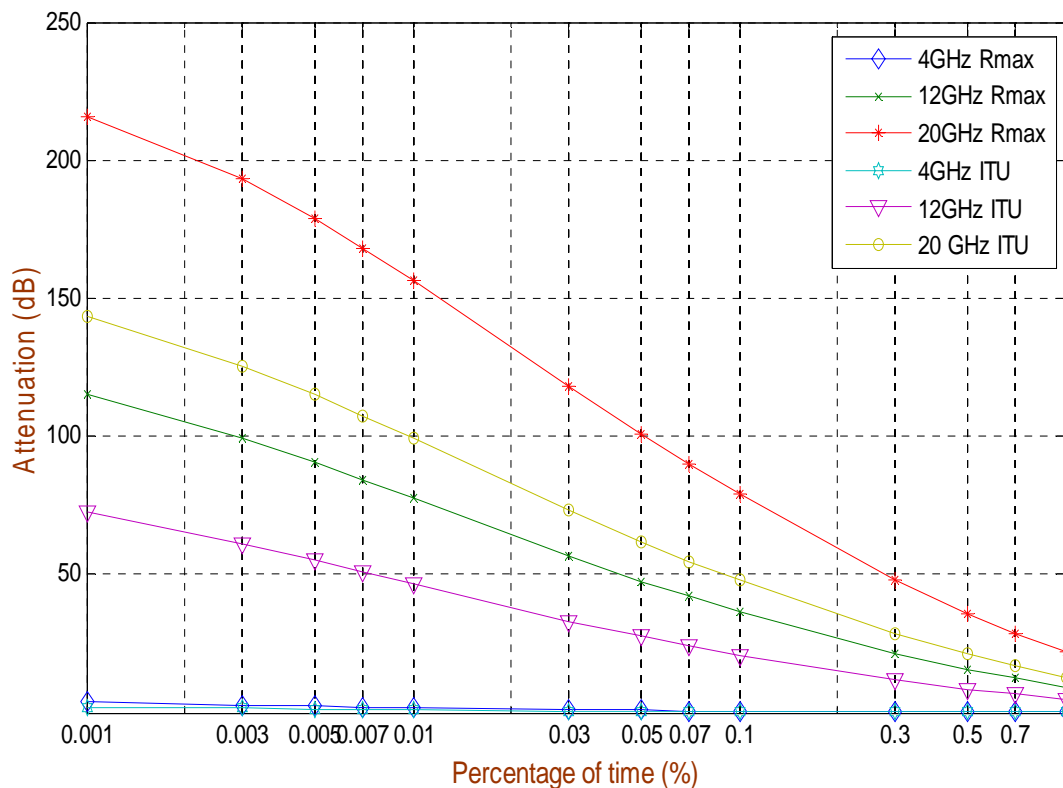


Fig. 4.1: Comparison Curves between Predicted Attenuation at Measured Maximum $R_{0.01}$ and ITU-R Predicted Attenuation for C/Ku/Ka-Band at Horizontal Polarization.

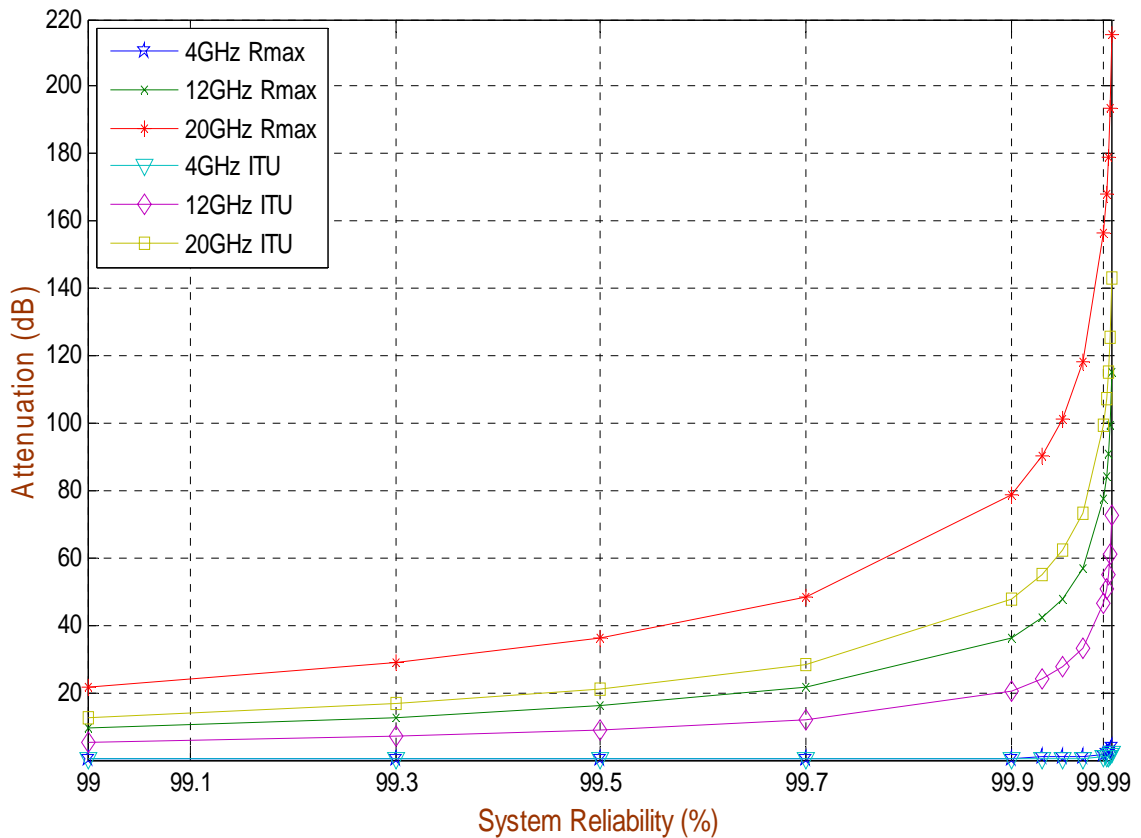


Fig. 4.2: Attenuation vs. System Reliability Curves at Horizontal Polarization for Measured Maximum $R_{0.01}$

Fig. 4.1 shows variations between attenuation at measured maximum $R_{0.01}$ and ITU-R predicted attenuation for three frequency bands at different percentages of time at Horizontal polarization. From the curve for 0.01% of the time, it is observed that at C-band the difference between measured and ITU-R predicted value is 0.75 dB, at Ku-band the difference is 31 dB and at Ka-band it is 57 dB. It is obvious that ITU-R predicted rain attenuation are lower than those predicted using measured rain rate in all three frequency bands. Fig.4.2 shows attenuation vs. system reliability curves of predicted attenuation for measured maximum and ITU-R predicted $R_{0.01}$ for three frequency bands. The difference between C and Ku band is 30.25 dB and C and Ka band is about 56.25 dB for the design of earth-satellite link with 99.99% reliability. Hence to design reliable earth to satellite microwave link is very critical at Ku and Ka bands.

4.3.2 COMPARISON BETWEEN PREDICTED ATTENUATION AT MEASURED MINIMUM $R_{0.01}$ AND ITU-R PREDICTED ATTENUATION FOR C/KU/KA-BAND AT HORIZONTAL POLARIZATION

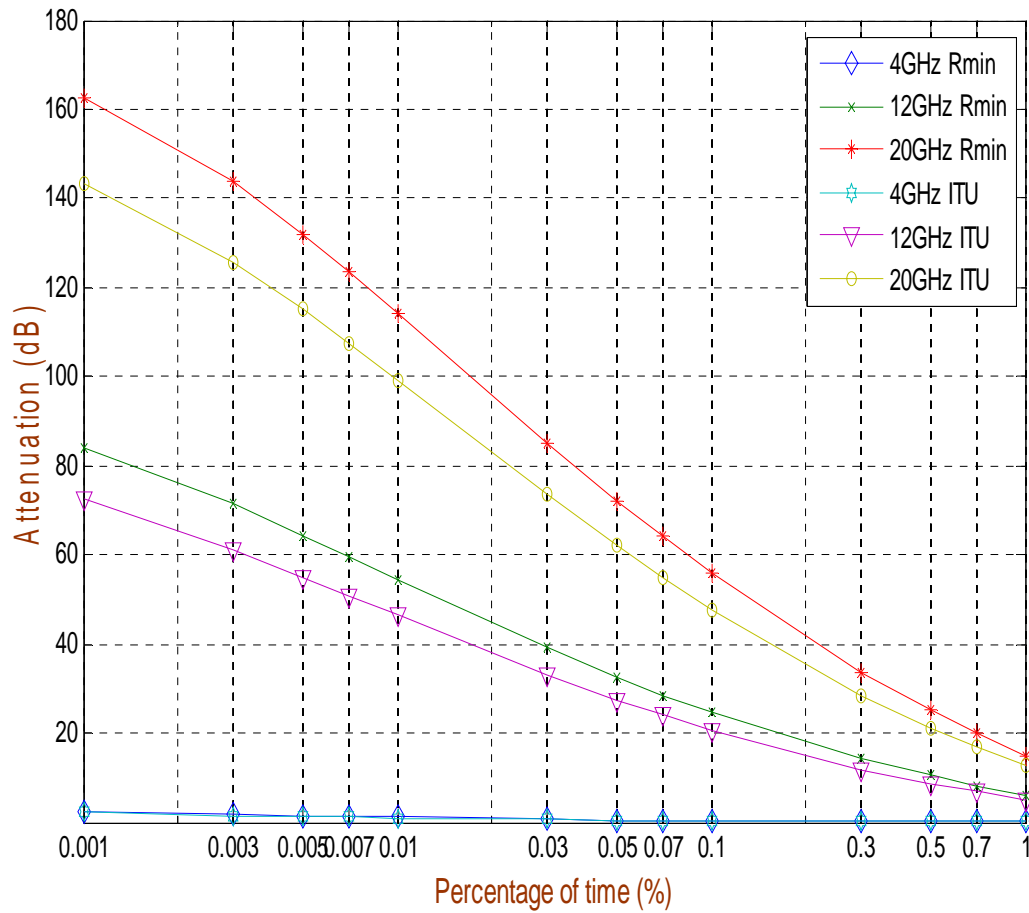


Fig. 4.3: Comparison Curves between Predicted Attenuation at Measured Minimum $R_{0.01}$ and ITU-R Predicted Attenuation for C/Ku/Ka-Band at Horizontal Polarization.

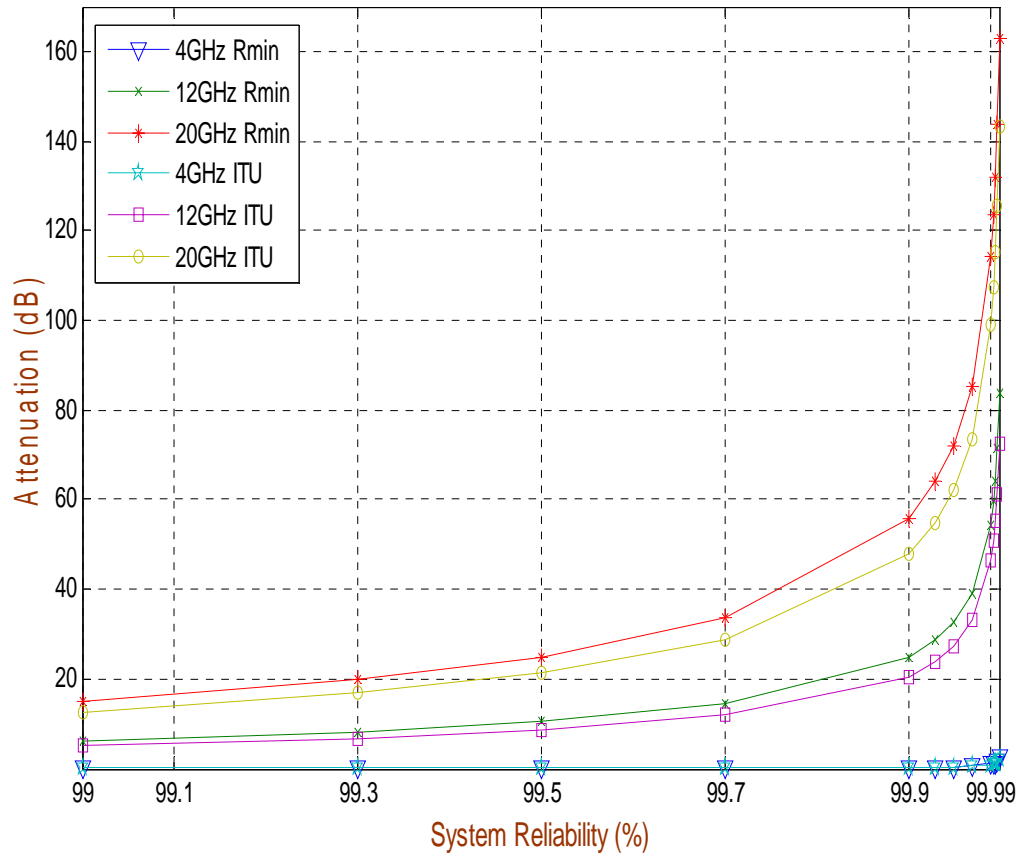


Fig.4.4: Attenuation vs. System Reliability Curves at Horizontal Polarization for Measured Minimum $R_{0.01}$

In Fig. 4.3 variations between attenuation at measured minimum $R_{0.01}$ and ITU-R predicted attenuation for three frequency bands at different percentages of time at Horizontal polarization are shown. From the curve, it is observed that at C-band the difference between measured and ITU-R predicted value is 0.18 dB, at Ku-band the difference is 8.5 dB and at Ka-band it is 15 dB for 0.01% of the time. So, it is obvious that ITU-R underestimated the rain attenuation in all three frequency bands. Fig.4.4 shows attenuation vs. system reliability curves of predicted attenuation for measured minimum and ITU-R predicted $R_{0.01}$ for three frequency bands. The difference between C and Ku band is 8.32 dB and C and Ka band is about 14.8 dB for the design of earth-satellite link with 99.99% reliability.

4.3.3 COMPARISON BETWEEN PREDICTED ATTENUATION AT MEASURED MAXIMUM $R_{0.01}$ AND ITU-R PREDICTED ATTENUATION FOR C/KU/KA-BAND AT VERTICAL POLARIZATION

Table 4.2: Comparison among predicted attenuations for measured maximum $R_{0.01}$, minimum $R_{0.01}$ and ITU-R predicted $R_{0.01}$ at vertical polarization

Frequency	For Measured Max. $R_{0.01}$ ($R_{0.01} = 148.4576$ mm/h) Attenuation, $A_{0.01}$ (dB)	For Measured Min. $R_{0.01}$ ($R_{0.01} = 109.4259$ mm/h) Attenuation, $A_{0.01}$ (dB)	ITU-R Predicted $R_{0.01}$ ($R_{0.01} = 95$ mm/h) Attenuation, $A_{0.01}$ (dB)
	Vertical polarization	Vertical polarization	Vertical polarization
4 GHz	1.4145	0.9446	0.7788
12 GHz	72.960	51.4537	43.618
20 GHz	145.8613	107.1226	92.4976

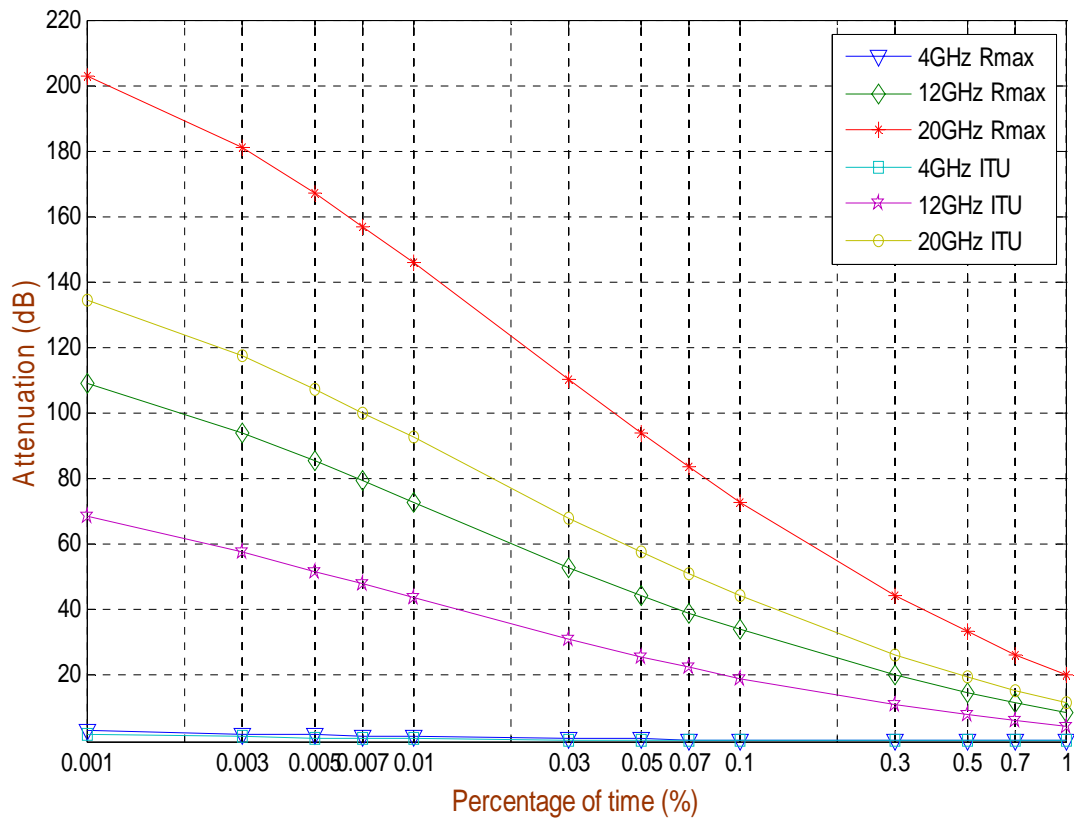


Fig. 4.5: Comparison Curves between Predicted Attenuation at Measured Maximum $R_{0.01}$ and ITU-R Predicted Attenuation for C/Ku/Ka-Band at Vertical Polarization.

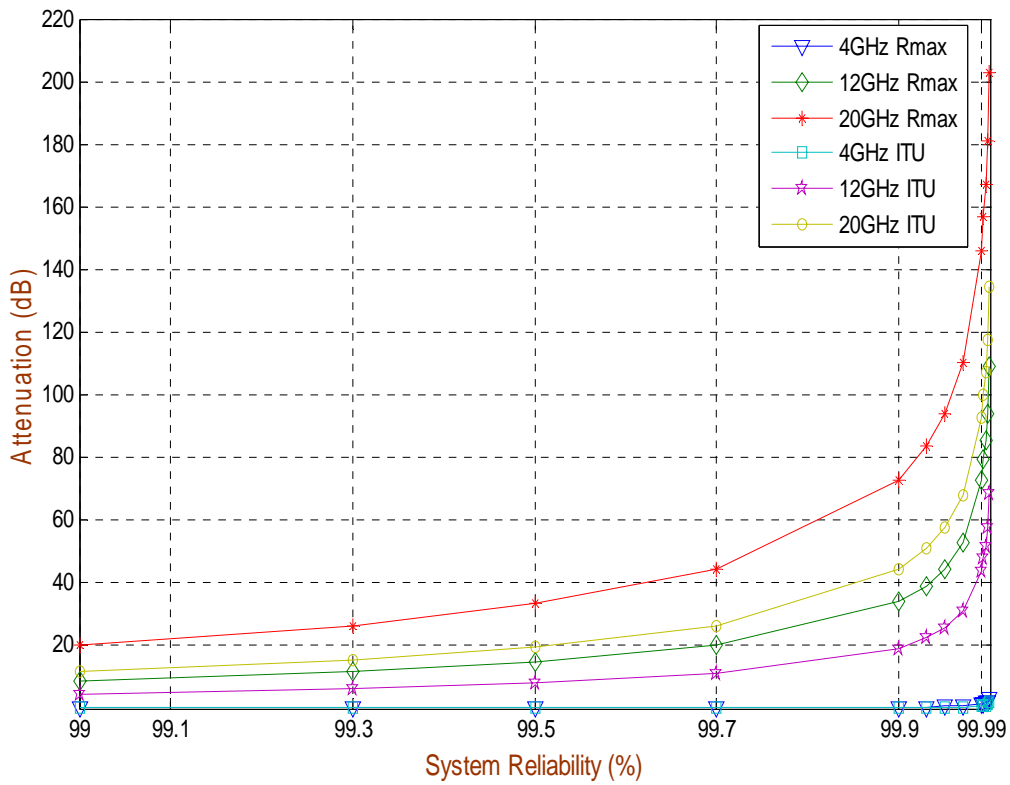


Fig.4.6: Attenuation vs. System Reliability Curves at Vertical Polarization for Measured Maximum $R_{0.01}$

In Fig. 4.5 variations between attenuation at measured maximum $R_{0.01}$ and ITU-R predicted attenuation for three frequency bands at different percentages of time at Vertical polarization are shown. From the curve for 0.01% of the time, it is observed that at C-band the attenuation for measured maximum $R_{0.01}$ is 0.6 dB higher than ITU-R predicted value, at Ku-band it is 29.35 dB and at Ka-band it is 53.3 dB higher respectively. Fig.4.6 shows attenuation vs. system reliability curves of predicted attenuation for measured maximum and ITU-R predicted $R_{0.01}$ for three frequency bands. The difference between C and Ku band is 28.7 dB and C and Ka band is about 52.7 dB for the design of earth-satellite link with 99.99% reliability.

4.3.4 COMPARISON BETWEEN PREDICTED ATTENUATION AT MEASURED MINIMUM $R_{0.01}$ AND ITU-R PREDICTED ATTENUATION FOR C/KU/KA-BAND AT VERTICAL POLARIZATION

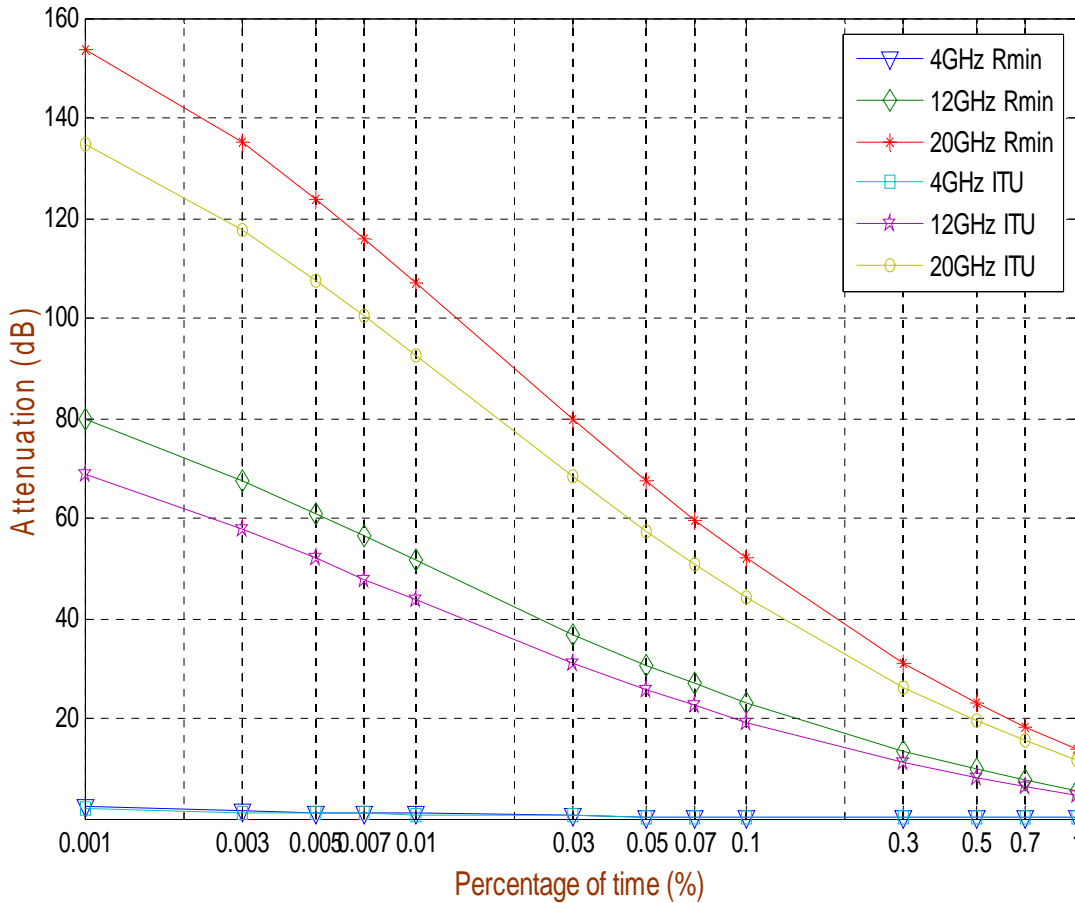


Fig. 4.7: Comparison Curves between Predicted Attenuation at Measured Minimum $R_{0.01}$ and ITU-R Predicted Attenuation for C/Ku/Ka-Band at Vertical Polarization.

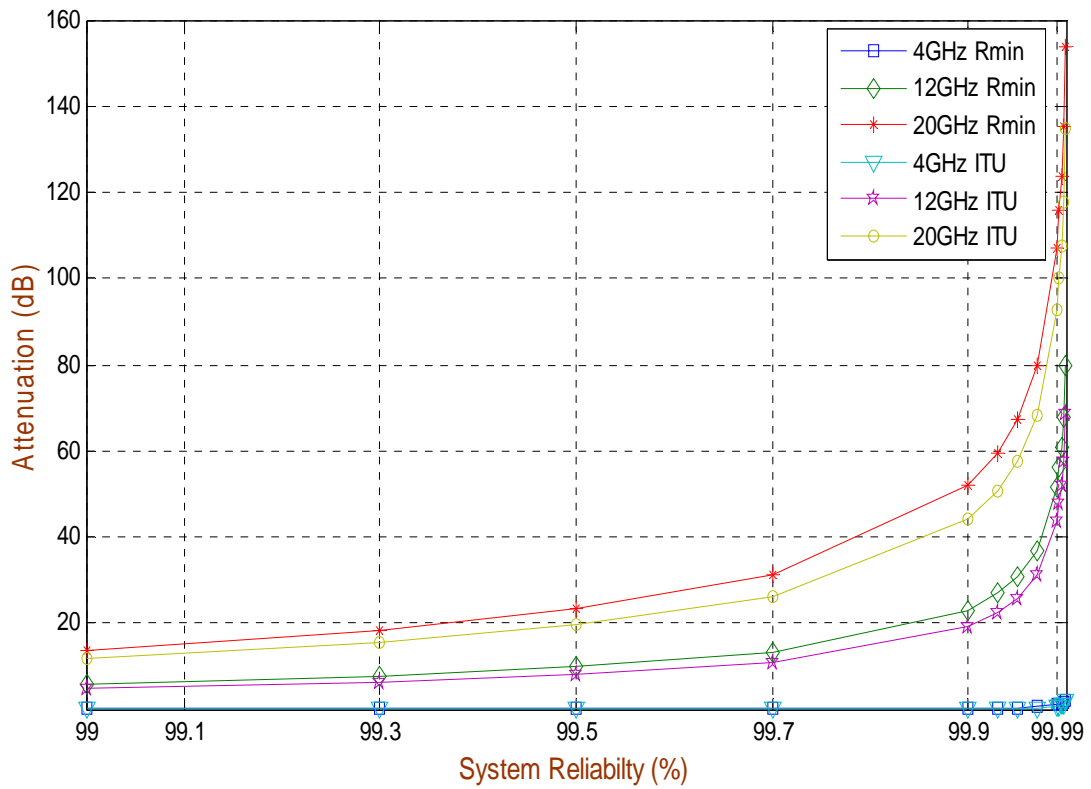


Fig. 4.8: Attenuation vs. System Reliability Curves at Vertical Polarization for Measured Minimum $R_{0.01}$

Fig. 4.5 shows variations between attenuation at measured minimum $R_{0.01}$ and ITU-R predicted attenuation for three frequency bands at different percentages of time at Vertical polarization. From the curve for 0.01% of the time, it is observed that at C-band the difference between measured and ITU-R predicted value is 0.16 dB, at Ku-band the difference is 7.84 dB and at Ka-band it is 14.6 dB. Fig.4.8 shows attenuation vs. system reliability curves of predicted attenuation for measured minimum and ITU-R predicted $R_{0.01}$ for three frequency bands. For the design of earth-satellite link with 99.99% reliability the difference between C and Ku band is 7.6 dB and C and Ka band is about 14.4 dB.

4.3.5 COMPARISON BETWEEN PREDICTED ATTENUATION AT MEASURED MAXIMUM $R_{0.01}$ AND ITU-R PREDICTED ATTENUATION FOR C/KU/KA-BAND AT CIRCULAR POLARIZATION

Table 4.3: Comparison among predicted attenuations for measured maximum $R_{0.01}$, minimum $R_{0.01}$ and ITU-R predicted $R_{0.01}$ at circular polarization

Frequency	For Measured Max. $R_{0.01}$ ($R_{0.01} = 148.4576$ mm/h) Attenuation, $A_{0.01}$ (dB)	For Measured Min. $R_{0.01}$ ($R_{0.01} = 109.4259$ mm/h) Attenuation, $A_{0.01}$ (dB)	For ITU-R Predicted $R_{0.01}$ ($R_{0.01} = 95$ mm/h) Attenuation, $A_{0.01}$ (dB)
	Circular polarization	Circular polarization	Circular polarization
4 GHz	1.5155	1.0025	0.8279
12 GHz	75.232	52.945	44.99
20 GHz	151.006	110.6315	95.777

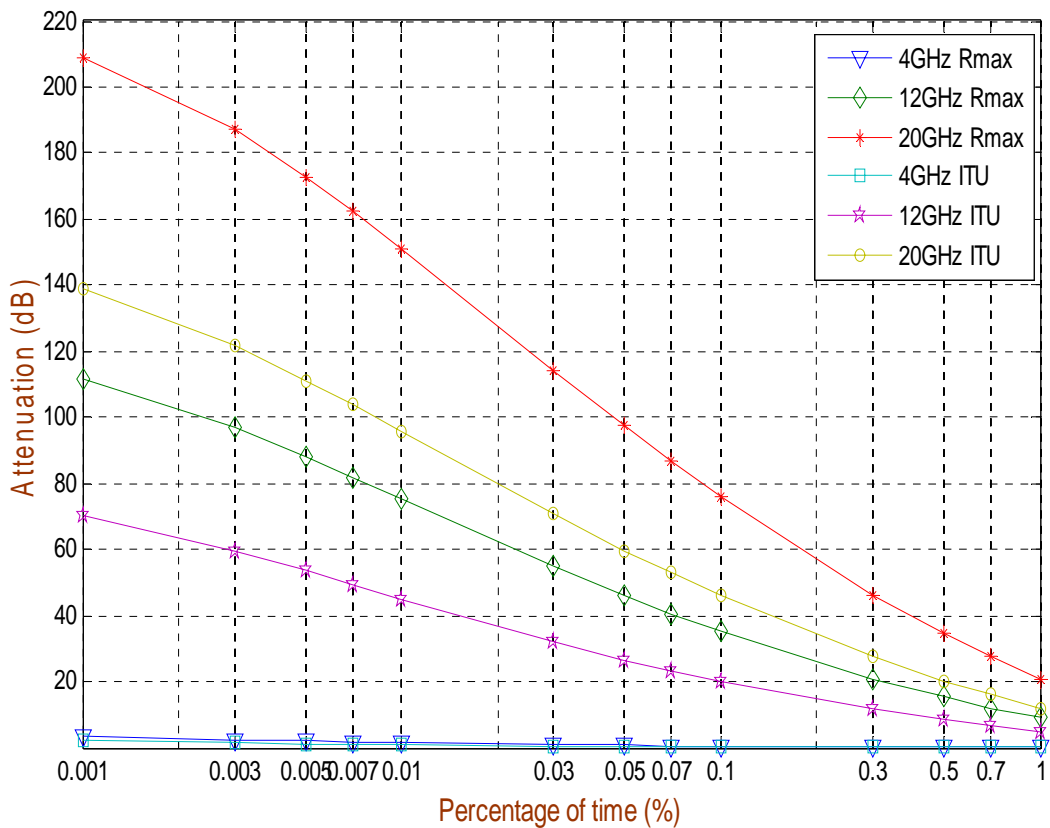


Fig. 4.9: Comparison Curves between Predicted Attenuation at Measured Maximum $R_{0.01}$ and ITU-R Predicted Attenuation for C/Ku/Ka-Band at Circular Polarization.

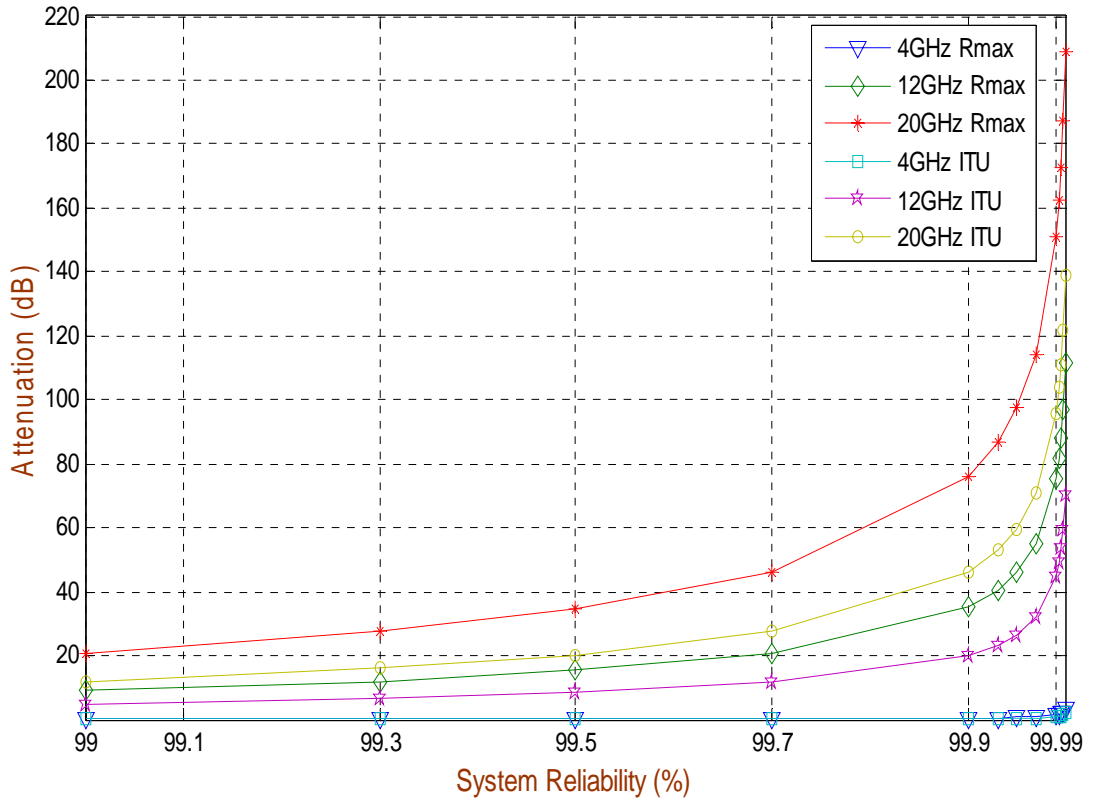


Fig.4.10: Attenuation vs. System Reliability Curves at Circular Polarization for Measured Maximum $R_{0.01}$

In Fig. 4.9 variations between attenuation at measured maximum $R_{0.01}$ and ITU-R predicted attenuation for three frequency bands at different percentages of time at Circular polarization are shown. It is observed from the curve that at C-band the difference between measured and ITU-R predicted value is 0.68 dB, at Ku-band the difference is 30.24 dB and at Ka-band it is 55.22 dB for 0.01% of the time. Fig.4.10 shows attenuation vs. system reliability curves of predicted attenuation for measured maximum and ITU-R predicted $R_{0.01}$ for three frequency bands. The difference between C and Ku band is 29.5 dB and C and Ka band is about 54.5 dB for the design of earth-satellite link with 99.99% reliability.

4.3.6 COMPARISON BETWEEN PREDICTED ATTENUATION AT MEASURED MINIMUM $R_{0.01}$ AND ITU-R PREDICTED ATTENUATION FOR C/KU/KA-BAND AT CIRCULAR POLARIZATION

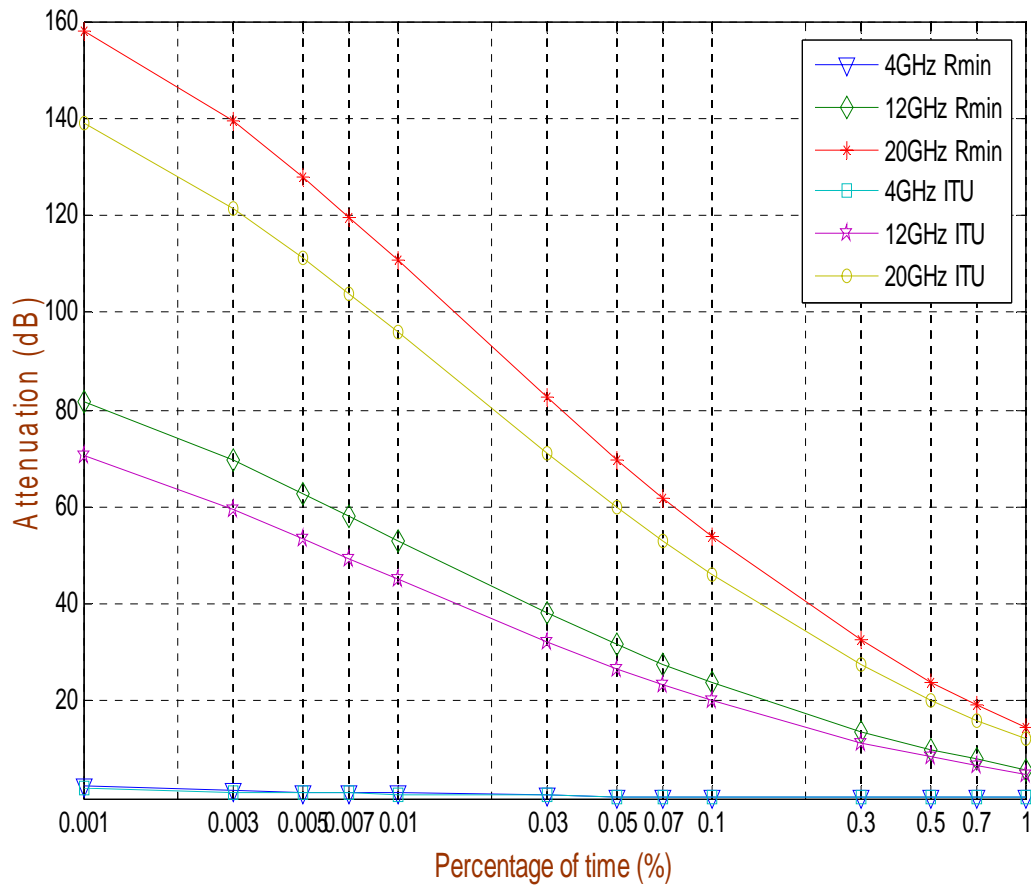


Fig. 4.11: Comparison Curves between Predicted Attenuation at Measured Minimum $R_{0.01}$ and ITU-R Predicted Attenuation for C/Ku/Ka-Band at Circular Polarization.

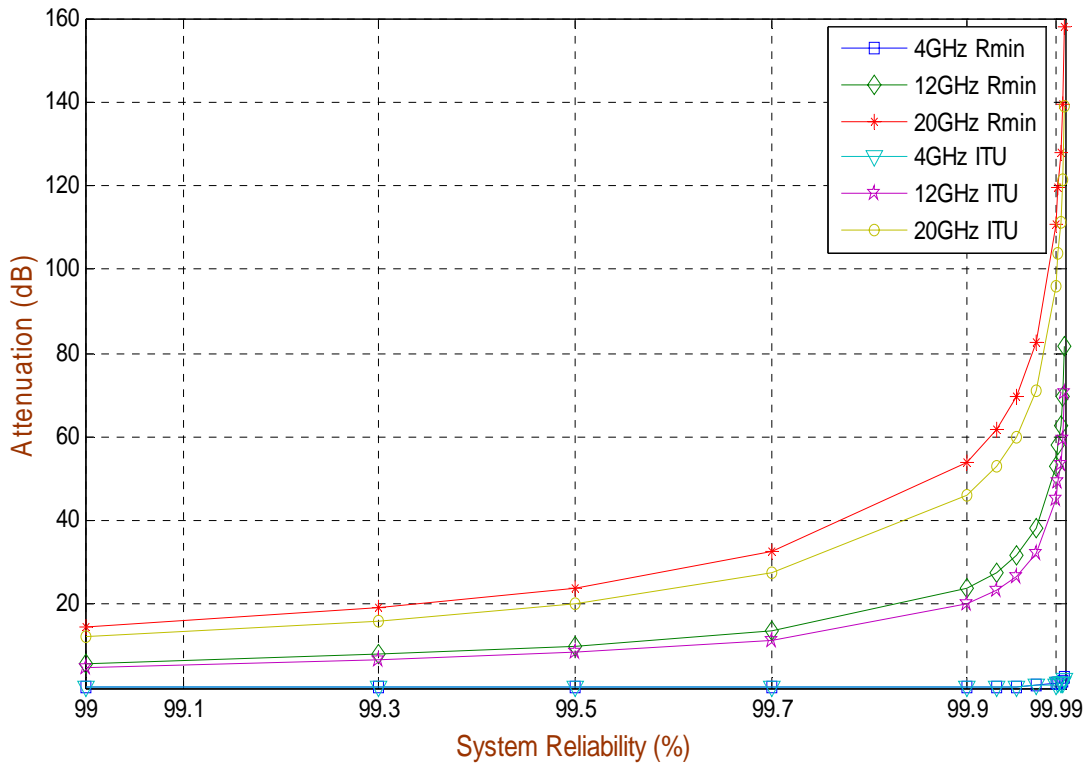


Fig.4.12: Attenuation vs. System Reliability Curves at Circular Polarization for Measured Minimum $R_{0.01}$

Fig. 4.11 shows variations between attenuation at measured minimum $R_{0.01}$ and ITU-R predicted attenuation for three frequency bands at different percentages of time at Circular polarization. For 0.01% of the time, it is observed that at C-band the attenuation for measured minimum $R_{0.01}$ is 0.17 dB higher than ITU-R predicted value, at Ku-band it is 7.9 dB and at Ka-band it is 14.86 dB higher respectively. Fig.4.12 shows attenuation vs. system reliability curves of predicted attenuation for measured minimum and ITU-R predicted $R_{0.01}$ for three frequency bands. For the design of earth-satellite link with 99.99% reliability the difference between C and Ku band is 7.7 dB and C and Ka band is about 14.6 dB. Hence to design reliable microwave link is very critical at Ku and Ka-bands and needs careful and accurate estimation of rain attenuation in Bangladesh. It is also observed that horizontally polarized wave suffers the most and the vertically polarized wave is the least. The circularly polarized wave is middle.

4.4 DEVIATION CALCULATION FOR EARTH TO SATELLITE LINK

Table 4.4: Deviation between predicted attenuation for measured maximum $R_{0.01}$ and ITU-R predicted attenuation at horizontal polarization

System Reliability (%)	$A_{0.01}$ for measured maximum $R_{0.01}$ (dB)			$A_{0.01}$ for ITU-R predicted $R_{0.01}$ (dB)			Deviation (dB)		
	4 GHz	12 GHz	20 GHz	4 GHz	12 GHz	20 GHz	4 GHz	12 GHz	20 GHz
99.999	3.66	115.03	215.61	2.12	72.57	143.39	1.544	42.45	72.21
99.997	2.62	99.59	193.26	1.47	61.26	125.67	1.150	38.33	67.59
99.995	2.18	90.64	178.75	1.21	55.10	115.02	0.97	35.54	63.72
99.993	1.92	84.39	168.19	1.05	50.90	107.48	0.86	33.48	60.70
99.99	1.65	77.59	156.39	0.90	46.41	99.21	0.75	31.17	57.17
99.97	1.00	56.73	118.38	0.52	33.08	73.43	0.47	23.64	44.94
99.95	0.77	47.64	101.02	0.40	27.45	62.01	0.37	20.18	39.01
99.93	0.64	42.00	90.02	0.33	24.02	54.88	0.31	17.98	35.14
99.90	0.52	36.38	78.85	0.26	20.63	47.72	0.25	15.74	31.12
99.70	0.25	21.50	48.25	0.12	11.89	28.55	0.12	9.61	19.70
99.50	0.17	15.83	36.11	0.08	8.65	21.15	0.08	7.18	14.96
99.30	0.12	12.52	28.85	0.06	6.78	16.78	0.06	5.73	12.07
99.00	0.09	9.36	21.82	0.04	5.03	12.59	0.04	4.32	9.22

Table 4.5: Deviation between measured attenuation for measured minimum $R_{0.01}$ and ITU-R predicted attenuation at horizontal polarization

System Reliability (%)	$A_{0.01}$ for measured minimum $R_{0.01}$ (dB)			$A_{0.01}$ for ITU-R predicted $R_{0.01}$ (dB)			Deviation (dB)		
	4 GHz	12 GHz	20 GHz	4 GHz	12 GHz	20 GHz	4 GHz	12 GHz	20 GHz
99.999	2.50	83.79	162.77	2.12	72.57	143.39	0.385	11.21	19.38
99.997	1.75	71.29	143.65	1.47	61.26	125.67	0.2835	10.03	17.98
99.995	1.44	64.36	131.91	1.21	55.10	115.02	0.2391	9.26	16.89
99.993	1.26	59.60	123.53	1.05	50.90	107.48	0.2117	8.69	16.04
99.99	1.08	54.49	114.29	0.90	46.41	99.21	0.1844	8.07	15.07
99.97	0.64	39.15	85.18	0.52	33.08	73.43	0.114	6.06	11.74
99.95	0.48	32.61	72.17	0.40	27.45	62.01	0.0885	5.15	10.15
99.93	0.40	28.59	64.00	0.33	24.02	54.88	0.0741	4.57	9.12
99.90	0.32	24.63	55.78	0.26	20.63	47.72	0.0607	3.99	8.06
99.70	0.15	14.30	33.61	0.12	11.89	28.55	0.0302	2.41	5.05
99.50	0.10	10.45	24.97	0.08	8.65	21.15	0.0206	1.79	3.82
99.30	0.07	8.21	19.86	0.06	6.78	16.78	0.0154	1.42	3.07
99.00	0.05	6.11	14.94	0.04	5.03	12.59	0.0109	1.075	2.34

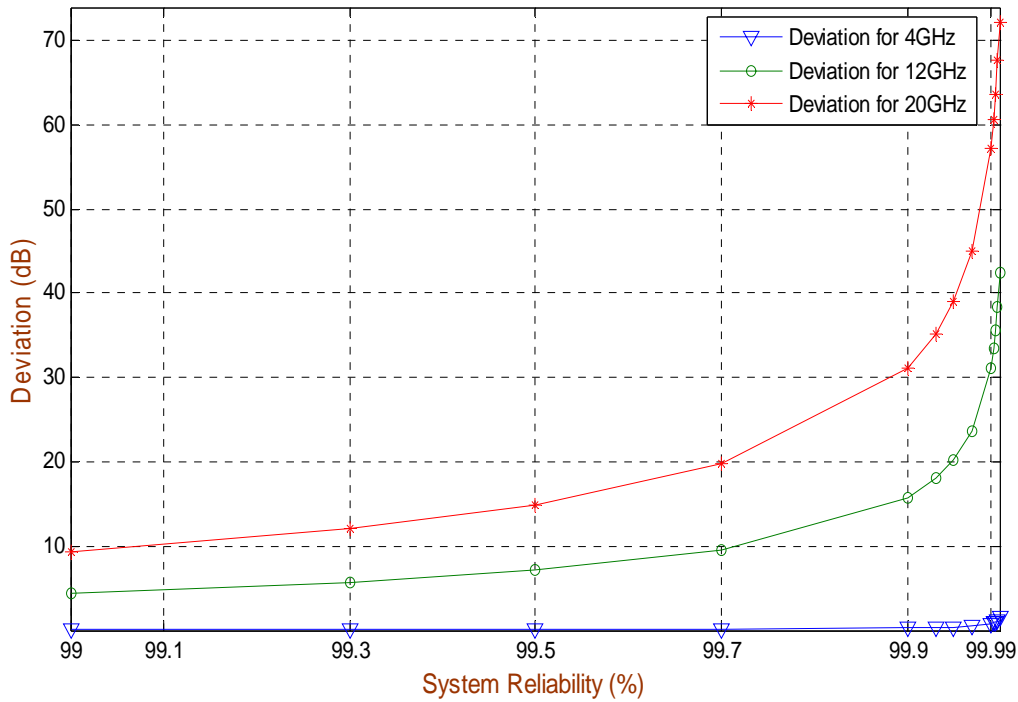


Fig.4.13: Deviation vs. System Reliability Curves for Measured Maximum $R_{0.01}$

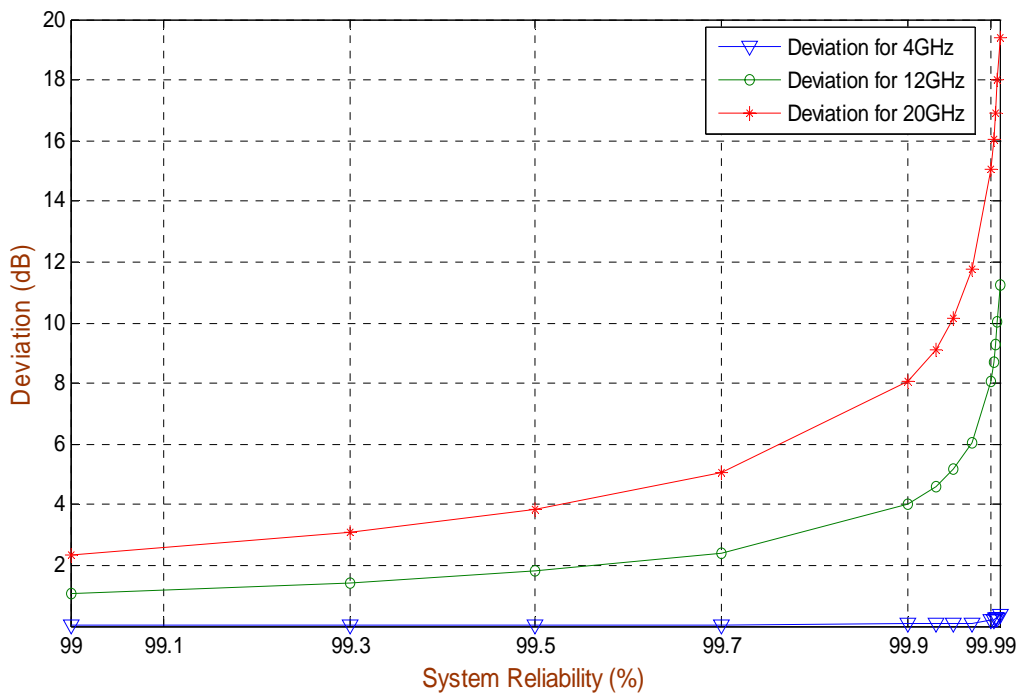


Fig.4.14: Deviation vs. System Reliability Curves for Measured Minimum $R_{0.01}$

From the above deviation curves it is observed that with the increase of system reliability, deviation between measured attenuation and ITU-R predicted attenuation increases. So it is clear that ITU-R recommendation underestimates the rain rate measured in Bangladesh and consequently the rain fade estimation introduces significant errors especially at Ku and Ka-bands.

4.5 COMPARISON STUDY FOR TERRESTRIAL LINK

4.5.1 COMPARISON BETWEEN PREDICTED ATTENUATION AT MEASURED MAXIMUM $R_{0.01}$ AND ITU-R PREDICTED ATTENUATION FOR C/KU/KA-BAND AT HORIZONTAL POLARIZATION

Table 4.6: Comparison among predicted attenuations for measured maximum $R_{0.01}$, minimum $R_{0.01}$ and ITU-R predicted $R_{0.01}$ at horizontal polarization

Frequency	For Measured Max. $R_{0.01}$ ($R_{0.01} = 148.4576$ mm/h) Attenuation, $A_{0.01}$ (dB)	For Measured Min. $R_{0.01}$ ($R_{0.01} = 109.4259$ mm/h) Attenuation, $A_{0.01}$ (dB)	For ITU-R Predicted $R_{0.01}$ ($R_{0.01} = 95$ mm/h) Attenuation, $A_{0.01}$ (dB)
	Horizontal polarization	Horizontal polarization	Horizontal polarization
4 GHz	0.9503	0.6217	0.5444
12 GHz	44.425	31.200	28.033
20 GHz	89.5448	65.4412	59.9210

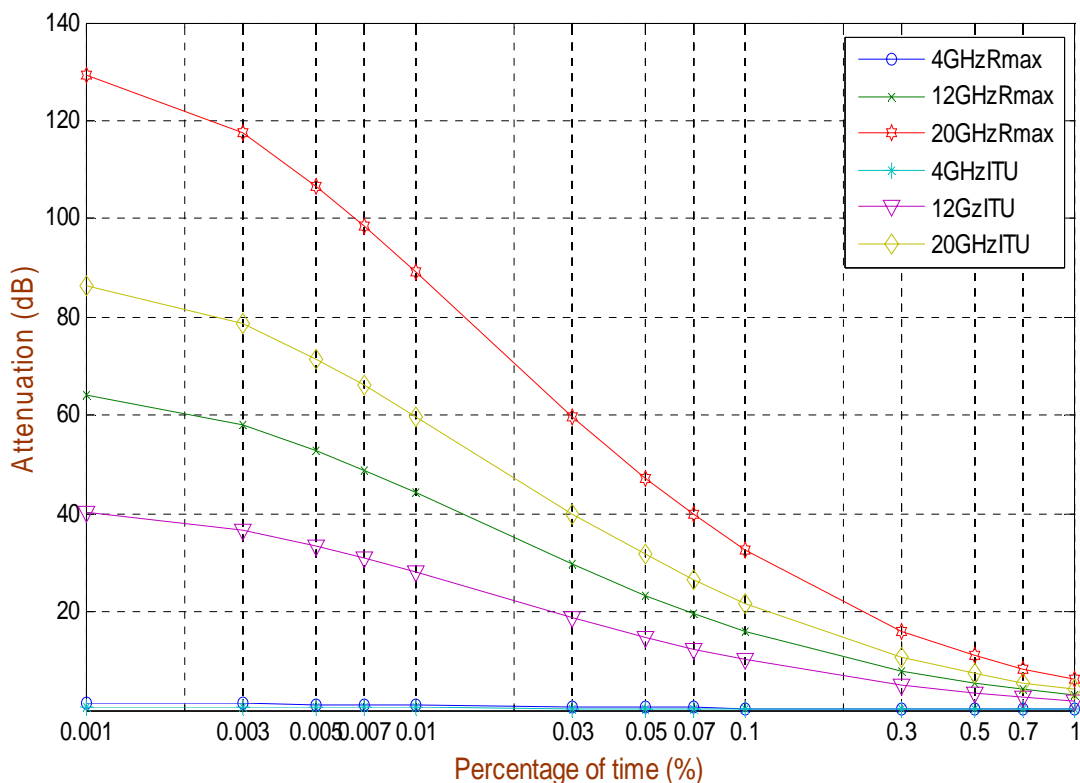


Fig. 4.15: Comparison Curves between Predicted Attenuation at Measured Maximum $R_{0.01}$ and ITU-R Predicted Attenuation for C/Ku/Ka-Band at Horizontal Polarization.

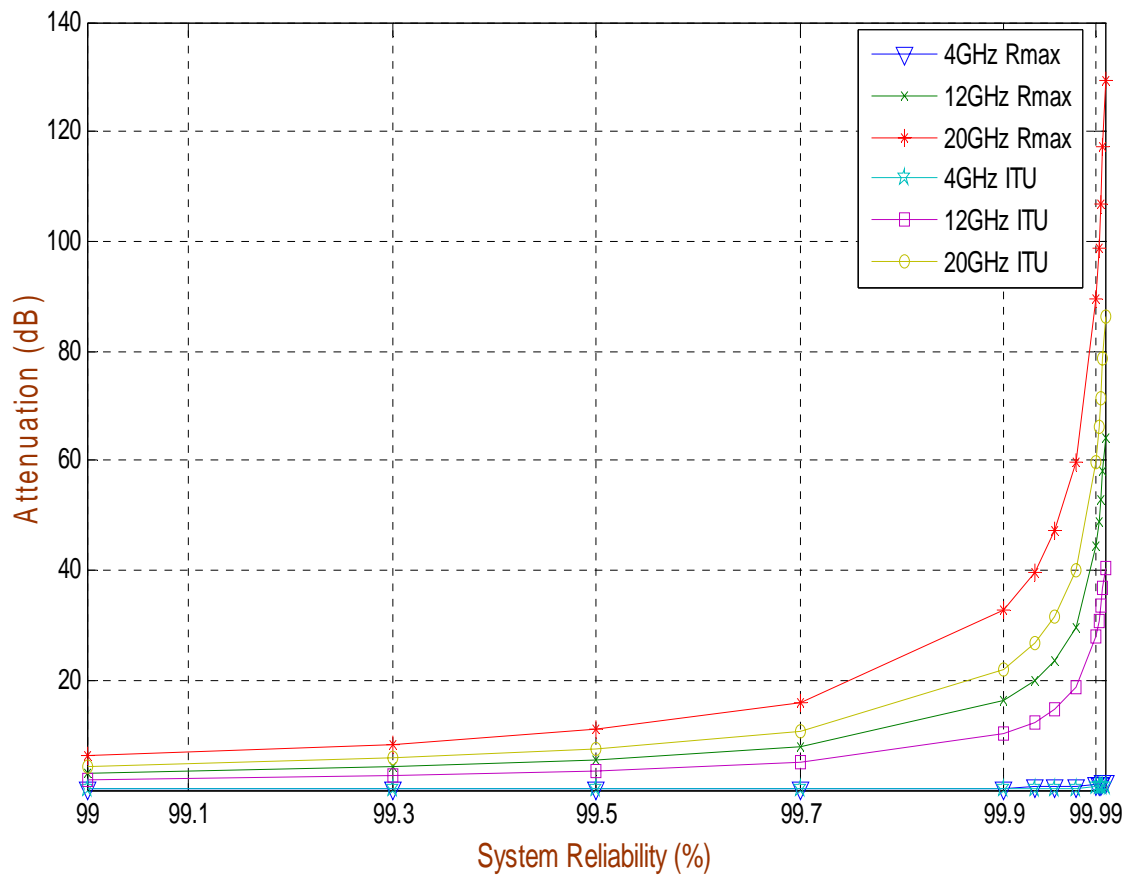


Fig.4.16: Attenuation vs. System Reliability Curves at Horizontal Polarization for Measured Maximum $R_{0.01}$

Fig. 4.15 shows variations between attenuation at measured maximum $R_{0.01}$ and ITU-R predicted attenuation for three frequency bands at different percentages of time at Horizontal polarization. It is observed from the curve that at C-band the difference between measured and ITU-R predicted value is 0.40 dB, at Ku-band the difference is 16.39 dB and at Ka-band it is 29.62 dB for 0.01% of the time. Fig.4.16 shows attenuation vs. system reliability curves of predicted attenuation for measured maximum and ITU-R predicted $R_{0.01}$ for three frequency bands. The difference between C and Ku band is 16 dB and C and Ka band is about 29.2 dB for the design of terrestrial link with 99.99% reliability. Hence to design reliable terrestrial microwave link is also very critical at Ku and Ka bands.

4.5.2 COMPARISON BETWEEN PREDICTED ATTENUATION AT MEASURED MINIMUM $R_{0.01}$ AND ITU-R PREDICTED ATTENUATION FOR C/KU/KA-BAND AT HORIZONTAL POLARIZATION

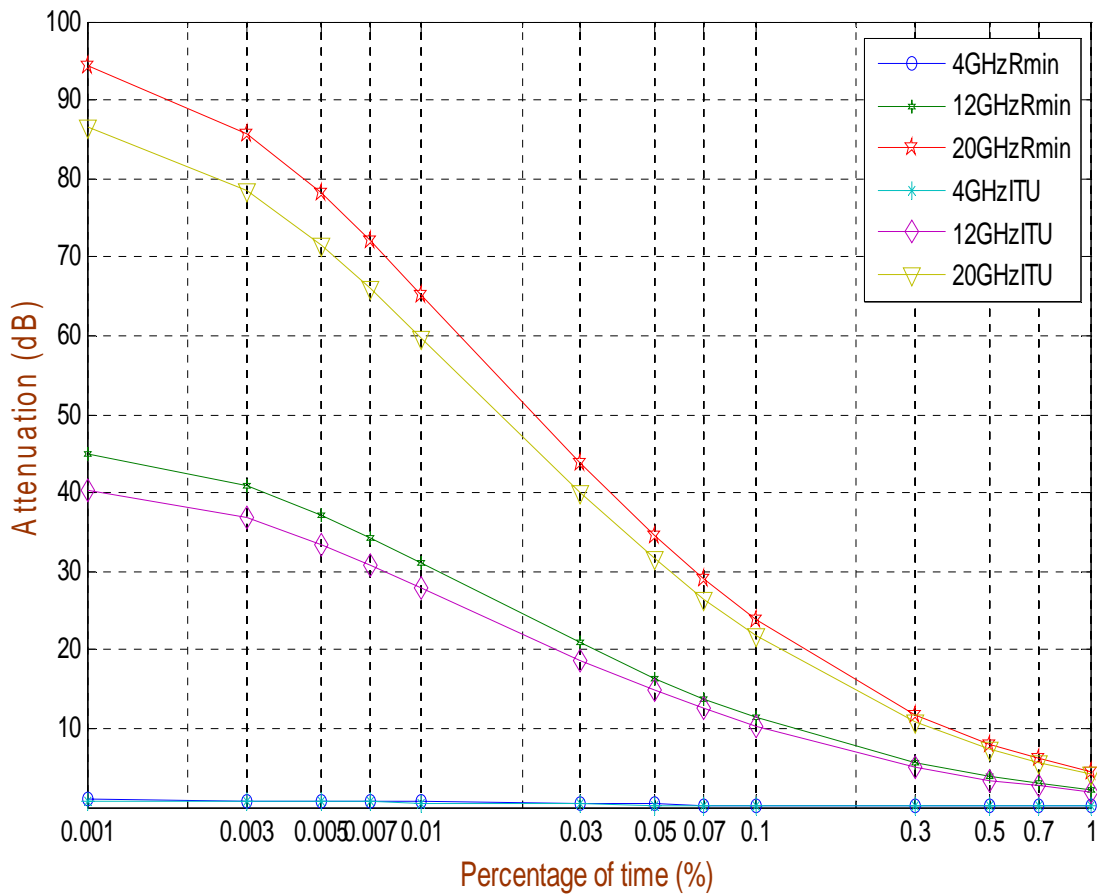


Fig. 4.17: Comparison Curves between Predicted Attenuation at Measured Minimum $R_{0.01}$ and ITU-R Predicted Attenuation for C/Ku/Ka-Band at Horizontal Polarization.

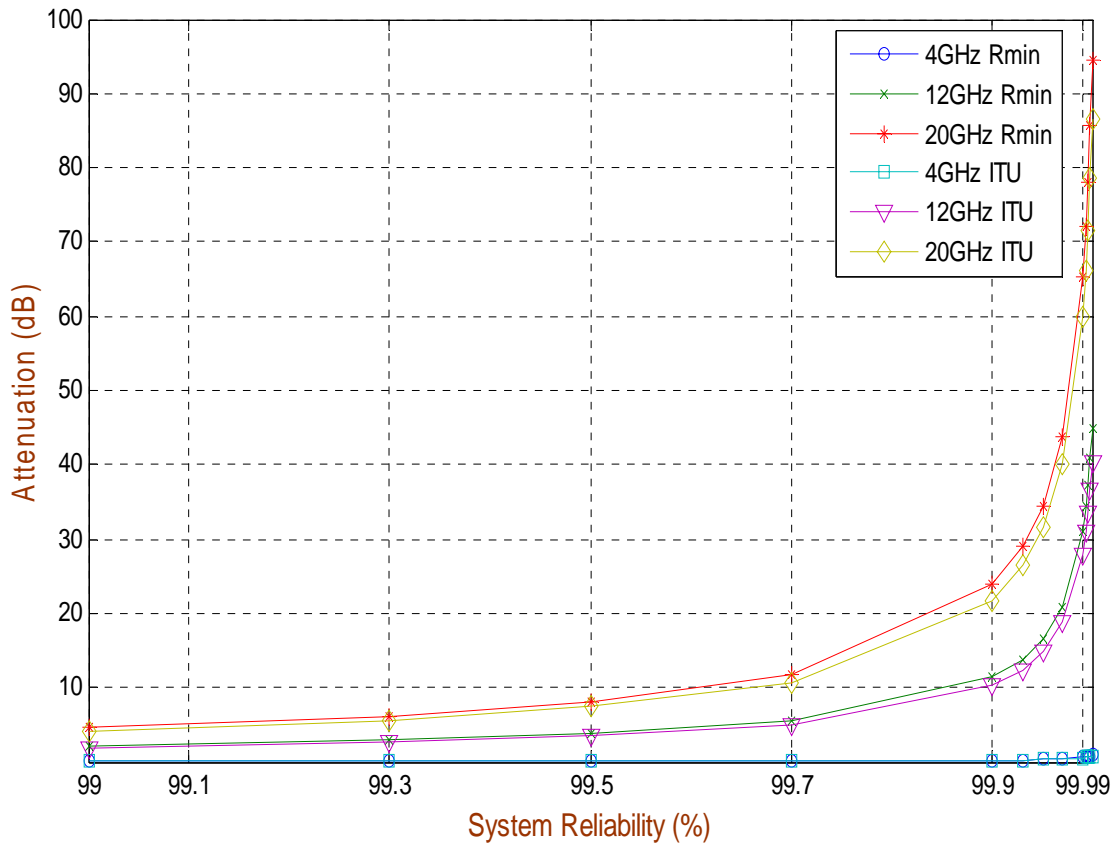


Fig.4.18: Attenuation vs. System Reliability Curves at Horizontal Polarization for Measured Minimum $R_{0.01}$

In Fig. 4.17 variations between attenuation at measured minimum $R_{0.01}$ and ITU-R predicted attenuation for three frequency bands at different percentages of time at Horizontal polarization are shown. For 0.01% of the time, it is observed that at C-band the difference between measured and ITU-R predicted value is 0.07 dB, at Ku-band the difference is 3.16 dB and at Ka-band it is 5.52 dB. Fig.4.18 shows attenuation vs. system reliability curves of predicted attenuation for measured minimum and ITU-R predicted $R_{0.01}$ for three frequency bands. For the design of terrestrial link with 99.99% reliability, it is observed that the difference between C and Ku band is 3.09 dB and C and Ka band is about 5.4 dB.

4.5.3 COMPARISON BETWEEN PREDICTED ATTENUATION AT MEASURED MAXIMUM $R_{0.01}$ AND ITU-R PREDICTED ATTENUATION FOR C/KU/KA-BAND AT VERTICAL POLARIZATION

Table 4.7: Comparison among predicted attenuations for measured maximum $R_{0.01}$, minimum $R_{0.01}$ and ITU-R predicted $R_{0.01}$ at vertical polarization

Frequency	For Measured Max. $R_{0.01}$ ($R_{0.01} = 148.4576$ mm/h) Attenuation, $A_{0.01}$ (dB)	For Measured Min. $R_{0.01}$ ($R_{0.01} = 109.4259$ mm/h) Attenuation, $A_{0.01}$ (dB)	For ITU-R Predicted $R_{0.01}$ ($R_{0.01} = 95$ mm/h) Attenuation, $A_{0.01}$ (dB)
	Vertical polarization	Vertical polarization	Vertical polarization
4 GHz	0.8099	0.5409	0.4704
12 GHz	41.7735	29.460	26.343
20 GHz	83.5133	61.3334	55.8624

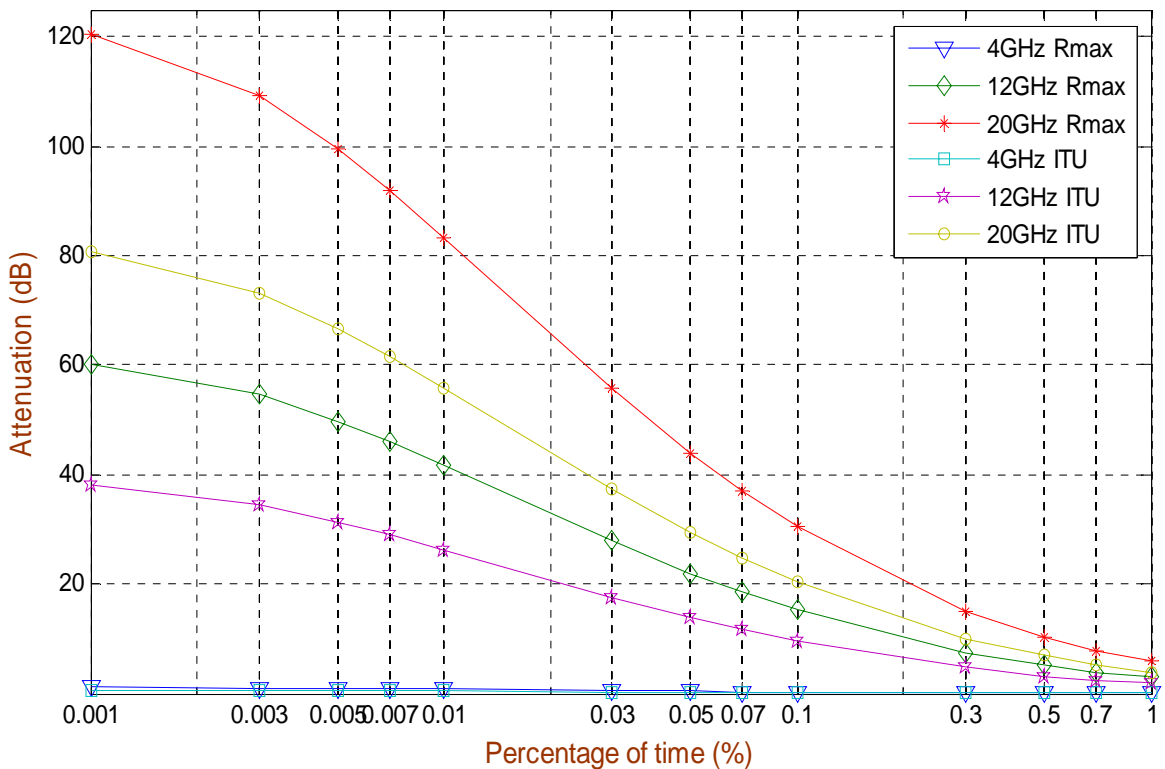


Fig. 4.19: Comparison Curves between Predicted Attenuation at Measured Maximum $R_{0.01}$ and ITU-R Predicted Attenuation for C/Ku/Ka-Band at Vertical Polarization.

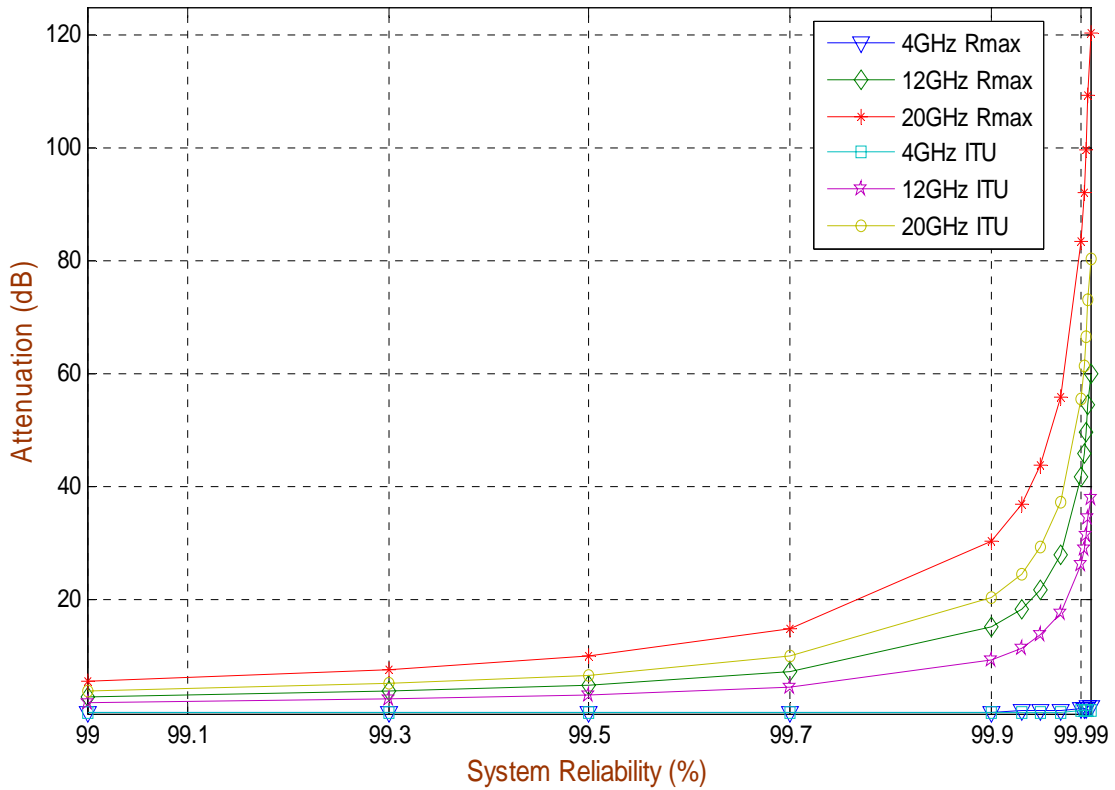


Fig.4.20: Attenuation vs. System Reliability Curves at Vertical Polarization for Measured Maximum $R_{0.01}$

In Fig. 4.19 variations between attenuation at measured maximum $R_{0.01}$ and ITU-R predicted attenuation for three frequency bands at different percentages of time at Vertical polarization are shown. From the curve for 0.01% of the time, it is observed that at C-band the attenuation for measured maximum $R_{0.01}$ is 0.34 dB higher than ITU-R predicted value, at Ku-band the attenuation is 15.43 dB and at Ka-band it is 27.65 dB higher respectively. Fig.4.20 shows attenuation vs. system reliability curves of predicted attenuation for measured maximum and ITU-R predicted $R_{0.01}$ for three frequency bands. The difference between C and Ku band is 15.09 dB and C and Ka band is about 27.3 dB for the design of terrestrial link with 99.99% reliability.

4.5.4 COMPARISON BETWEEN PREDICTED ATTENUATION AT MEASURED MINIMUM $R_{0.01}$ AND ITU-R PREDICTED ATTENUATION FOR C/KU/KA-BAND AT VERTICAL POLARIZATION

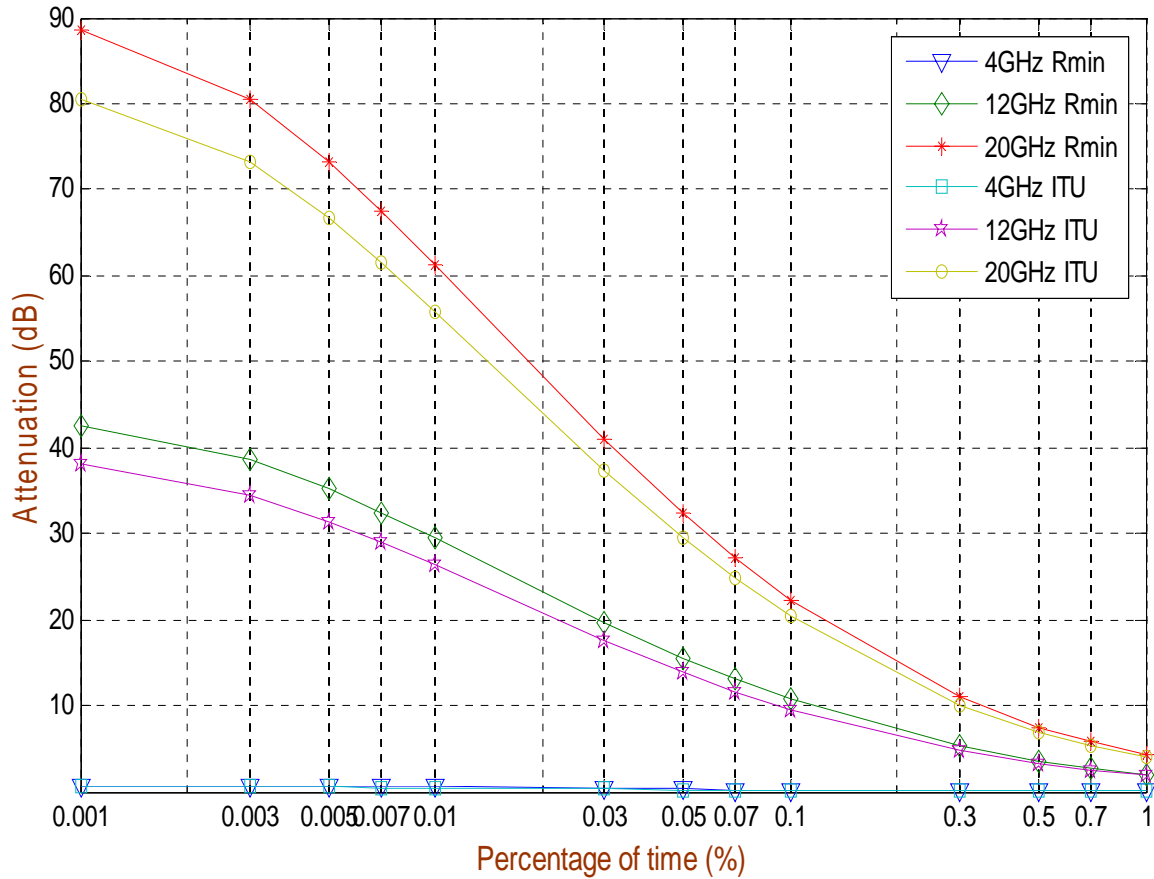


Fig. 4.21: Comparison Curves between Predicted Attenuation at Measured Minimum $R_{0.01}$ and ITU-R Predicted Attenuation for C/Ku/Ka-Band at Vertical Polarization.

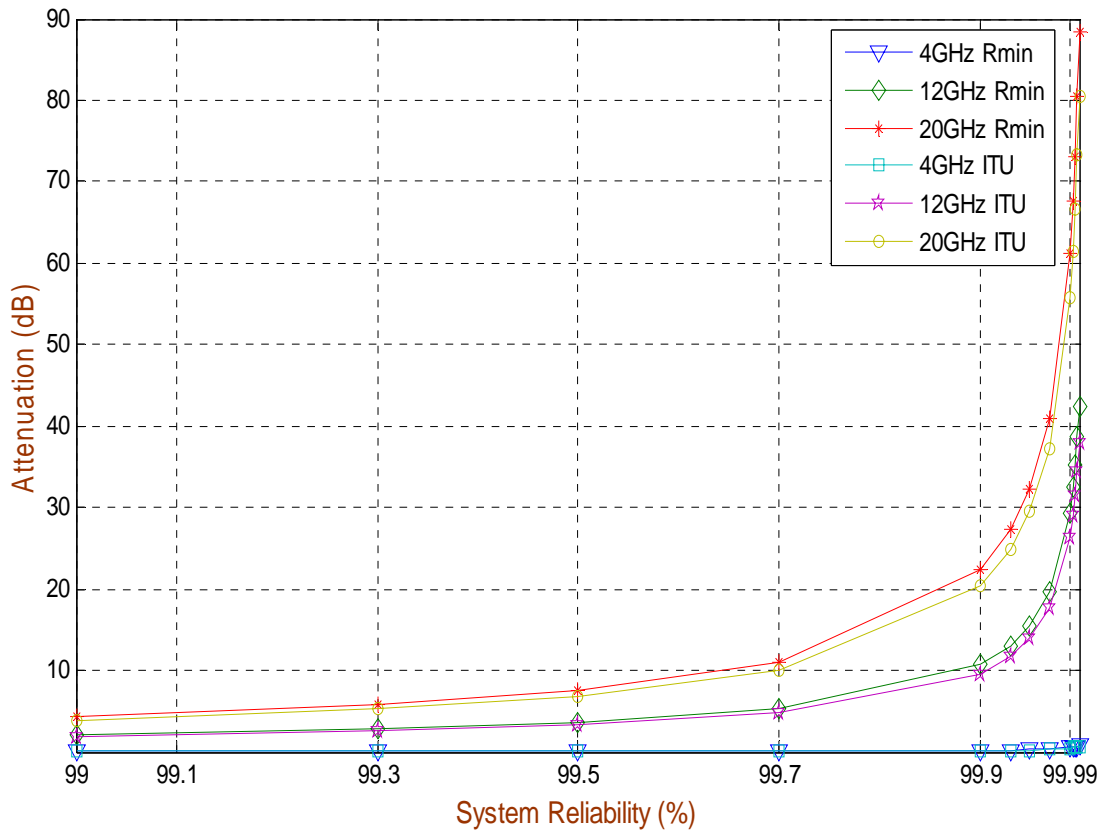


Fig.4.22: Attenuation vs. System Reliability Curves at Vertical Polarization for Measured Minimum $R_{0.01}$

Fig. 4.21 shows variations between attenuation at measured minimum $R_{0.01}$ and ITU-R predicted attenuation for three frequency bands at different percentages of time at Vertical polarization. From the curve for 0.01% of the time, it is observed that at C-band the difference between measured and ITU-R predicted value is 0.07 dB, at Ku-band the difference is 3.12 dB and at Ka-band it is 5.47 dB. Fig.4.22 shows attenuation vs. system reliability curves of predicted attenuation for measured minimum and ITU-R predicted $R_{0.01}$ for three frequency bands. The difference between C and Ku band is 3 dB and C and Ka band is about 5.4 dB for the design of terrestrial link with 99.99% reliability.

4.5.5 COMPARISON BETWEEN PREDICTED ATTENUATION AT MEASURED MAXIMUM $R_{0.01}$ AND ITU-R PREDICTED ATTENUATION FOR C/KU/KA-BAND AT CIRCULAR POLARIZATION

Table 4.8: Comparison among predicted attenuations for measured maximum $R_{0.01}$, minimum $R_{0.01}$ and ITU-R predicted $R_{0.01}$ at circular polarization

Frequency	For Measured Max. $R_{0.01}$ ($R_{0.01} = 148.4576$ mm/h) Attenuation, $A_{0.01}$ (dB)	For Measured Min. $R_{0.01}$ ($R_{0.01} = 109.4259$ mm/h) Attenuation, $A_{0.01}$ (dB)	For ITU-R Predicted $R_{0.01}$ ($R_{0.01} = 95$ mm/h) Attenuation, $A_{0.01}$ (dB)
	Circular polarization	Circular polarization	Circular polarization
4 GHz	0.8677	0.5740	0.500
12 GHz	43.0743	30.3143	27.172
20 GHz	86.4591	63.3424	57.8430

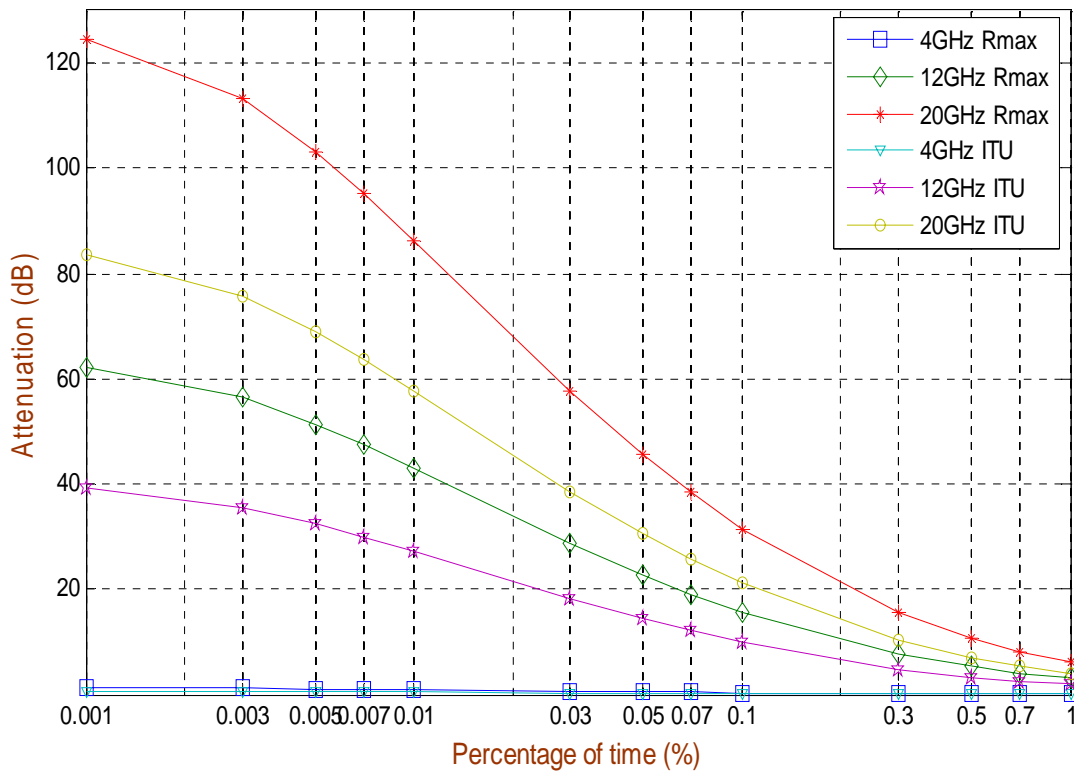


Fig. 4.23: Comparison Curves between Predicted Attenuation at Measured Maximum $R_{0.01}$ and ITU-R Predicted Attenuation for C/Ku/Ka-Band at Circular Polarization.

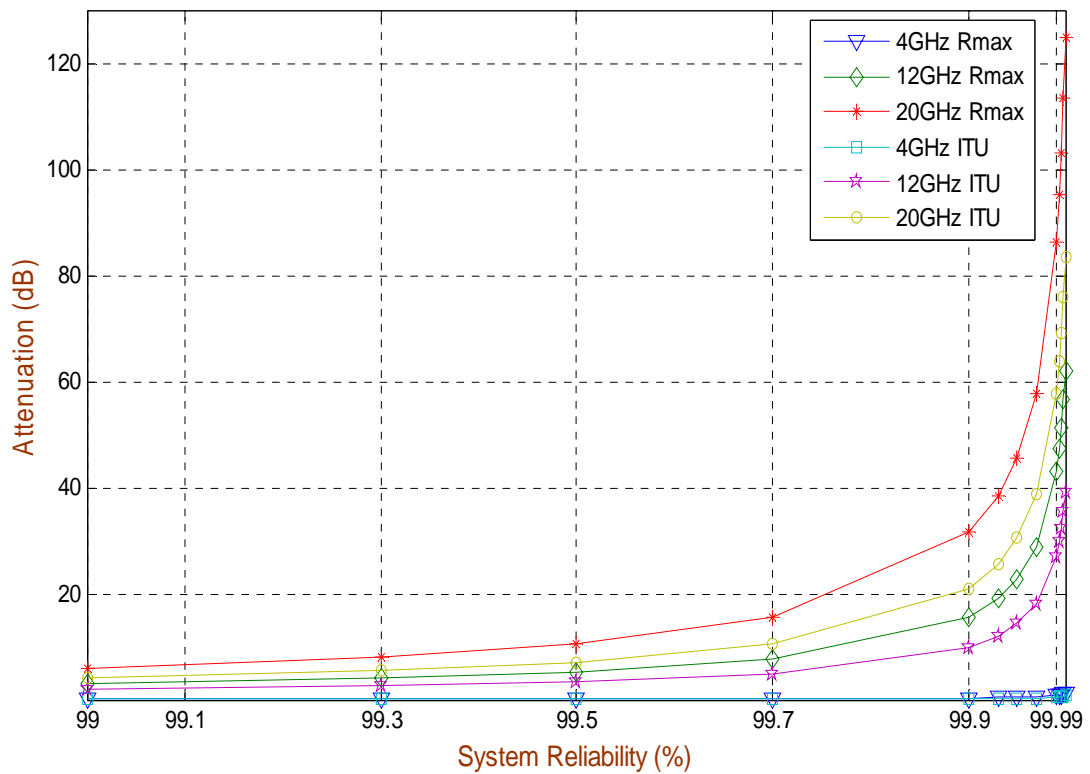


Fig.4.24: Attenuation vs. System Reliability Curves at Circular Polarization for Measured Maximum $R_{0.01}$

In Fig. 4.23 variations between attenuation at measured maximum $R_{0.01}$ and ITU-R predicted attenuation for three frequency bands at different percentages of time at Circular polarization is shown. From the curve it is observed that at C-band the difference between measured and ITU-R predicted value is 0.36 dB, at Ku-band the difference is 15.9 dB and at Ka-band it is 28.62 dB for 0.01% of the time. Fig.4.24 shows attenuation vs. system reliability curves of predicted attenuation for measured maximum and ITU-R predicted $R_{0.01}$ for three frequency bands. For the design of terrestrial link with 99.99% reliability the difference between C and Ku band is 15.54 dB and C and Ka band is about 28.2 dB.

4.5.6 COMPARISON BETWEEN PREDICTED ATTENUATION AT MEASURED MINIMUM $R_{0.01}$ AND ITU-R PREDICTED ATTENUATION FOR C/KU/KA-BAND AT CIRCULAR POLARIZATION

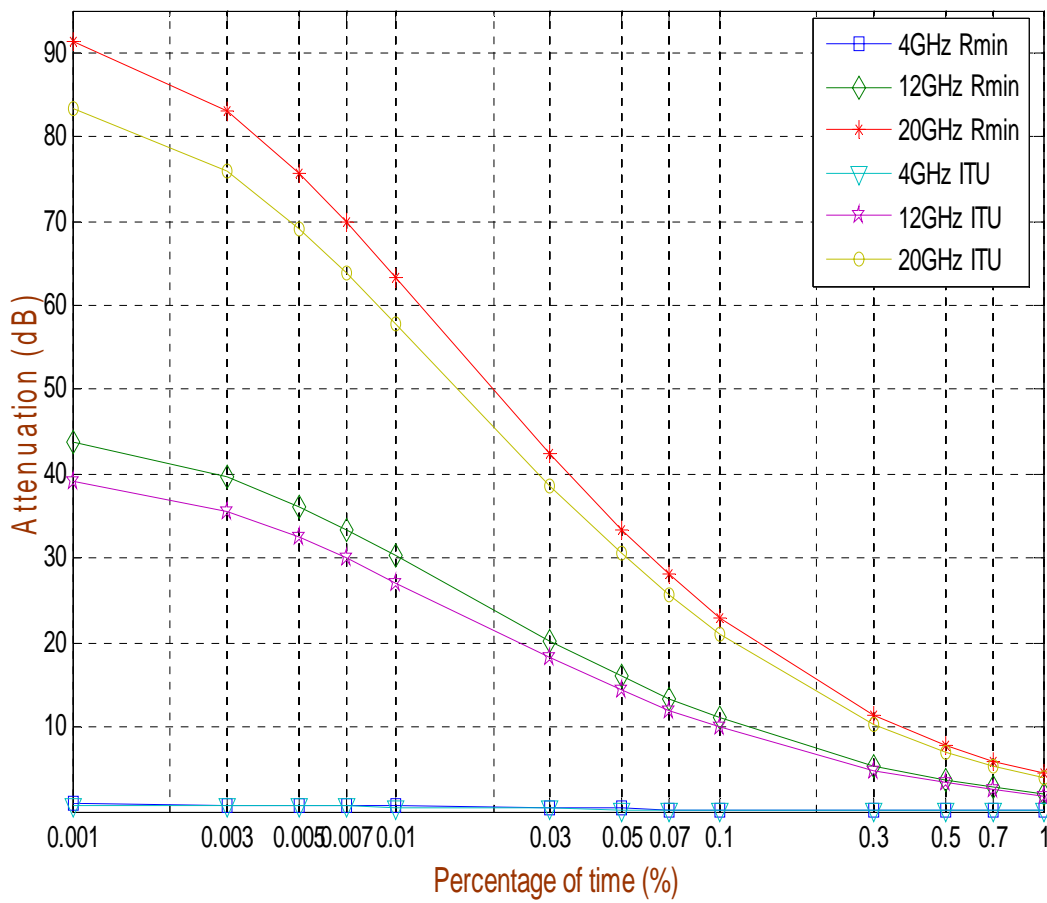


Fig. 4.25: Comparison Curves between Predicted Attenuation at Measured Minimum $R_{0.01}$ and ITU-R Predicted Attenuation for C/Ku/Ka-Band at Circular Polarization.

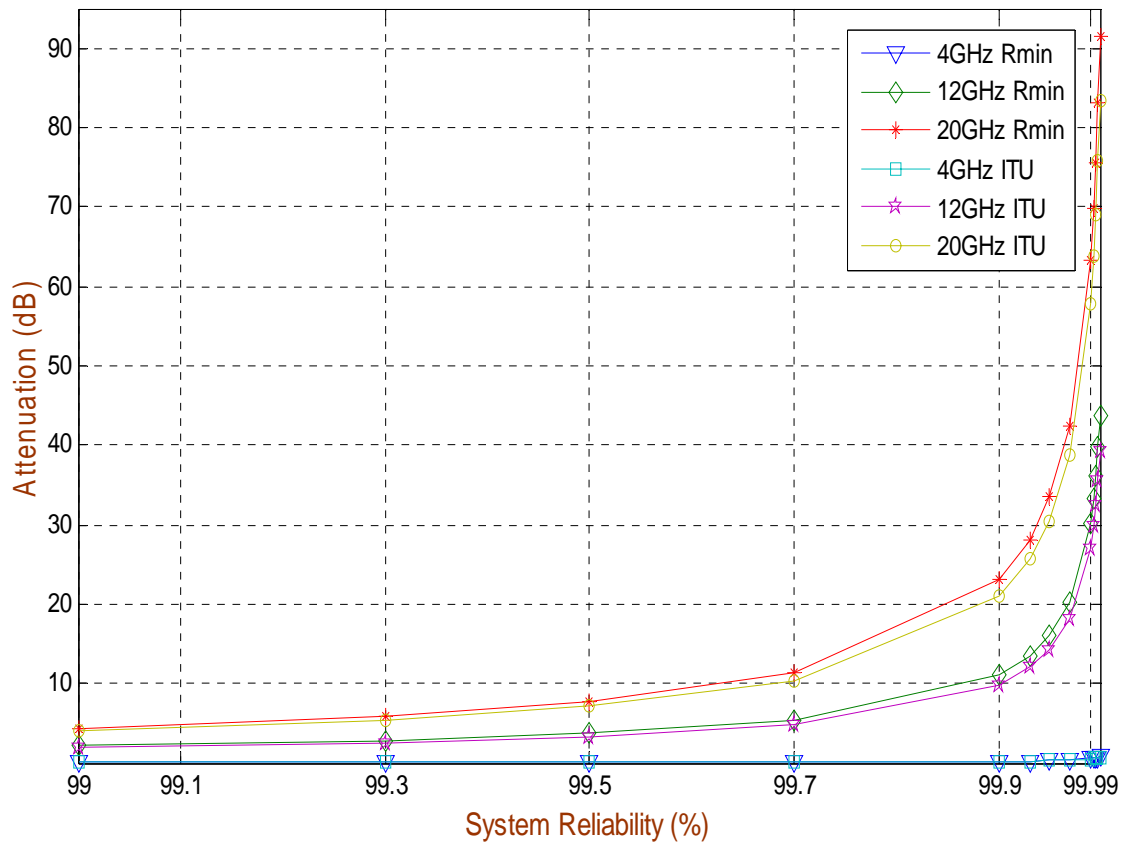


Fig.4.26: Attenuation vs. System Reliability Curves at Circular Polarization for Measured Minimum $R_{0.01}$

In Fig. 4.25 variations between attenuation at measured minimum $R_{0.01}$ and ITU-R predicted attenuation for three frequency bands at different percentages of time at Circular polarization are shown. It is observed from the curve that at C-band the attenuation for measured minimum $R_{0.01}$ is 0.07 dB higher than ITU-R predicted value, at Ku-band the attenuation is 3.14 dB and at Ka-band it is 5.49 dB higher respectively for 0.01% of the time. Fig.4.26 shows attenuation vs. system reliability curves of predicted attenuation for measured minimum and ITU-R predicted $R_{0.01}$ for three frequency bands. The difference between C and Ku band is 3.07 dB and C and Ka band is about 5.4 dB for the design of terrestrial link with 99.99% reliability. It is also observed that horizontally polarized wave suffers the most and the vertically polarized wave is the least. The circularly polarized wave is middle.

4.6 DEVIATION CALCULATION FOR TERRESTRIAL LINK

Table 4.9: Deviation between predicted attenuation for measured maximum $R_{0.01}$ and ITU-R predicted attenuation at horizontal polarization

System Reliability (%)	$A_{0.01}$ for measured maximum $R_{0.01}$ (dB)			$A_{0.01}$ for ITU-R predicted $R_{0.01}$ (dB)			Deviation (dB)		
	4 GHz	12 GHz	20 GHz	4 GHz	12 GHz	20 GHz	4 GHz	12 GHz	20 GHz
99.999	1.37	64.08	129.16	0.78	40.43	86.43	0.59	23.65	42.73
99.997	1.24	58.21	117.34	0.71	36.73	78.52	0.53	21.48	38.82
99.995	1.13	52.98	106.79	0.64	33.43	71.46	0.49	19.55	35.33
99.993	1.04	48.94	98.65	0.59	30.88	66.01	0.45	18.06	32.64
99.99	0.94	44.33	89.35	0.54	27.97	59.79	0.4	16.36	29.56
99.97	0.63	29.67	59.81	0.36	18.72	40.02	0.27	10.95	19.79
99.95	0.50	23.43	47.23	0.28	14.78	31.60	0.22	8.65	15.63
99.93	0.42	19.71	39.73	0.24	12.43	26.59	0.18	7.28	13.14
99.90	0.34	16.17	32.59	0.19	10.20	21.81	0.15	5.97	10.78
99.70	0.17	7.97	16.07	0.09	5.03	10.75	0.08	2.94	5.32
99.50	0.11	5.46	11.01	0.06	3.44	7.36	0.05	2.02	3.65
99.30	0.08	4.18	8.43	0.05	2.64	5.64	0.03	1.54	2.79
99.00	0.06	3.10	6.26	0.03	1.96	4.19	0.03	1.14	2.07

Table 4.10: Deviation between predicted attenuation for measured minimum $R_{0.01}$ and ITU-R predicted attenuation at horizontal polarization

System Reliability (%)	$A_{0.01}$ for measured minimum $R_{0.01}$ (dB)			$A_{0.01}$ for ITU-R predicted $R_{0.01}$ (dB)			Deviation (dB)		
	4 GHz	12 GHz	20 GHz	4 GHz	12 GHz	20 GHz	4 GHz	12 GHz	20 GHz
99.999	0.89	45.00	94.39	0.78	40.43	86.43	0.11	4.57	7.96
99.997	0.81	40.88	85.76	0.71	36.73	78.52	0.1	4.15	7.24
99.995	0.74	37.21	78.04	0.64	33.43	71.46	0.1	3.78	6.58
99.993	0.68	34.37	72.09	0.59	30.88	66.01	0.09	3.49	6.08
99.99	0.62	31.13	65.30	0.54	27.97	59.79	0.08	3.16	5.51
99.97	0.41	20.84	43.71	0.36	18.72	40.02	0.05	2.12	3.69
99.95	0.32	16.45	34.51	0.28	14.78	31.60	0.04	1.67	2.91
99.93	0.27	13.84	29.03	0.24	12.43	26.59	0.03	1.41	2.44
99.90	0.22	11.35	23.82	0.19	10.20	21.81	0.03	1.15	2.01
99.70	0.11	5.60	11.74	0.09	5.03	10.75	0.02	0.57	0.99
99.50	0.07	3.83	8.04	0.06	3.44	7.36	0.01	0.39	0.68
99.30	0.058	2.94	6.16	0.051	2.64	5.64	0.007	0.3	0.52
99.00	0.043	2.18	4.580	0.038	1.96	4.19	0.005	0.22	0.39

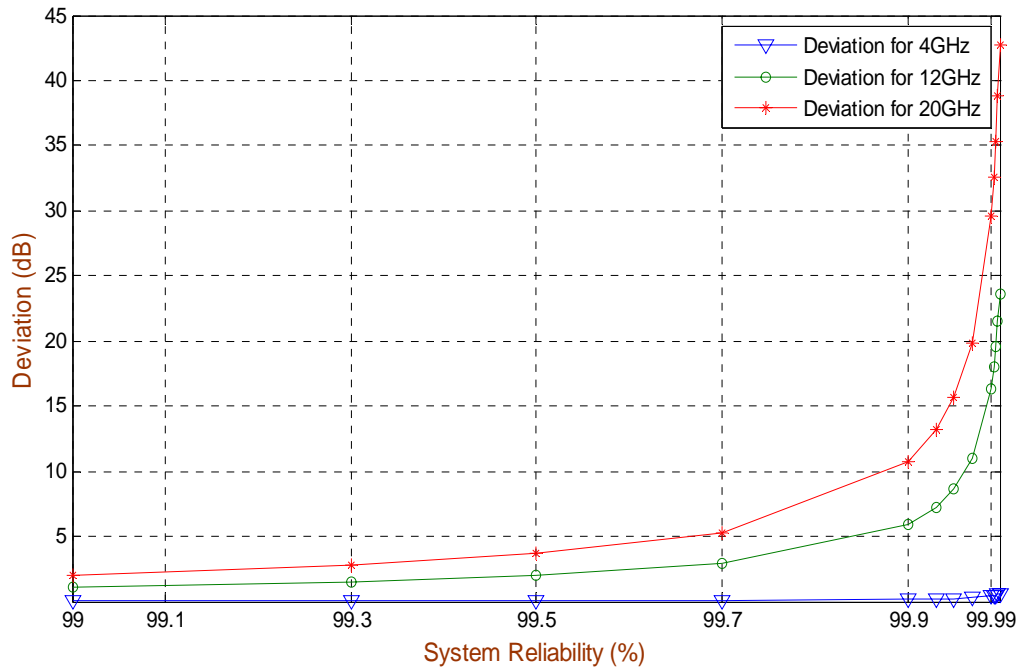


Fig.4.27: Deviation vs. System Reliability Curves for Measured Maximum $R_{0.01}$

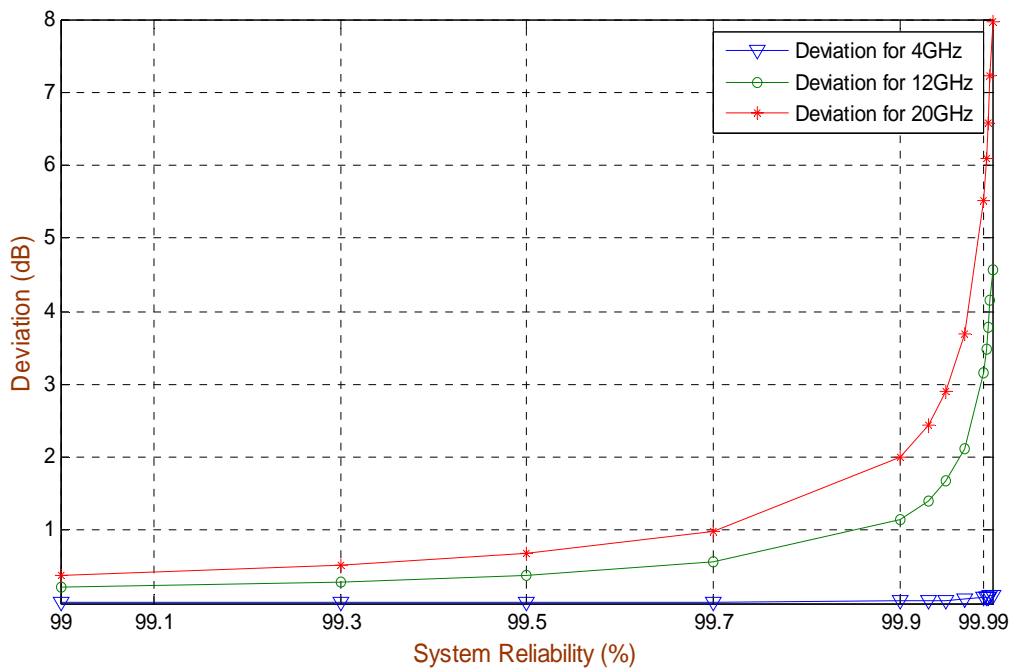


Fig.4.28: Deviation vs. System Reliability Curves for Measured Minimum $R_{0.01}$

From the above deviation curves it is observed that with the increase of system reliability, deviation between measured attenuation and ITU-R predicted attenuation increases. So it is clear that ITU-R recommendation underestimates the rain rate measured in Bangladesh and consequently the rain fade estimation introduces significant errors especially at Ku and Ka-bands.

4.7 LINK BUDGET ANALYSIS FOR EARTH-TO-SATELLITE DOWNLINK AT C/KU/KA- BANDS USING ITU-R PROPOSED AND MEASURED RAIN RATE AT HORIZONTAL POLARIZATION FOR BANGLADESH

Table 4.11: Link Budget Analysis for Earth-To-Satellite downlink:

	For ITU-R Predicted $R_{0.01}$			For Maximum $R_{0.01}$ (Worst Case)		
	4GHz	12GHz	20GHz	4GHz	12GHz	20GHz
Downlink Power Budget	4GHz	12GHz	20GHz	4GHz	12GHz	20GHz
EIRP	65	65	65	65	65	65
B_0 = Transponder Output Back off	-2	-2	-2	-2	-2	-2
G_r =Receiving Antenna Gain	33.93	43.47	47.91	33.93	43.47	47.91
[FSL]=Free Space Path Loss	-199.7	-206.6	-209.7	-199.7	-206.6	-209.7
L_{ant} =Edge of beam loss for Satellite Antenna	-3	-3	-3	-3	-3	-3
[AA]=Clear air atmospheric loss	-0.075	-0.11	-0.4	-0.075	-0.11	-0.4
L_m = Other losses	-0.5	-0.5	-0.5	-0.5	-0.5	-0.5
P_r = Received power at receiver station (Clear Air)	-106.34	-103.74	-102.69	-106.34	-103.74	-102.69
Rain Attenuation, A_{rain}	0.901	46.417	99.21	1.659	77.591	156.39
P_r (due to rain)	-107.25	-150.16	-201.91	-108.0	-181.33	-259.08
Downlink Noise Budget	4GHz	12GHz	20GHz	4GHz	12GHz	20GHz
k =Boltzmann's Constant in dBW/K/Hz	-228.6	-228.6	-228.6	-228.6	-228.6	-228.6
T_s =System noise temperature, 140K	21.46	21.46	21.46	21.46	21.46	21.46
B_n = Noise bandwidth, 36MHz	75.56	75.56	75.56	75.56	75.56	75.56
N =Receiver Noise Power (Clear Air)	-131.58	-131.58	-131.58	-131.58	-131.58	-131.58
Increased due to rain (ΔN)	1.38	4.63	4.45	2.068	4.629	4.45
N =Receiver Noise Power (due to rain)	-130.2	-126.95	-127.13	-129.512	-126.951	-127.13
C/N Ratio in Receiver	4GHz	12GHz	20GHz	4GHz	12GHz	20GHz
C/N= Clear Air	25.235	27.84	28.89	25.235	27.84	28.89
C/N=Due to rain	22.95	-23.21	-74.78	21.512	-54.38	-131.95

4.8 LINK BUDGET ANALYSIS FOR TERRESTRIAL DOWNLINK AT C/KU/KA- BANDS USING ITU-R PROPOSED AND MEASURED RAIN RATE AT HORIZONTAL POLARIZATION FOR BANGLADESH

Table 4.12: Link Budget Analysis for Terrestrial downlink:

	For ITU-R Predicted $R_{0.01}$			For Maximum $R_{0.01}$ (Worst Case)		
	4GHz	12GHz	20GHz	4GHz	12GHz	20GHz
Downlink Power Budget	4GHz	12GHz	20GHz	4GHz	12GHz	20GHz
EIRP	65	65	65	65	65	65
B_0 = Transponder Output Back off	-2	-2	-2	-2	-2	-2
G_r =Receiving Antenna Gain	33.93	43.47	47.91	33.93	43.47	47.91
[FSL]=Free Space Path Loss	-199.7	-206.6	-209.7	-199.7	-206.6	-209.7
L_{ant} =Edge of beam loss for Satellite Antenna	-3	-3	-3	-3	-3	-3
[AA]=Clear air atmospheric loss	-0.075	-0.11	-0.4	-0.075	-0.11	-0.4
L_m = Other losses	-0.5	-0.5	-0.5	-0.5	-0.5	-0.5
P_r = Received power at receiver station (Clear Air)	-106.34	-103.74	-102.69	-106.34	-103.74	-102.69
Rain Attenuation, A_{rain}	0.544	28.033	59.92	0.95	44.425	89.54
P_r (due to rain)	-106.89	-131.77	-162.61	-107.29	-148.16	-192.23
<hr/>						
Downlink Noise Budget	4GHz	12GHz	20GHz	4GHz	12GHz	20GHz
k =Boltzmann's Constant in dBW/K/Hz	-228.6	-228.6	-228.6	-228.6	-228.6	-228.6
T_s =System noise temperature, 140K	21.46	21.46	21.46	21.46	21.46	21.46
B_n = Noise bandwidth, 36MHz	75.56	75.56	75.56	75.56	75.56	75.56
N =Receiver Noise Power (Clear Air)	-131.58	-131.58	-131.58	-131.58	-131.58	-131.58
Increased due to rain (ΔN)	1.38	4.63	4.45	2.068	4.629	4.45
N =Receiver Noise Power (due to rain)	-130.2	-126.95	-127.13	-129.512	-126.951	-127.13
<hr/>						
C/N Ratio in Receiver	4GHz	12GHz	20GHz	4GHz	12GHz	20GHz
C/N= Clear Air	25.235	27.84	28.89	25.235	27.84	28.89
C/N=Due to rain	23.31	- 4.82	- 35.48	22.22	- 21.21	- 65.1

From all the above comparison curves and tables, it is clear that ITU-R recommendation underestimates the rain rate measured in Bangladesh and consequently the link budget estimations have introduced significant errors especially at Ku and Ka-bands both for Earth-to-Satellite and terrestrial downlink. Even though the C/N ratio is about 2.6-3.65 dB higher in Ku and Ka-bands than C-band during clear air condition but during the rains C/N ratios fall to 22.95 dB at C-band, -23.21 dB at Ku-band and -74.78 dB at Ka-band for Earth-to-Satellite downlink. In the case of terrestrial downlink, the C/N ratios fall to 23.31 dB at C-band, -4.82 dB at Ku-band and -35.48 dB at Ka-band during rain. These estimations are based on ITU-R recommended rain rates. But our estimation is done based on converted measured rain rate and for measured maximum $R_{0.01}$ (Worst Case), the C/N ratio is fallen to -54.38 dB at Ku-band and -131.95 dB at Ka-band during rain for Earth-to-Satellite downlink. For terrestrial downlink, the value of C/N ratio during rain is -21.21 dB at Ku-band and -65.1 dB at Ka-band. These predictions show that using of Ku and Ka-bands is very challenging and critical in this region like Bangladesh. However, the measured rain rate data is converted from measured long term annual rainfall data, it is too preliminary to comment correctly. Therefore, it is necessary to measure rain intensity and rain drop size distribution urgently for the design of reliable microwave link in Bangladesh.

4.9 THE MEASUREMENTS AND DEVIATIONS IN DIFFERENT COUNTRIES

From various studies [1-2, 4, 35] it has been observed that for some countries ITU-R underestimates the value of rainfall rate, $R_{0.01}$ (mm/hr) and sometimes overestimates. For example in Malaysia the value of ITU-R predicted $R_{0.01}$ is 145 mm/hr at any locations where measured $R_{0.01}$ varies from 80-150 mm/hr [1]. So for areas with lower rainfall such as Chuping, Temerloh, Kuala Lumpur and Senai $R_{0.01}$ is lower than the ITU-R value. It is observed that for areas with higher rainfall rate such as Taiping, Jerangau and Tapah, $R_{0.01}$ is 145mm/h where the ITU-R value is quite acceptable [2]. Also ITU-R rain zoning overestimated rain rate values in Nigeria [4]. Here deviation between Measured $A_{0.01}$ and ITU-R predicted $A_{0.01}$ at Ku-Band (12.675 GHz) is approximately 19.6 dB. In Brazil for different locations ITU – R underestimated rain rate values and the deviation is approximately 4-5 dB at Ku – Band (11.452 GHz) [35]. The measured $R_{0.01}$ rainfall rate at Bandung is 120 mm/hr. The ITU-R, has categorized Indonesia as Region P, countries with very high rain precipitation. According to ITU-R rain intensity that will cause the interruption of a communication link for 0.01% per year is 145 mm/hr. Therefore, the P region of ITU-R model is over estimate for Bandung in Indonesia. The measured $R_{0.01}$ rainfall rate at Cibinong is 159 mm/hr and ITU-R model is under estimate for Cibinong in Indonesia [36, 37].

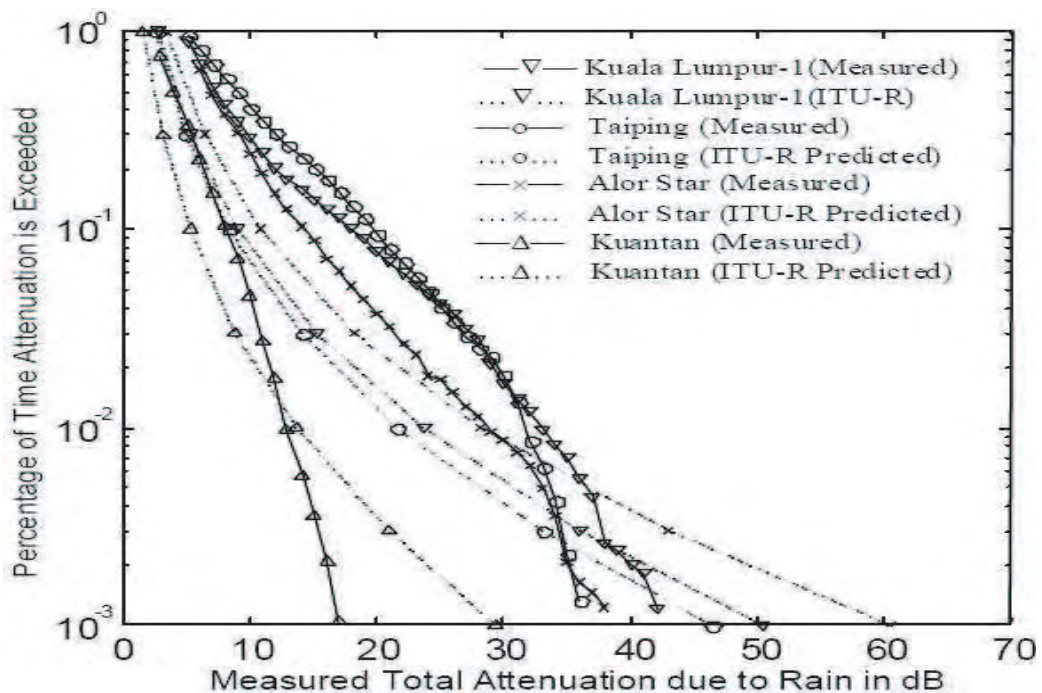


Fig.4.29: Rain attenuation distribution measured at 15 GHz frequency over microwave links at Kuala Lumpur-1, Taiping, Alor star and Kuantan and those predicted by ITU-R.

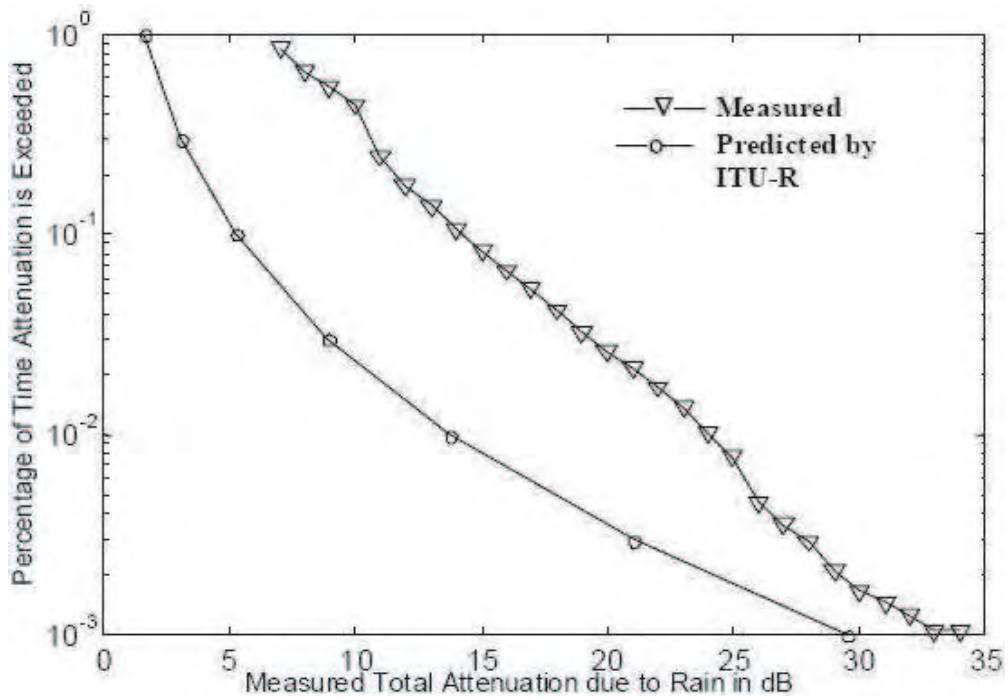


Fig.4.30: Rain attenuation distribution measured at 23 GHz frequency over microwave links at Kuala Lumpur -2 and those predicted by ITU-R.

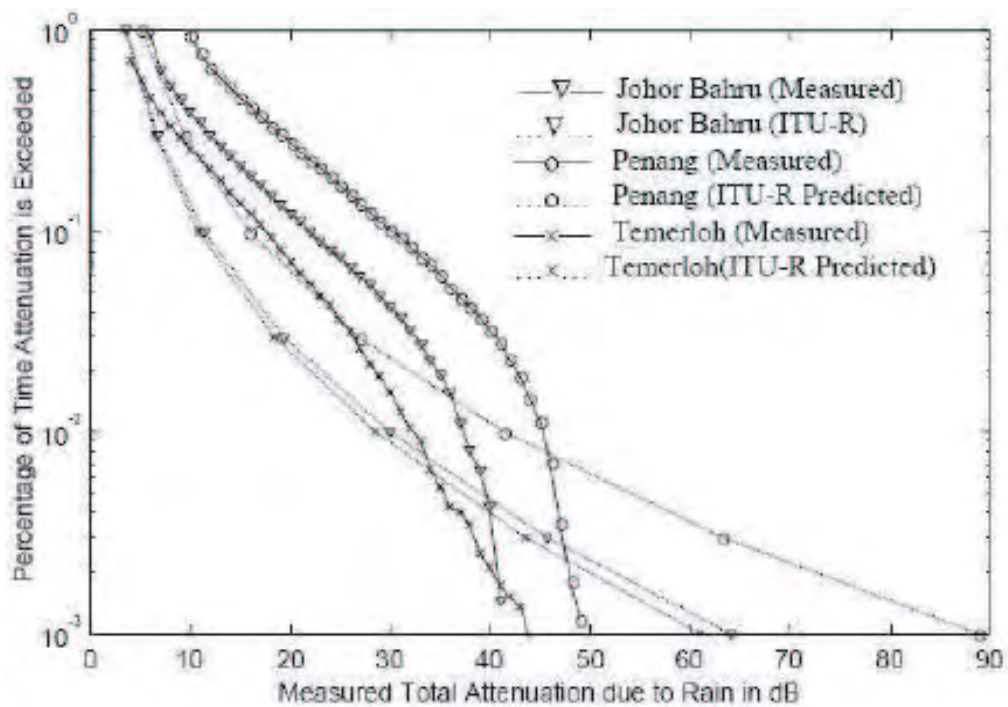


Fig.4.31: Rain attenuation distribution measured at 15 GHz frequency over microwave links at Johor Bahru, Penang and Temerloh and those predicted by ITU-R.

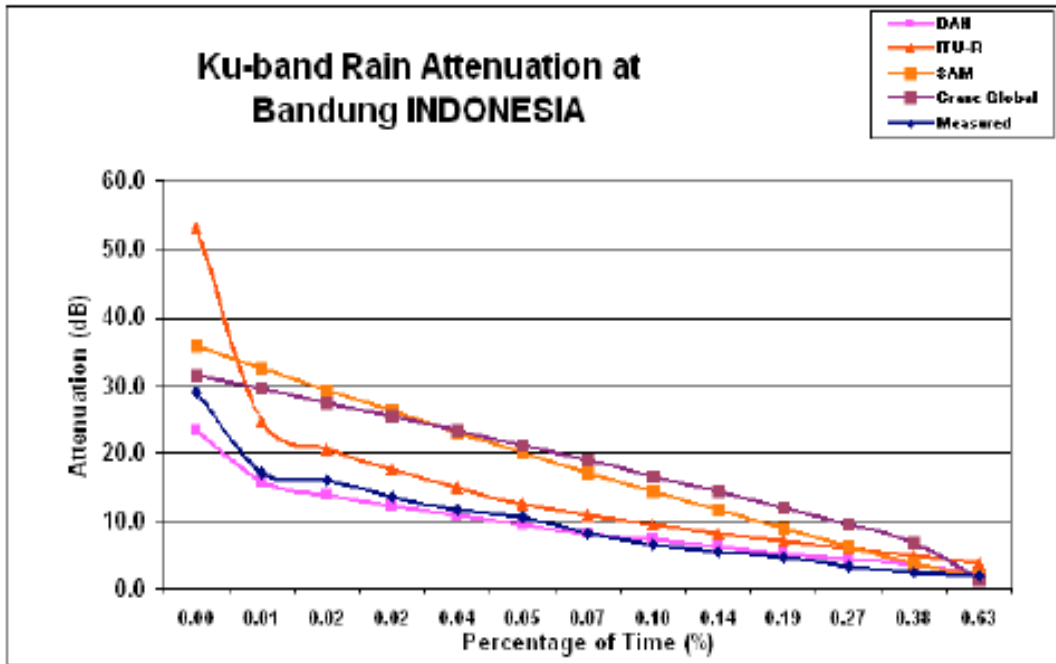


Fig.4.32: Measured vs. Predicted Rain Attenuation at Bandung, Indonesia for 12.24 GHz at Horizontal Polarization.

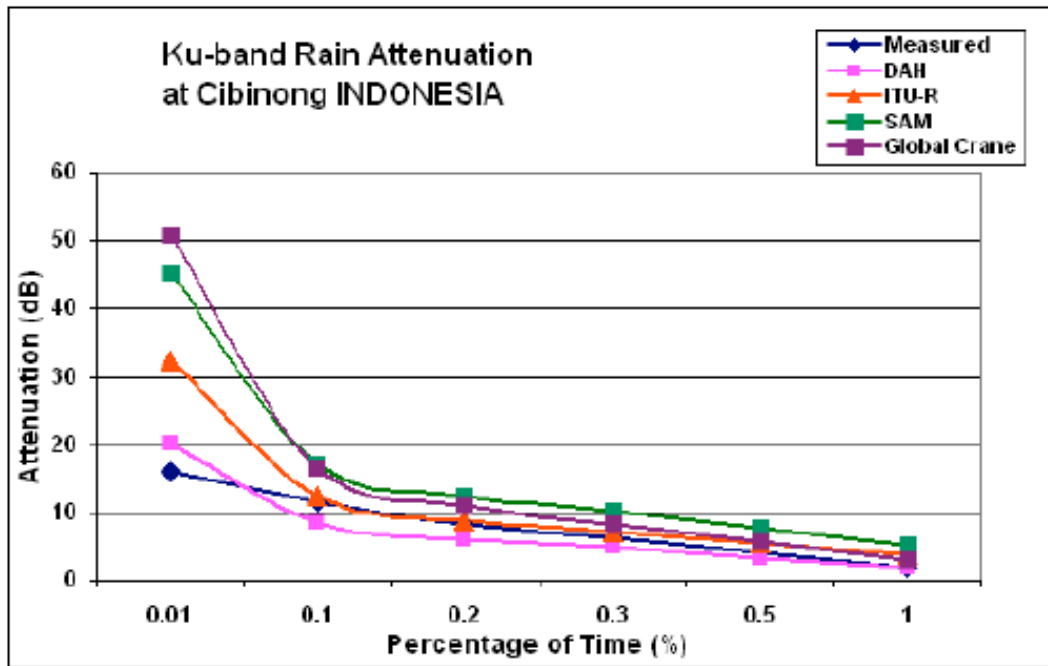


Fig.4.33: Measured vs. Predicted Rain Attenuation at Cibinong, Indonesia for 11.2 GHz at Circular Polarization.

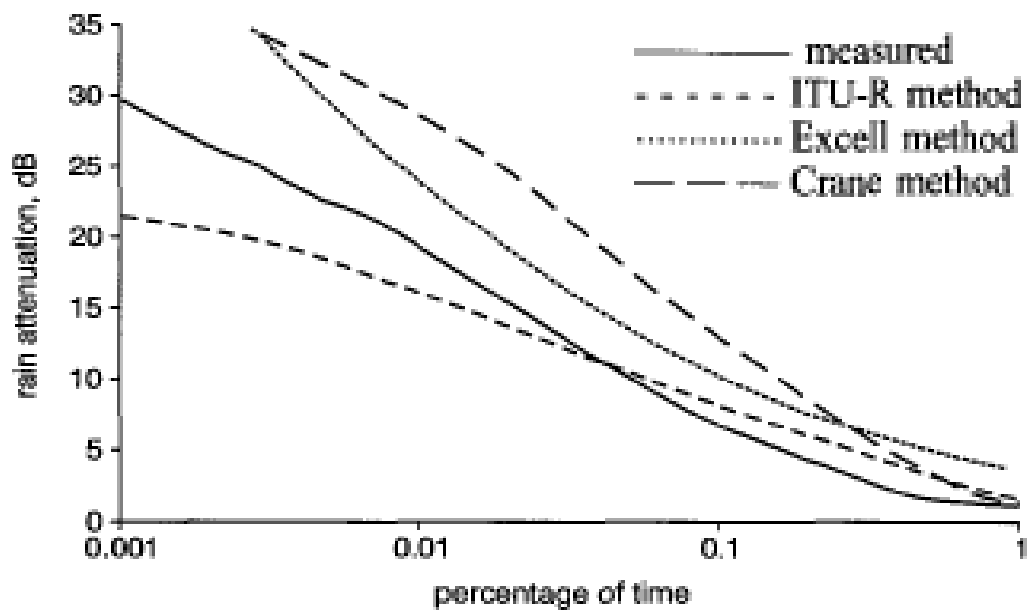


Fig.4.34: Measured and predicted attenuation distributions at Belim in Brazil for 11.45 GHz at Circular Polarization.

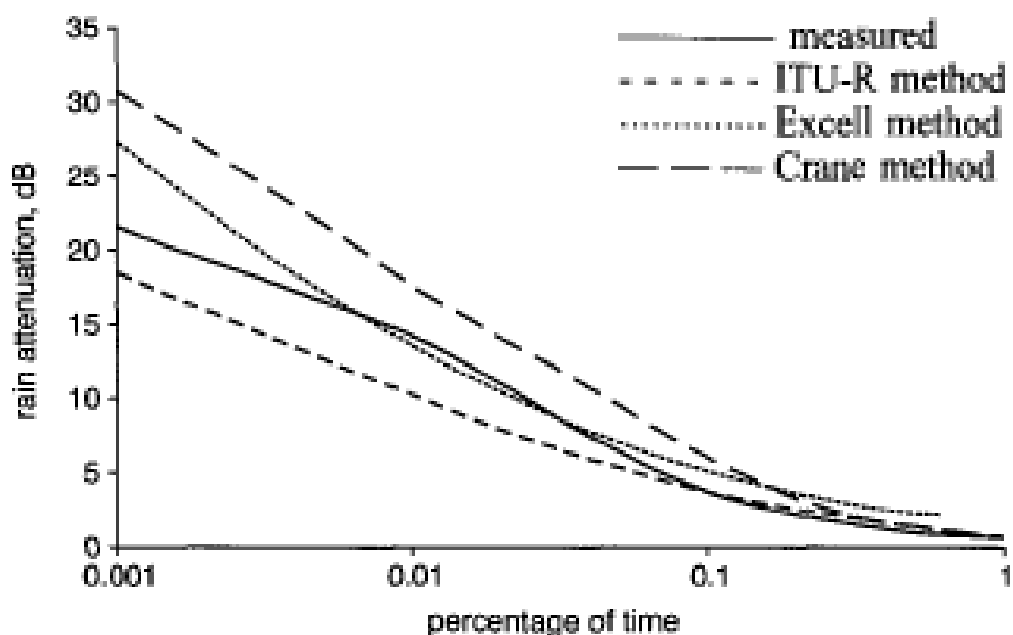


Fig.4.35: Measured and predicted attenuation distributions at Rio de Janeiro in Brazil for 11.45 GHz at Circular Polarization.

APPENDIX - A:

The daily rain fall data were collected from 'Abohawa Odhidoptor' (Meteorological Department) of Bangladesh of 34 different rain stations for the period of 13 years.

Sample of a converted data in Microsoft Excel sheet from Word pad:

Station Name: Ishurdi

Year	Month	Day	-1	2	3	4	5	6	7	8	9	10	11	12	13	14	15	16	17	18	19	20	21	22	23	24	25	26	27	28	29	30	31	Rainfall/Month (mm)	Rainfall/Year (mm)	
1995	1		0	0	0	0	0	0	0	0	1	6	0	0	0	0	0	0	0	1	0	0	0	0	0	0	0	0	0	0	0	0	0	8		
1995	2		0	0	0	0	0	3	0	0	0	0	0	0	0	0	4	0	0	2	0	0	0	0	0	15	0	0	0	0				24		
1995	3		0	0	0	0	0	0	0	0	0	0	0	0	0	0	0	0	0	0	0	0	0	0	0	0	0	0	18	0	0	2		20		
1995	4		0	0	0	0	0	0	0	0	0	1	0	0	0	0	0	0	0	0	0	0	0	0	0	0	0	0	0	0	0	0		1		
1995	5		0	0	0	0	0	0	0	0	9	0	0	0	27	0	0	18	5	1	0	0	0	45	0	0	0	0	0	0	0	0		105		
1995	6		0	0	0	0	0	14	0	4	0	0	2	39	0	0	0	0	6	20	53	28	10	0	2	14	6	15	0	1	1	0		215		
1995	7		4	3	2	3	45	19	16	34	0	3	6	0	0	3	0	2	4	6	16	24	4	4	2	7	8	0	0	4	3	0	2		224	
1995	8		0	24	0	55	32	0	5	0	14	11	0	6	68	5	23	1	2	12	6	1	9	2	27	2	0	0	0	0	0	2	0		307	
1995	9		0	0	35	18	15	24	1	0	0	0	0	0	0	0	0	0	7	28	7	22	0	5	1	38	11	1	17	16	93	6		345		
1995	10		0	0	0	0	0	0	0	0	0	0	0	0	0	0	0	0	0	0	0	0	0	8	0	0	0	0	0	0	0	0		8		
1995	11		5	0	0	0	0	0	0	0	0	57	3	0	0	0	0	0	0	0	1	0	0	0	0	0	0	1	3	0	0	0		70		
1995	12		0	0	0	0	0	0	0	0	0	0	0	0	0	0	0	0	0	0	0	0	0	0	0	0	3	0	0	0	0	0		3	1330	
1996	1		0	0	0	0	0	0	0	0	0	0	0	0	0	0	0	0	0	0	0	0	0	0	0	0	0	0	0	0	0	0		0		
1996	2		0	0	0	0	0	0	0	0	0	0	0	0	0	0	0	0	0	0	0	0	1	0	0	0	11	2	11	0	0			25		
1996	3		0	0	0	0	0	0	0	0	0	0	0	0	0	0	0	0	0	0	0	0	0	0	14	0	0	0	3	0	0	0		17		
1996	4		0	0	0	0	0	0	0	0	0	0	0	3	0	0	0	0	0	0	0	0	0	0	1	14	8	21	0	0	57	0		104		
1996	5		0	18	0	0	0	0	0	0	0	0	0	22	0	0	0	0	0	8	0	0	0	0	0	0	0	1	0	0	11	21		81		
1996	6		0	2	2	1	41	0	0	16	0	1	0	0	1	0	0	0	0	0	0	56	19	7	9	2	0	40	16	2	0	80		295		
1996	7		19	4	0	18	2	19	3	6	24	0	5	0	0	3	0	10	0	8	0	0	5	2	8	2	0	11	2	0	4	0		155		
1996	8		13	4	4	37	7	1	9	12	1	0	1	0	0	1	13	48	43	19	9	20	6	0	0	0	0	0	10	4	9			271		
1996	9		9	7	5	0	1	6	21	1	5	6	0	0	0	0	0	0	45	2	0	0	0	10	0	0	52	8	23	68	0			269		
1996	10		0	0	0	5	0	65	0	0	0	0	0	0	0	0	0	0	0	0	0	0	0	0	0	0	0	0	0	13	98	2	0		183	
1996	11		0	0	0	0	0	0	0	0	0	0	0	0	0	0	0	0	0	0	0	0	0	0	0	0	0	0	0	0	0	0		0		
1996	12		0	0	0	0	0	0	0	0	0	0	0	0	0	0	0	0	0	0	0	0	0	0	0	0	0	0	0	0	0	0		0	1400	
1997	1		0	0	0	0	0	0	0	0	0	0	0	0	0	0	0	0	1	0	0	0	3	0	0	0	0	0	0	0	0	0		4		
1997	2		0	0	0	1	0	0	0	0	0	0	0	0	0	0	0	0	0	0	0	6	0	0	0	0	0	10	26					43		
1997	3		0	0	0	0	0	0	0	0	0	0	0	0	0	0	0	0	0	0	0	0	0	0	23	0	2	0	17	0	0	0		42		
1997	4		0	0	12	0	0	0	0	0	0	0	1	0	5	0	0	19	0	0	0	0	0	0	0	13	0	19	0	12	29	0		110		
1997	5		1	0	0	0	0	0	0	0	0	0	0	0	0	1	8	0	15	0	0	0	25	0	0	1	35	4	0	1	37	4	0		132	
1997	6		0	0	15	0	0	0	0	40	8	24	7	0	0	0	0	27	0	0	0	16	0	0	0	37	4	8	2	11				199		
1997	7		31	61	29	9	0	10	11	2	15	51	105	23	24	3	45	0	0	0	0	17	7	21	7	2	0	0	0	7	0	3	3		486	
1997	8		10	19	0	4	21	0	2	0	0	2	0	16	27	10	15	48	0	0	0	13	0	4	23	0	0	0	2	1	57	27		301		
1997	9		0	6	1	0	0	60	36	0	0	2	24	0	0	83	13	0	3	1	14	46	37	0	5	41	2	76	23	0	0		473			
1997	10		4	10	0	12	0	0	0	0	0	27	0	0	0	0	0	0	0	0	0	0	0	0	0	0	0	0	0	0	0		0	53		
1997	11		0	0	0	0	0	0	0	0	0	0	0	0	0	15	0	0	0	0	0	0	0	0	0	0	0	0	0	0	0		0	15		
1997	12		0	0	0	0	0	0	0	0	10	10	0	0	0	0	0	0	0	0	0	0	0	0	0	0	0	0	0	0	0		0	20	1878	

1998	1	0	0	0	0	0	0	0	0	0	0	0	0	0	0	0	0	0	1	0	0	3	6	0	0	0	0	0	0	0	6	0	0	16	
1998	2	0	0	0	0	0	0	0	0	0	0	0	0	0	0	0	0	0	3	0	0	0	0	0	0	0	2	7	0				12		
1998	3	0	0	0	0	0	0	13	0	0	0	0	0	2	0	0	0	0	0	0	0	0	0	0	31	0	0	0	0	0	6	16		68	
1998	4	0	0	0	0	0	0	5	0	17	0	0	0	0	0	0	0	1	1	4	1	0	1	63	1	14	0	0	1	0			109		
1998	5	0	23	0	27	0	37	0	11	0	21	0	0	0	2	0	8	1	0	0	0	0	39	0	0	0	4	69	6	5	0	16		269	
1998	6	0	0	0	0	0	0	0	0	0	0	0	0	0	12	15	4	0	0	31	0	0	6	5	1	2	0	4	2	19	0		101		
1998	7	0	3	1	3	5	2	5	77	5	22	2	4	57	43	5	74	15	7	10	15	17	1	25	1	7	0	0	0	0	1	6		413	
1998	8	0	9	0	6	0	2	13	10	0	0	4	3	5	107	3	1	6	3	0	8	7	0	0	0	0	0	0	0	17	0	21		225	
1998	9	3	1	12	10	0	2	15	0	6	19	75	49	21	0	0	0	10	45	0	0	0	0	0	0	0	0	0	0	17	0			285	
1998	10	0	3	0	10	1	0	0	0	0	0	11	4	0	0	0	4	0	9	0	1	12	3	24	4	0	0	0	0	0	0	10		96	
1998	11	2	10	0	0	0	0	0	0	0	0	7	0	0	0	0	0	0	0	0	0	0	0	21	2	0	0	0	0	0	0	0		42	
1998	12	0	0	0	0	0	0	0	0	0	0	0	0	0	0	0	0	0	0	0	0	0	0	0	0	0	0	0	0	0	0	0	0		1636
1999	1	0	0	0	0	0	0	0	0	0	0	0	0	0	0	0	0	0	0	0	0	0	0	0	0	0	0	0	0	0	0	0	0		0
1999	2	0	0	0	0	0	0	0	0	0	0	0	0	0	0	0	0	0	0	0	0	0	0	0	0	0	0	0	0	0	0	0	0		0
1999	3	0	0	0	0	0	0	0	0	0	0	0	0	0	0	0	0	0	0	0	0	0	0	0	0	0	0	0	0	0	0	0	0		0
1999	4	0	0	0	0	0	0	0	0	0	2	0	0	0	0	0	0	0	0	0	0	0	0	0	0	0	0	0	0	0	0	0	0		2
1999	5	0	0	0	0	0	0	1	0	4	5	0	8	0	15	13	6	0	3	0	0	0	0	3	0	54	0	47	5	39	0			203	
1999	6	0	0	0	0	0	0	0	0	16	8	25	0	0	45	0	0	1	5	0	0	25	121	51	8	17	8	38	17	1				386	
1999	7	18	54	8	25	0	0	0	0	0	31	11	17	64	8	3	7	0	0	35	38	25	10	4	0	0	0	9	3	23	14	0		407	
1999	8	0	0	0	0	0	2	1	16	0	14	0	63	5	38	4	10	2	0	0	2	2	0	0	14	41	1	15	15	3	1			249	
1999	9	0	6	0	3	0	0	0	0	5	0	15	19	4	22	1	2	0	19	5	0	29	52	6	30	29	38	3	0	9	0			297	
1999	10	3	9	0	2	4	0	1	3	5	0	0	0	0	58	0	0	98	13	5	3	0	1	0	0	0	0	0	0	0	0	0		205	
1999	11	0	3	0	0	0	0	0	0	0	0	0	0	0	0	0	0	0	0	0	0	0	0	0	0	0	0	0	0	0	0	0		3	
1999	12	0	0	0	0	0	0	0	0	0	0	0	0	0	0	0	0	0	0	0	0	0	0	0	0	0	0	0	0	0	0	0	0		1752
2000	1	0	0	0	0	0	0	0	0	0	0	0	0	0	0	4	0	0	0	0	0	0	0	0	0	0	0	0	0	4	0	0		8	
2000	2	0	0	2	0	0	40	12	0	0	0	0	2	5	0	0	0	0	0	0	0	0	0	0	0	0	0	0	0	0	0	0		61	
2000	3	0	0	0	0	0	0	0	0	0	0	0	0	18	0	0	0	0	0	0	2	0	0	0	0	0	0	0	0	0	0	0		20	
2000	4	0	0	0	0	0	0	0	0	0	0	13	0	0	0	41	0	2	0	0	22	9	7	0	0	55	51	0	6	0			206		
2000	5	0	27	1	0	0	0	0	0	0	0	0	0	33	1	0	1	20	0	0	38	23	51	18	0	2	8	0	10	0	0		233		
2000	6	0	0	0	0	33	0	8	9	5	0	11	31	0	0	29	0	3	7	4	10	12	1	7	13	0	14	12	0	0	3		212		
2000	7	4	0	0	0	0	3	0	0	2	28	0	2	13	4	64	13	0	19	21	4	16	4	14	12	12	6	0	0	0	0		241		
2000	8	0	33	11	0	0	0	0	0	1	3	22	1	0	0	0	0	22	0	3	1	0	0	0	23	0	2	0	3	22			147		
2000	9	71	46	7	0	0	30	0	6	22	7	0	0	0	16	8	7	12	76	123	39	8	2	71	0	0	0	0	0	0	0		551		
2000	10	0	4	8	0	1	8	0	0	0	0	7	0	0	0	10	0	3	0	7	0	13	0	0	0	0	0	49	19	0	0		129		
2000	11	0	0	0	0	0	0	0	0	0	0	0	0	0	0	0	0	0	0	0	0	0	0	0	0	0	0	0	0	0	0		0		
2000	12	0	0	0	0	0	0	0	0	0	0	0	0	0	0	0	0	0	0	0	0	0	0	0	0	0	0	0	0	0	0	0		1808	
2001	1	0	0	0	0	0	0	0	0	0	0	0	0	0	0	0	0	0	0	0	0	0	0	0	0	0	0	0	0	0	0	0		0	
2001	2	0	0	0	0	0	0	0	0	0	0	0	0	0	0	0	0	0	0	0	0	0	0	0	0	0	0	0	0	0	0	0		0	
2001	3	0	0	0	0	0	0	0	0	0	0	0	0	0	5	0	0	0	0	0	0	0	15	0	0	0	0	0	0	0	0	0		20	
2001	4	0	12	0	0	0	0	0	0	0	0	0	0	3	23	0	6	0	0	0	0	0	0	0	0	0	0	0	7	1			52		
2001	5	7	0	7	16	0	1	0	47	0	15	7	0	0	0	0	0	0	0	6	31	41	0	27	27	13	0	1	0	0	11		257		
2001	6	6	6	2	67	4	0	0	0	0	0	1	0	3	18	18	61	47	58	17	75	0	3	6	5	0	0	7	0	5			409		
2001	7	4	27	0	0	0	0	0	0	3	9	6	2	0	1	3	20	0	0	1	5	10	30	3	0	0	22	0	4	12	3		165		
2001	8	4	7	37	0	0	0	0	1	5	2	0	0	2	0	0	0	2	3	0	0	1	7	9	1	4	17	1	0	55			158		
2001	9	10	5	7	0	46	3	0	103	3	15	58	6	5	0	15	0	0	28	3	0	0	0	0	0	0	0	0	27	0	0		334		
2001	10	8	8	16	16	8	1	0	1	2	1	0	0	0	1	0	2	10	0	0	0	0	0	0	0	0	0	0	0	0	0		74		
2001	11	0	0	0	9	0	0	0	0	0	0	0	1	0	0	0	0	0	0	0	0	0	0	0	0	0	0	0	0	0	0		10		
2001	12	0	0	0	0	0	0	0	0	0	0	0	0	0	0	0	0	0	0	0	0	0	0	0	0	0	0	0	0	0	0		1479		

Sample of a converted data in Microsoft Excel sheet from Word pad:

Station Name: Teknuf

Year	Month	Day -1	2	3	4	5	6	7	8	9	10	11	12	13	14	15	16	17	18	19	20	21	22	23	24	25	26	27	28	29	30	31	Rainfall/Month (mm)
1995	1	0	0	0	0	0	0	0	0	0	0	0	0	0	0	0	0	0	0	0	0	0	0	0	0	0	0	0	0	0	0	0	0
1995	2	0	0	0	0	0	0	0	0	0	0	0	0	0	0	0	0	0	0	0	0	3	0	0	0	0	0	0	0	0	0	0	0
1995	3	0	0	0	0	0	0	0	0	0	0	0	0	0	0	0	0	0	0	0	0	0	0	0	0	0	0	0	0	0	1	0	
1995	4	0	0	0	0	0	0	0	0	63	0	0	0	0	0	0	0	0	0	0	0	0	0	0	0	0	0	0	0	0	0	0	
1995	5	0	0	0	0	0	0	0	0	0	0	0	14	17	15	53	104	61	5	0	0	4	0	0	0	0	0	0	0	0	0	0	5
1995	6	0	0	24	31	3	9	48	66	12	88	263	92	62	38	0	4	17	17	1	14	50	57	60	69	43	21	29	0	5	0		
1995	7	48	171	80	43	103	7	0	14	15	0	6	47	58	38	34	40	45	9	14	16	63	140	16	4	0	15	5	13	0	36	140	
1995	8	19	11	77	18	14	6	60	42	36	0	10	50	3	94	56	0	3	54	25	8	14	9	4	9	0	0	0	0	0	0	0	
1995	9	0	67	66	58	36	58	16	0	0	48	17	0	6	1	23	9	30	22	9	1	3	3	33	6	3	22	16	0	10	0	0	
1995	10	0	0	1	6	0	0	8	8	0	0	0	0	0	0	0	4	0	0	14	6	0	0	0	0	0	0	0	0	0	0	0	
1995	11	10	55	14	0	3	0	8	0	1	0	49	44	6	0	0	0	0	0	30	91	0	12	0	0	25	17	0	0	0	0	0	
1995	12	0	0	0	0	0	0	0	0	0	0	0	0	0	0	0	0	0	0	0	0	0	0	0	0	0	0	0	0	0	0	0	
1996	1	0	0	0	0	0	0	0	0	0	0	0	0	0	0	0	0	0	0	0	0	0	0	0	0	0	0	0	0	0	0	0	
1996	2	0	0	0	0	0	0	0	0	0	0	0	0	0	0	0	0	0	0	0	0	0	0	3	8	77	0	0	0	0	0	0	
1996	3	0	0	0	0	0	0	0	0	0	0	0	0	0	0	0	0	0	0	0	0	0	0	0	0	0	0	0	0	0	0	0	
1996	4	0	4	0	0	0	0	0	0	0	0	0	0	0	0	0	0	0	0	0	0	0	0	0	0	0	59	12	4	0	0	4	
1996	5	0	0	0	0	0	21	26	11	15	0	0	45	7	0	20	5	0	0	3	0	0	0	0	0	0	78	15	2	0	13	0	
1996	6	0	0	8	0	30	0	0	0	0	0	4	0	0	0	0	20	19	69	144	115	7	28	65	23	18	0	15	26	58	0	0	
1996	7	29	8	73	30	26	86	37	0	0	0	17	0	6	0	27	3	0	7	16	24	28	52	59	168	57	266	43	58	91	0	1	
1996	8	59	20	40	65	89	31	37	139	8	10	0	0	9	2	15	20	22	18	25	15	92	21	0	27	49	13	0	24	11	5	0	
1996	9	0	24	26	14	8	21	4	0	0	7	15	0	0	0	0	13	105	37	11	0	27	32	4	26	1	32	51	0	0	0	0	
1996	10	0	0	0	237	45	38	33	2	0	0	0	0	0	0	0	0	1	0	0	0	0	0	0	0	0	0	17	62	90	136	26	
1996	11	0	0	0	5	0	13	0	0	0	0	0	0	0	0	0	0	0	0	0	0	0	0	0	0	0	0	0	0	0	0	0	
1996	12	0	0	0	0	0	0	0	0	0	0	0	0	0	0	0	0	0	0	0	0	0	0	0	0	0	0	0	0	0	0	0	
1997	1	0	0	0	0	0	0	0	0	0	0	0	0	0	0	0	0	0	0	0	0	0	0	0	0	0	0	0	0	0	0	0	0
1997	2	0	44	0	0	4	0	0	0	0	0	0	0	0	0	0	0	0	0	0	0	0	0	0	0	0	0	0	0	0	0	0	0
1997	3	0	0	0	0	0	0	0	0	0	0	0	0	0	0	0	0	0	0	0	0	1	0	0	27	5	0	0	0	0	0	0	0
1997	4	0	2	0	0	0	0	0	0	2	6	10	0	18	4	0	0	6	1	0	0	0	0	0	0	0	0	0	0	0	0	0	0
1997	5	0	0	0	0	0	0	0	0	0	0	0	0	0	0	0	0	0	26	75	0	0	3	41	9	15	15	8	49	2	0	0	
1997	6	0	0	0	15	0	29	7	1	0	0	7	1	15	118	71	0	27	17	23	109	8	0	52	1	13	45	6	3	17	0	0	
1997	7	115	48	64	21	99	78	47	12	84	33	27	26	27	5	4	1	7	44	48	64	133	112	37	11	0	19	0	7	21	75	84	
1997	8	115	125	73	0	22	44	3	4	0	25	34	26	34	68	42	0	4	0	3	7	3	0	0	0	0	23	0	0	62	11	14	
1997	9	0	0	0	38	12	60	42	141	0	0	0	0	3	63	21	0	0	10	4	0	0	0	9	0	87	59	63	13	19	22	0	0
1997	10	10	4	0	0	0	0	0	5	4	0	0	0	0	0	0	0	0	0	0	0	0	0	0	0	0	0	0	0	0	0	0	0
1997	11	0	0	0	0	0	0	0	32	0	0	5	6	3	0	0	0	0	0	0	0	0	0	0	0	0	0	0	0	0	0	0	0
1997	12	0	0	0	0	0	0	0	0	0	0	10	0	0	0	5	0	0	1	0	0	0	0	0	0	0	0	0	0	0	0	0	0

Rainfall/Year
(mm)

4285

4322

3807

4263

4720

4987

4595

3929

4451

4141

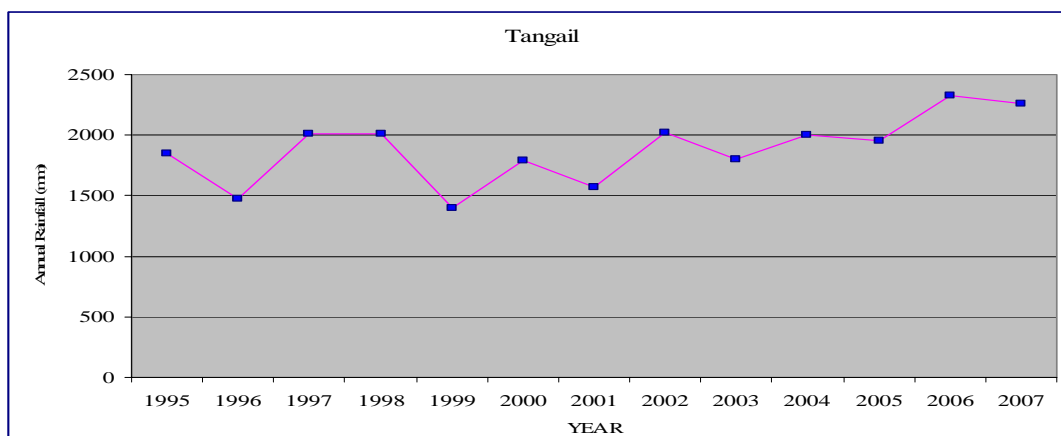
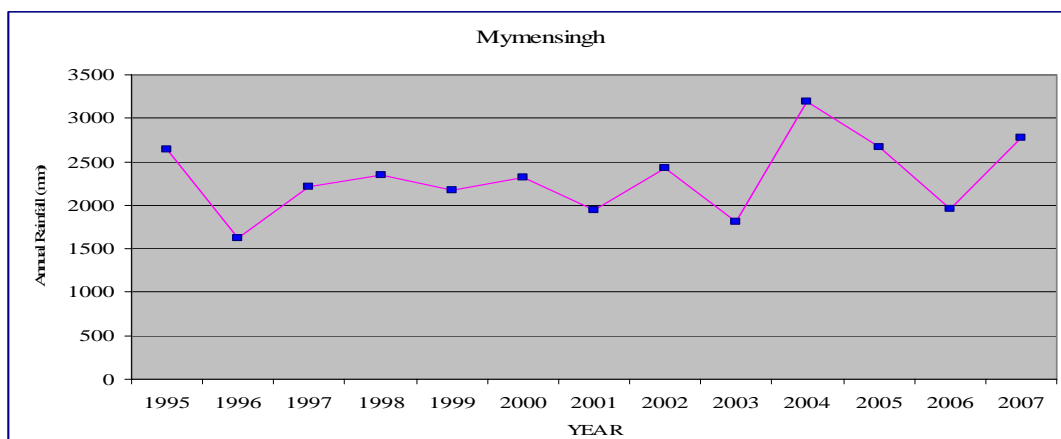
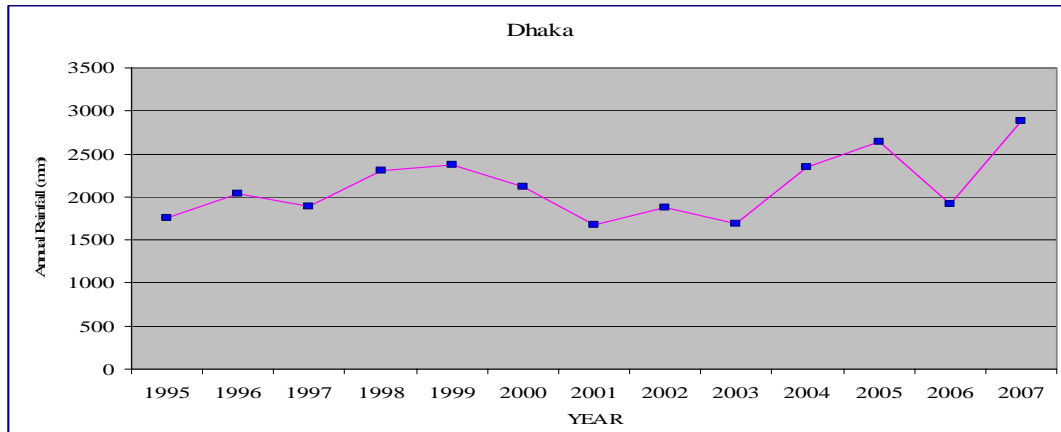
3992

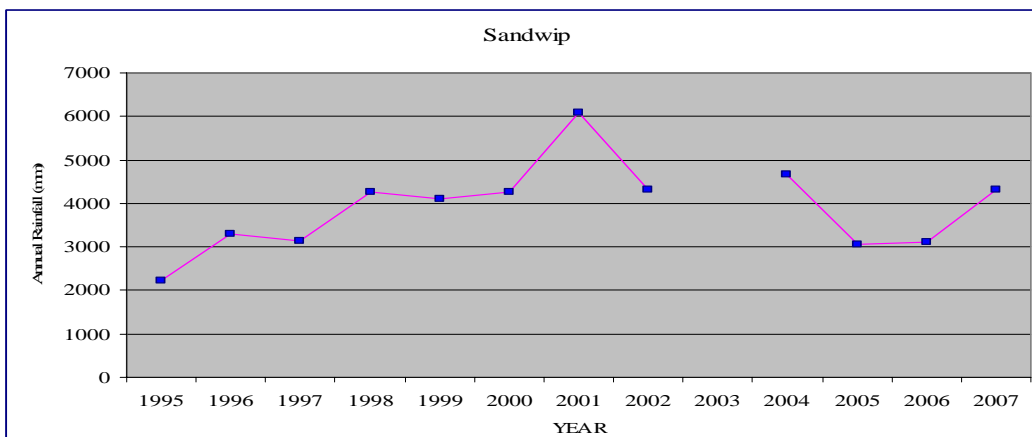
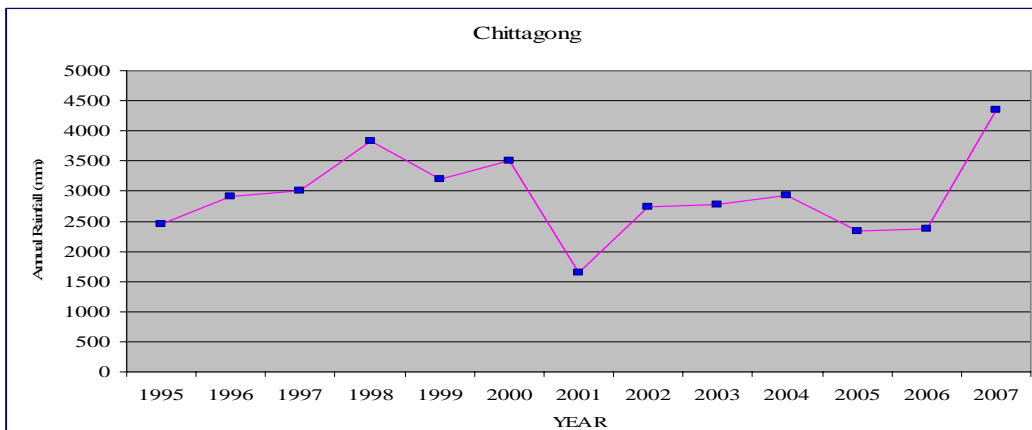
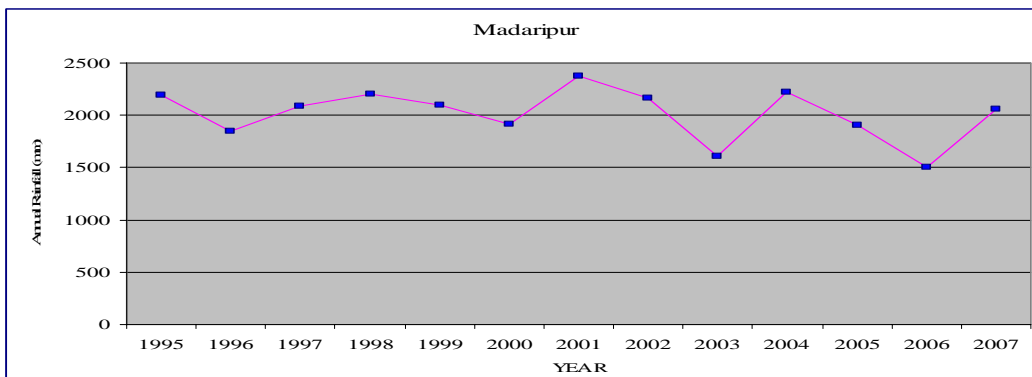
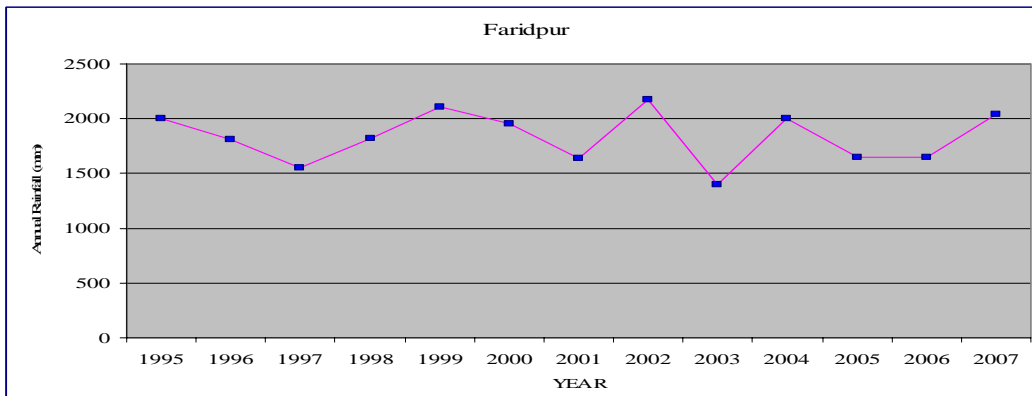
4732

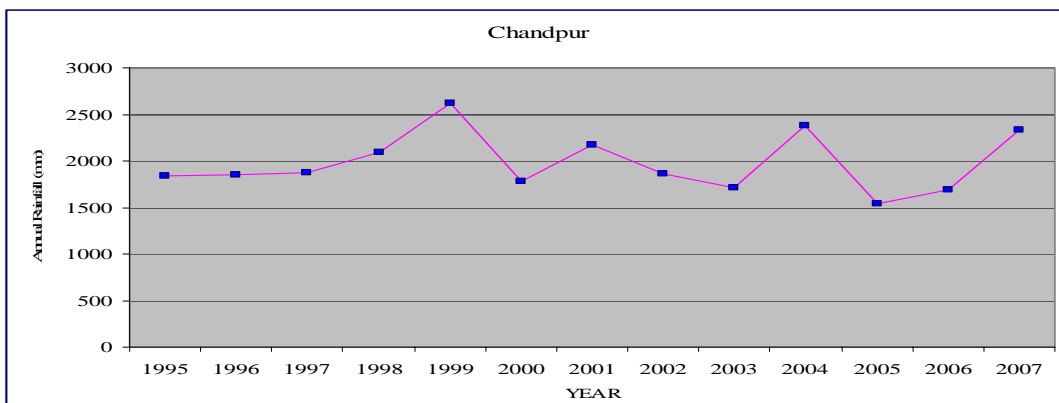
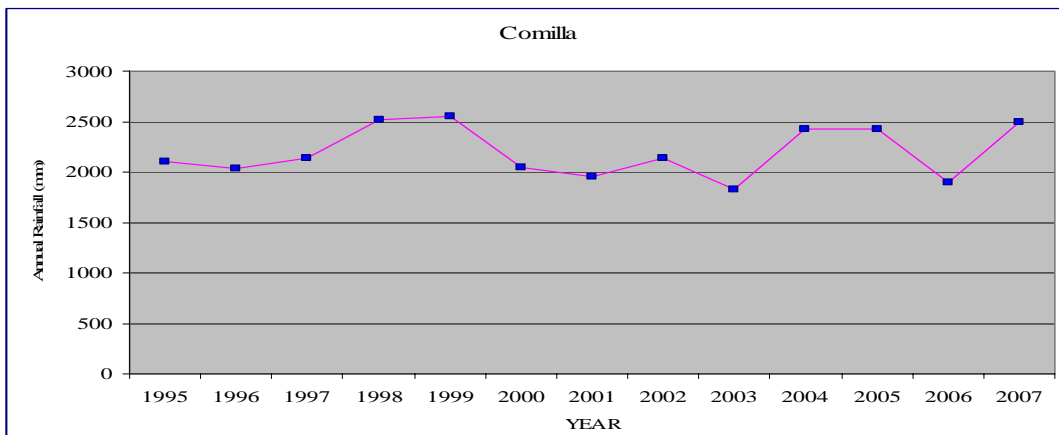
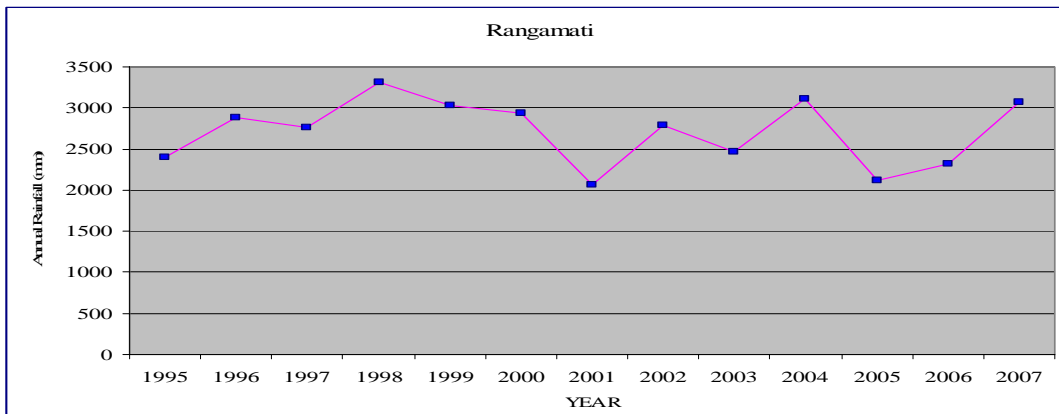
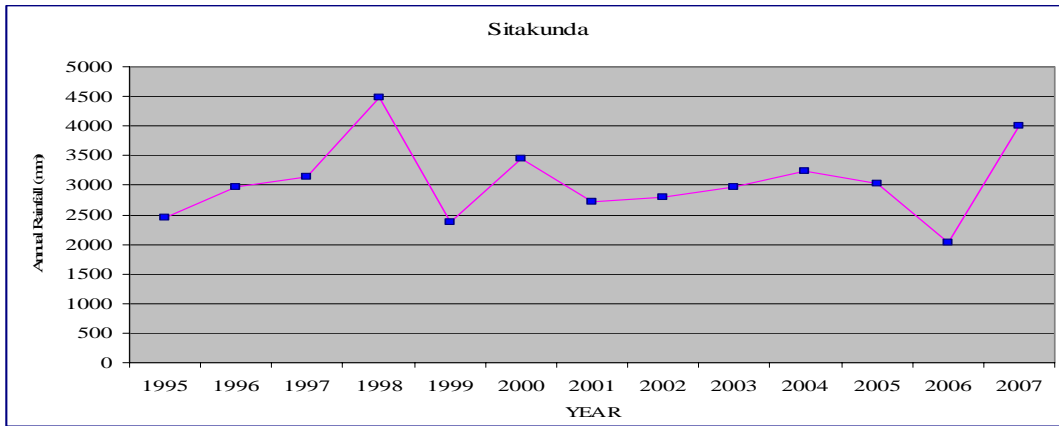
4465

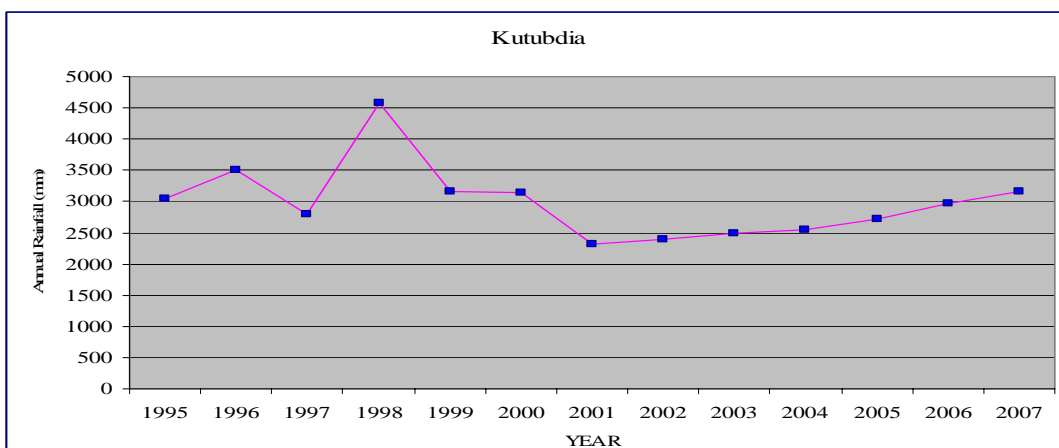
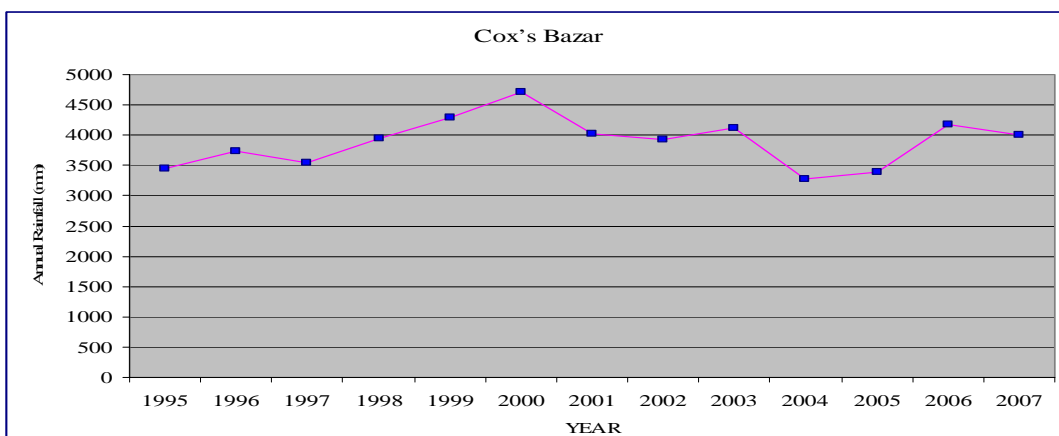
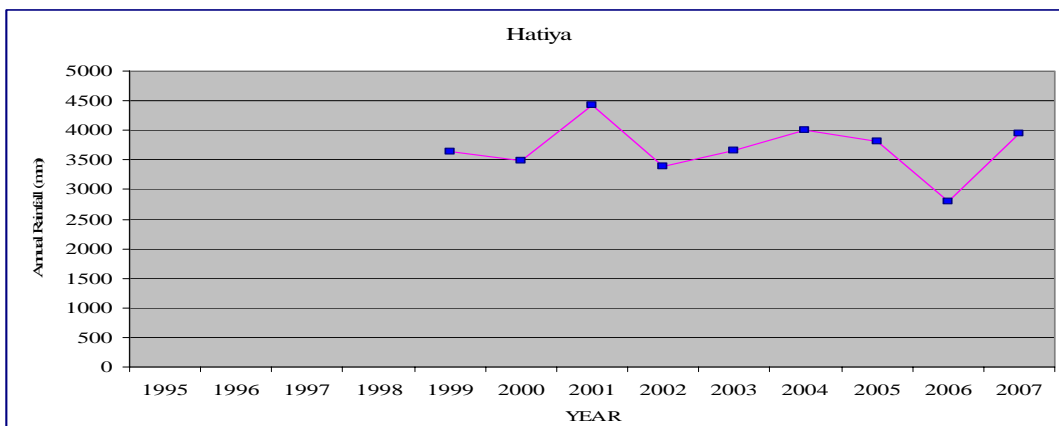
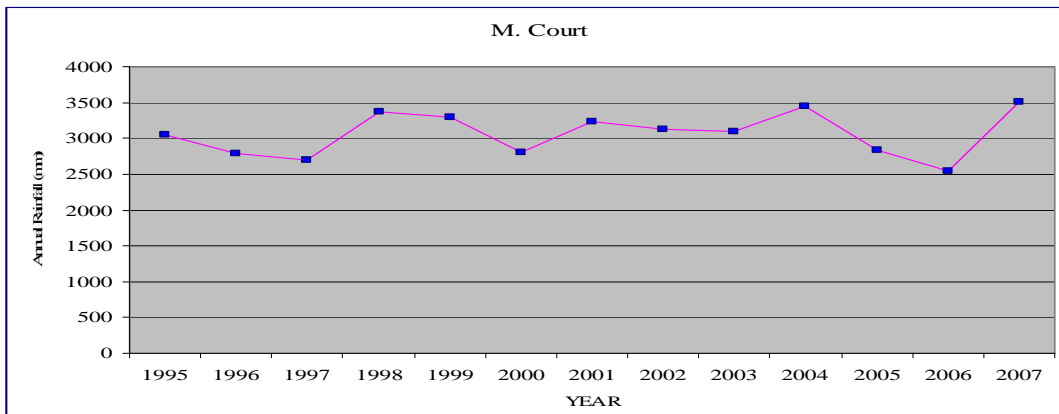
APPENDIX – B:

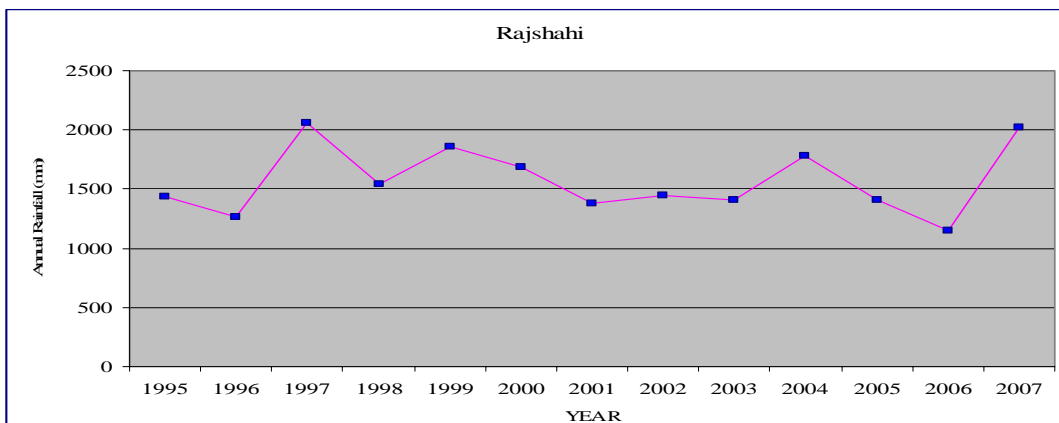
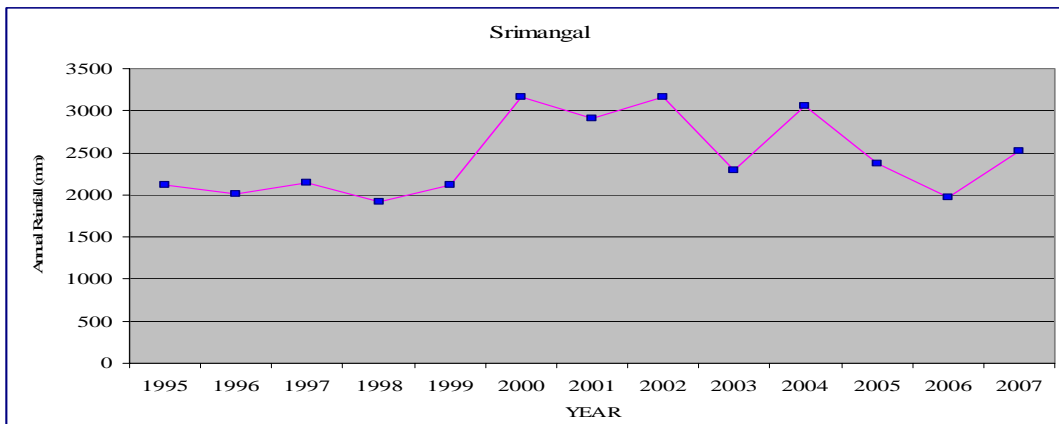
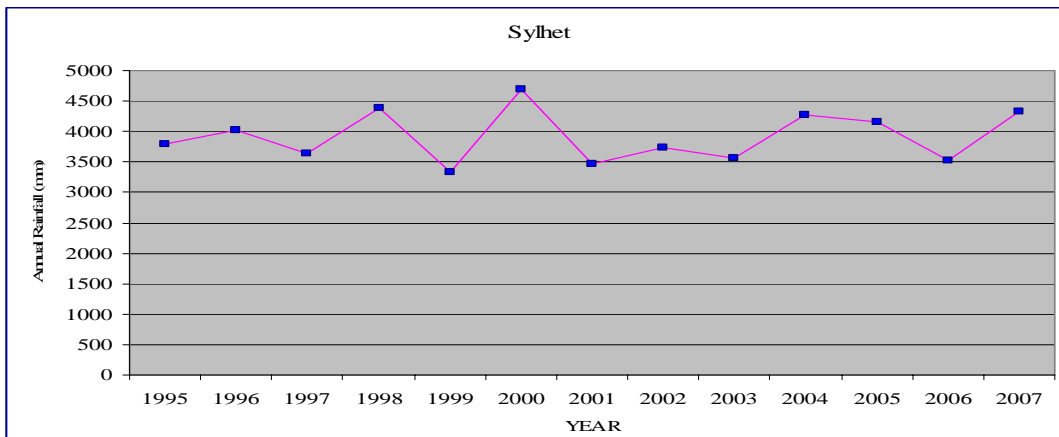
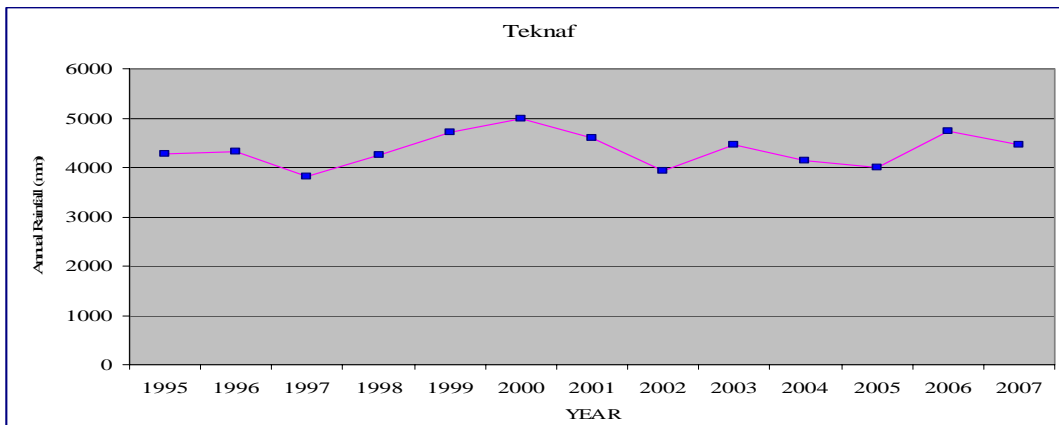
Annual rainfall rate of 34 rain gauge station for the period of 13 years are plotted as follows:

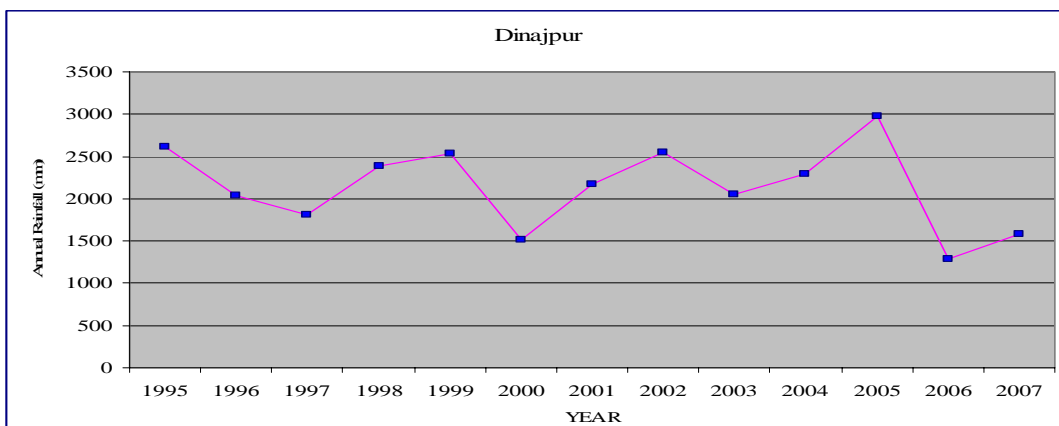
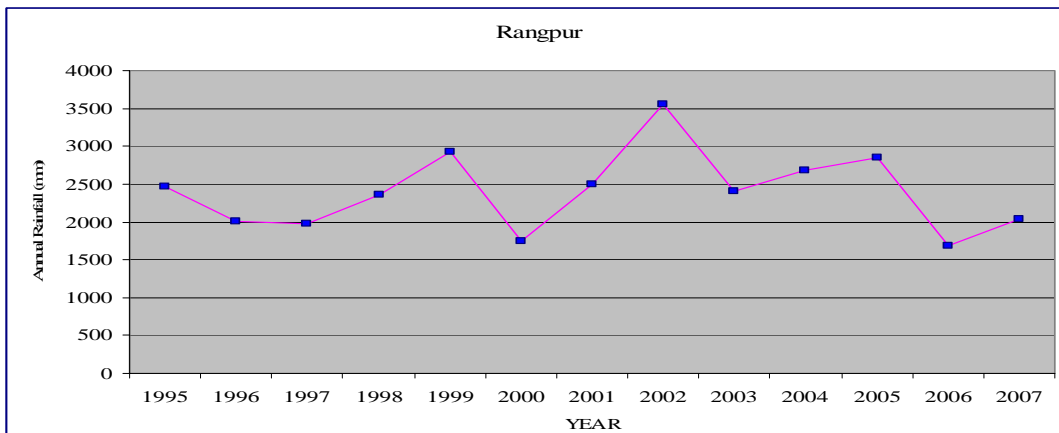
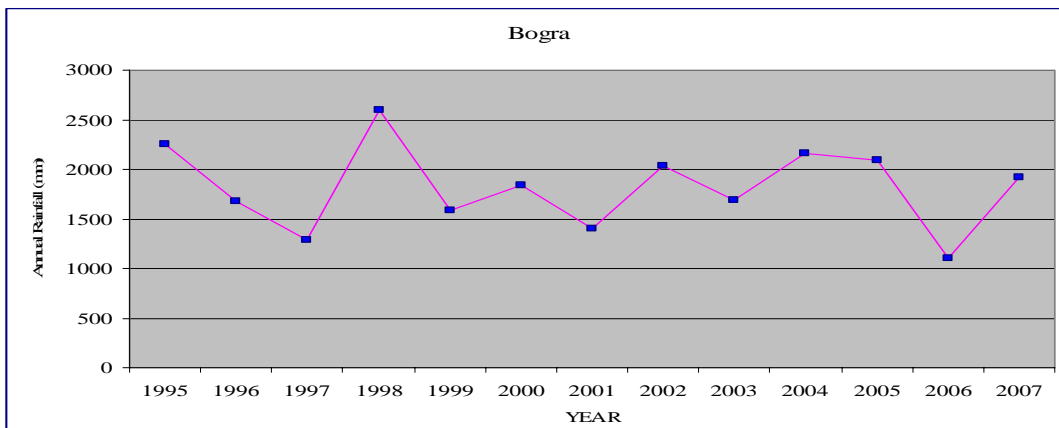
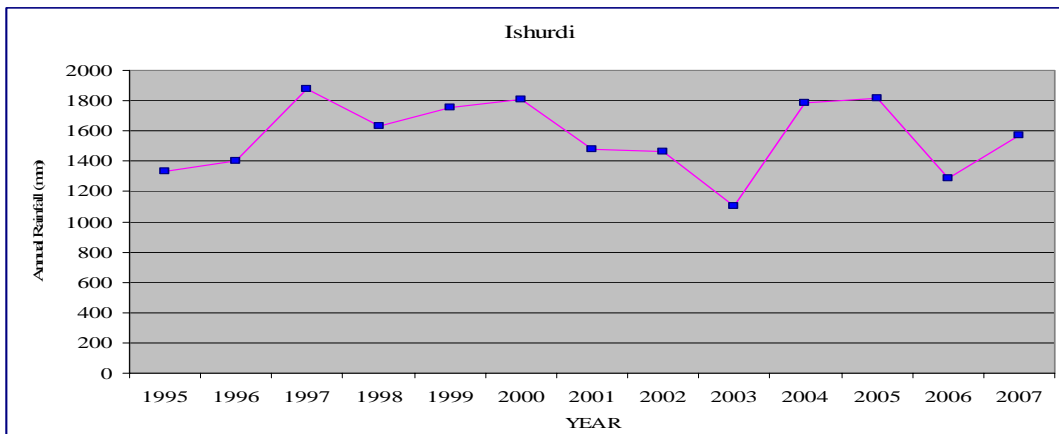


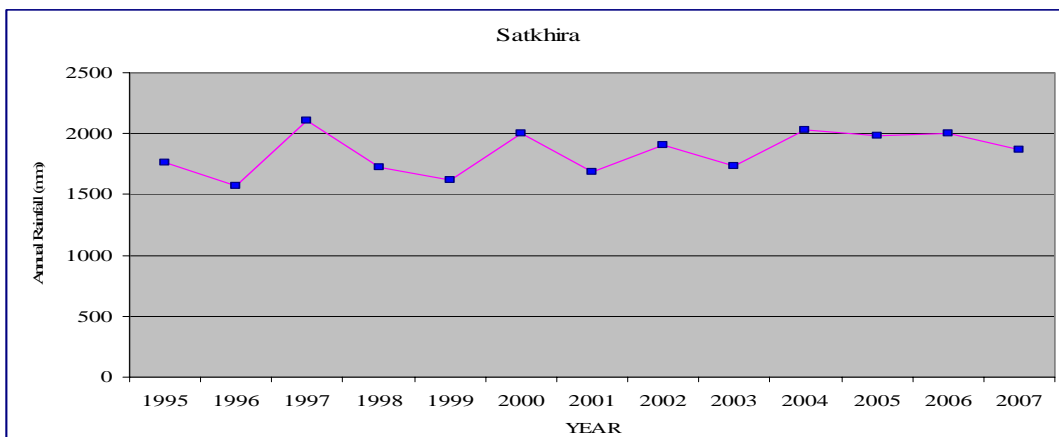
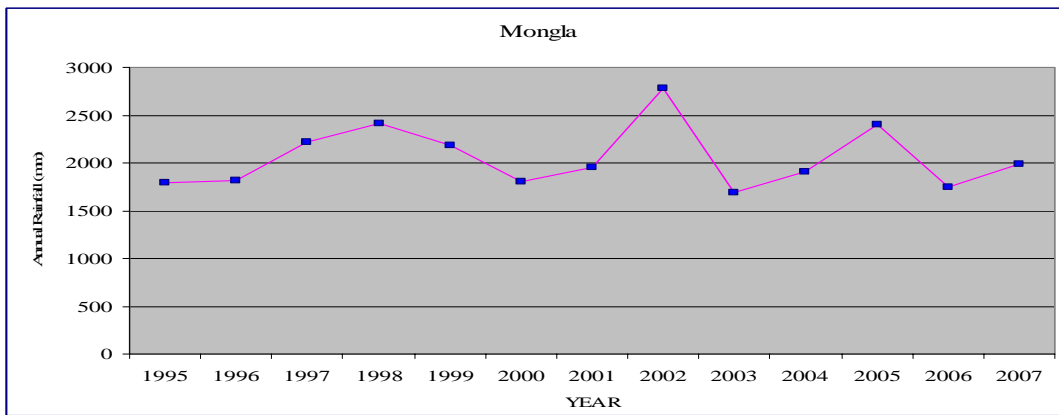
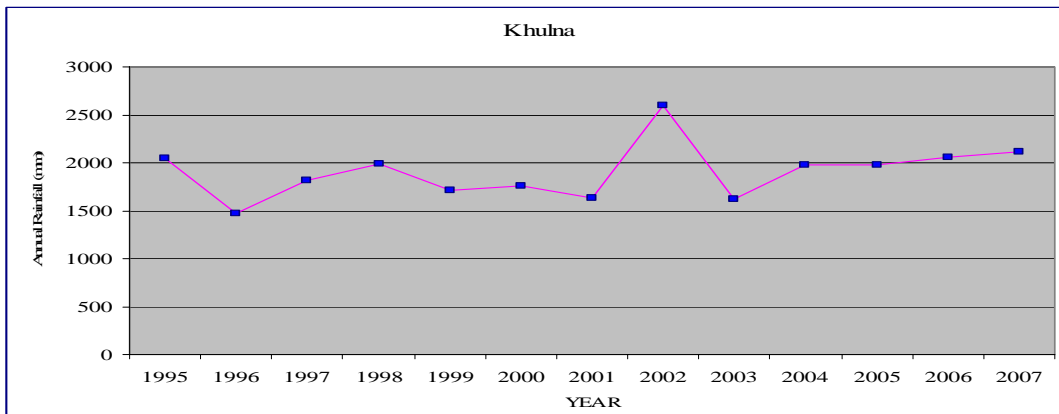
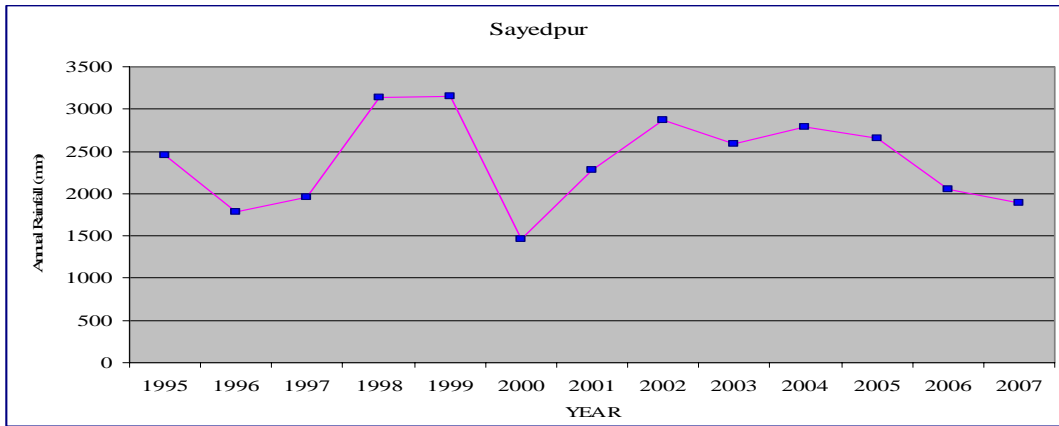


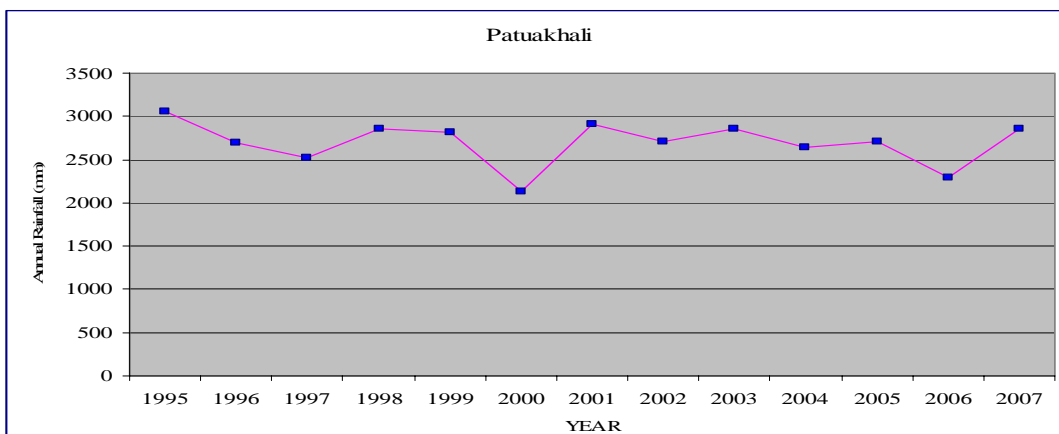
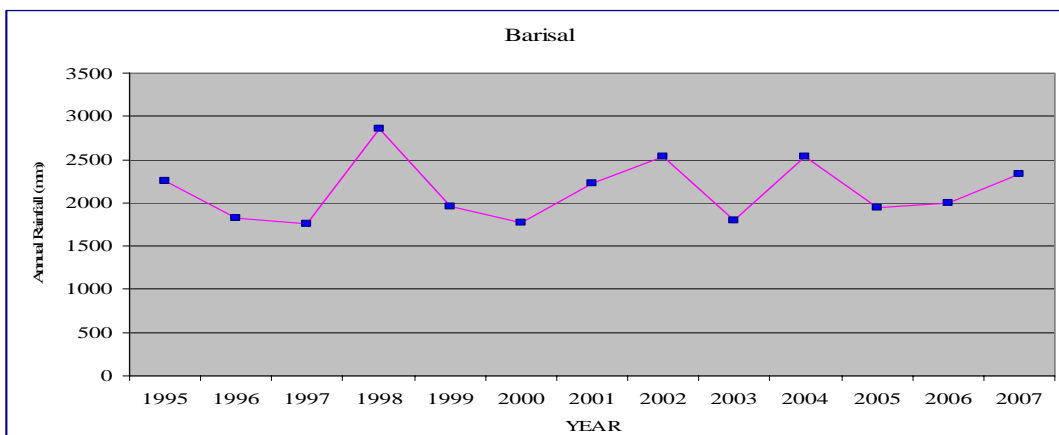
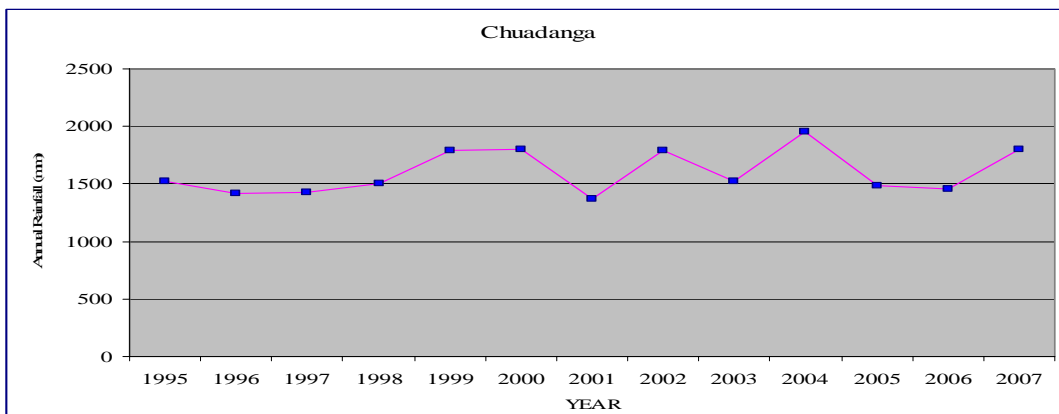
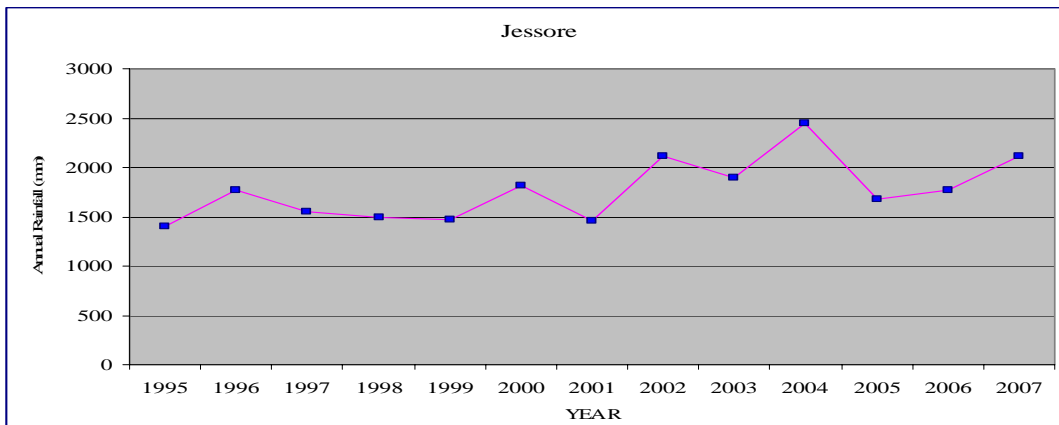


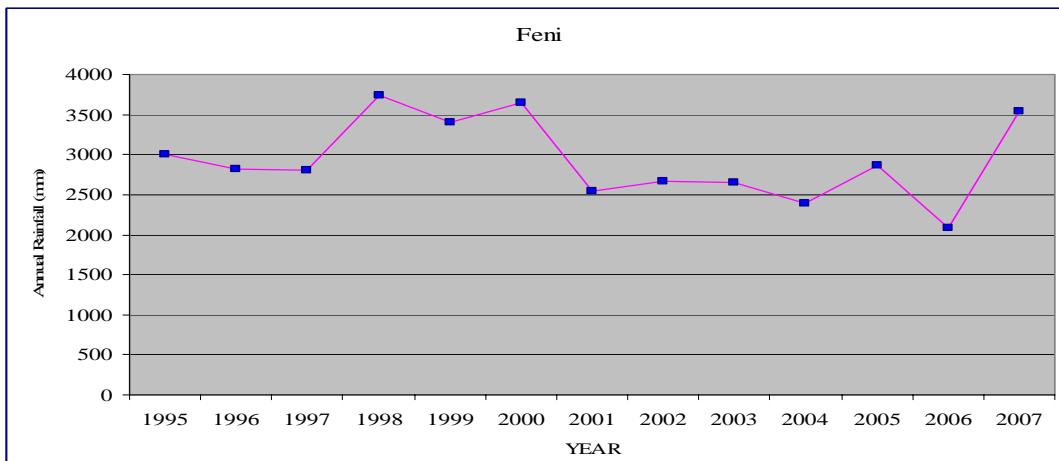
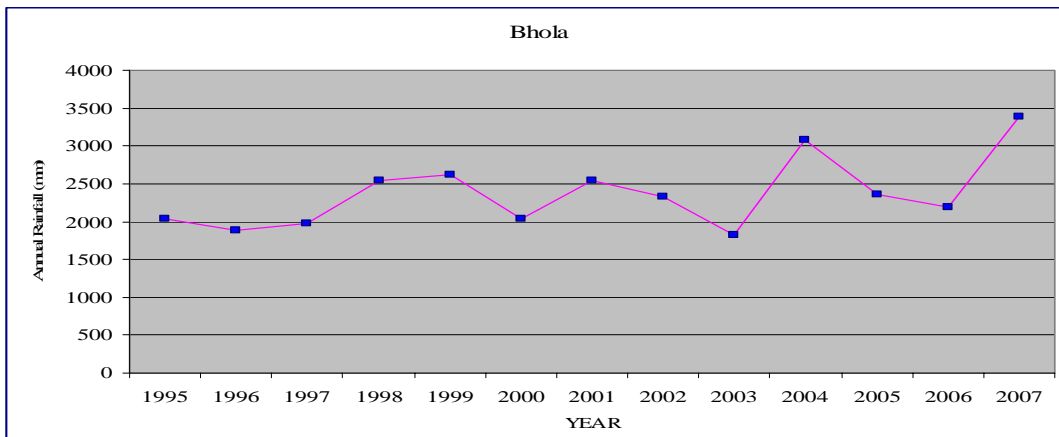
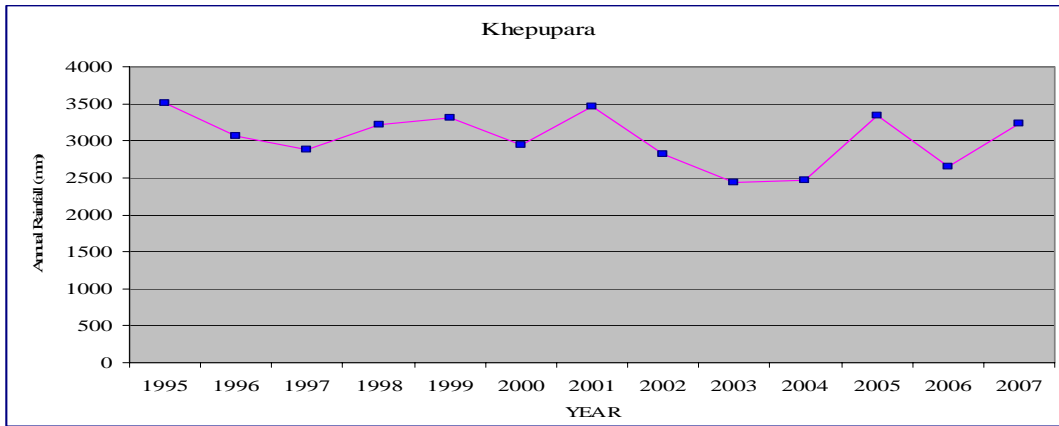












APPENDIX – C:

RECOMMENDATION ITU-R P.838-3

The specific attenuation γ_R (dB/km) is obtained from the rain rate R (mm/h) using the power-law relationship:

$$\gamma_R = kR^\alpha \quad (1)$$

Values for the coefficients k and α are determined as functions of frequency, f (GHz), in the range from 1 to 1 000 GHz, from the following equations, which have been developed from curve-fitting to power-law coefficients derived from scattering calculations:

$$\log_{10} k = \sum_{j=1}^4 a_j \exp \left[- \left(\frac{\log_{10} f - b_j}{c_j} \right)^2 \right] + m_k \log_{10} f + c_k \quad (2)$$

$$\alpha = \sum_{j=1}^5 a_j \exp \left[- \left(\frac{\log_{10} f - b_j}{c_j} \right)^2 \right] + m_\alpha \log_{10} f + c_\alpha \quad (3)$$

where:

- f : frequency (GHz)
- k : either k_H or k_V
- α : either α_H or α_V .

Values for the constants for the coefficient k_H for horizontal polarization are given in Table 1 and for the coefficient k_V for vertical polarization in Table 2. Table 3 gives the values for the constants for the coefficient α_H for horizontal polarization, and Table 4 gives the values for the constants for the coefficient α_V for vertical polarization.

TABLE 1
Coefficients for k_H

j	a_j	b_j	c_j	m_k	c_k
1	-5.33980	-0.10008	1.13098	-0.18961	0.71147
2	-0.35351	1.26970	0.45400		
3	-0.23789	0.86036	0.15354		
4	-0.94158	0.64552	0.16817		

TABLE 2
Coefficients for k_V

j	a_j	b_j	c_j	m_k	c_k
1	-3.80595	0.56934	0.81061	-0.16398	0.63297
2	-3.44965	-0.22911	0.51059		
3	-0.39902	0.73042	0.11899		
4	0.50167	1.07319	0.27195		

TABLE 3
Coefficients for α_H

j	a_j	b_j	c_j	m_α	c_α
1	-0.14318	1.82442	-0.55187	0.67849	-1.95537
2	0.29591	0.77564	0.19822		
3	0.32177	0.63773	0.13164		
4	-5.37610	-0.96230	1.47828		
5	16.1721	-3.29980	3.43990		

TABLE 4
Coefficients for α_V

j	a_j	b_j	c_j	m_α	c_α
1	-0.07771	2.33840	-0.76284	-0.053739	0.83433
2	0.56727	0.95545	0.54039		
3	-0.20238	1.14520	0.26809		
4	-48.2991	0.791669	0.116226		
5	48.5833	0.791459	0.116479		

For linear and circular polarization, and for all path geometries, the coefficients in equation (1) can be calculated from the values given by equations (2) and (3) using the following equations:

$$k = [k_H + k_V + (k_H - k_V) \cos^2 \theta \cos 2 \tau] / 2 \quad (4)$$

$$\alpha = [k_H \alpha_H + k_V \alpha_V + (k_H \alpha_H - k_V \alpha_V) \cos^2 \theta \cos 2 \tau] / 2k \quad (5)$$

where θ is the path elevation angle and τ is the polarization tilt angle relative to the horizontal ($\tau = 45^\circ$ for circular polarization).

For quick reference, the coefficients k and α are shown graphically in Figs. 1 to 4, and Table 5 lists numerical values for the coefficients at given frequencies.

TABLE 5
Frequency-dependent coefficients for estimating specific rain attenuation using equations (4), (5) and (1)

Frequency (GHz)	k_H	α_H	k_V	α_V
1	0.0000259	0.9691	0.0000308	0.8592
1.5	0.0000443	1.0185	0.0000574	0.8957
2	0.0000847	1.0664	0.0000998	0.9490

2.5	0.0001321	1.1209	0.0001464	1.0085
3	0.0001390	1.2322	0.0001942	1.0688
3.5	0.0001155	1.4189	0.0002346	1.1387
4	0.0001071	1.6009	0.0002461	1.2476
4.5	0.0001340	1.6948	0.0002347	1.3987
5	0.0002162	1.6969	0.0002428	1.5317
5.5	0.0003909	1.6499	0.0003115	1.5882
6	0.0007056	1.5900	0.0004878	1.5728
7	0.001915	1.4810	0.001425	1.4745
8	0.004115	1.3905	0.003450	1.3797
9	0.007535	1.3155	0.006691	1.2895
10	0.01217	1.2571	0.01129	1.2156
11	0.01772	1.2140	0.01731	1.1617
12	0.02386	1.1825	0.02455	1.1216
13	0.03041	1.1586	0.03266	1.0901
14	0.03738	1.1396	0.04126	1.0646
15	0.04481	1.1233	0.05008	1.0440
16	0.05282	1.1086	0.05899	1.0273
17	0.06146	1.0949	0.06797	1.0137
18	0.07078	1.0818	0.07708	1.0025
19	0.08084	1.0691	0.08642	0.9930
20	0.09164	1.0568	0.09611	0.9847
21	0.1032	1.0447	0.1063	0.9771
22	0.1155	1.0329	0.1170	0.9700
23	0.1286	1.0214	0.1284	0.9630
24	0.1425	1.0101	0.1404	0.9561
25	0.1571	0.9991	0.1533	0.9491
26	0.1724	0.9884	0.1669	0.9421
27	0.1884	0.9780	0.1813	0.9349
28	0.2051	0.9679	0.1964	0.9277
29	0.2224	0.9580	0.2124	0.9203
30	0.2403	0.9485	0.2291	0.9129
31	0.2588	0.9392	0.2465	0.9055
32	0.2778	0.9302	0.2646	0.8981
33	0.2972	0.9214	0.2833	0.8907
34	0.3171	0.9129	0.3026	0.8834

35	0.3374	0.9047	0.3224	0.8761
36	0.3580	0.8967	0.3427	0.8690
37	0.3789	0.8890	0.3633	0.8621
38	0.4001	0.8816	0.3844	0.8552
39	0.4215	0.8743	0.4058	0.8486
40	0.4431	0.8673	0.4274	0.8421
41	0.4647	0.8605	0.4492	0.8357
42	0.4865	0.8539	0.4712	0.8296
43	0.5084	0.8476	0.4932	0.8236
44	0.5302	0.8414	0.5153	0.8179
45	0.5521	0.8355	0.5375	0.8123
46	0.5738	0.8297	0.5596	0.8069
47	0.5956	0.8241	0.5817	0.8017
48	0.6172	0.8187	0.6037	0.7967
49	0.6386	0.8134	0.6255	0.7918
50	0.6600	0.8084	0.6472	0.7871
51	0.6811	0.8034	0.6687	0.7826
52	0.7020	0.7987	0.6901	0.7783
53	0.7228	0.7941	0.7112	0.7741
54	0.7433	0.7896	0.7321	0.7700
55	0.7635	0.7853	0.7527	0.7661
56	0.7835	0.7811	0.7730	0.7623
57	0.8032	0.7771	0.7931	0.7587
58	0.8226	0.7731	0.8129	0.7552
59	0.8418	0.7693	0.8324	0.7518
60	0.8606	0.7656	0.8515	0.7486
61	0.8791	0.7621	0.8704	0.7454
62	0.8974	0.7586	0.8889	0.7424
63	0.9153	0.7552	0.9071	0.7395
64	0.9328	0.7520	0.9250	0.7366
65	0.9501	0.7488	0.9425	0.7339
66	0.9670	0.7458	0.9598	0.7313
67	0.9836	0.7428	0.9767	0.7287
68	0.9999	0.7400	0.9932	0.7262
69	1.0159	0.7372	1.0094	0.7238
70	1.0315	0.7345	1.0253	0.7215
71	1.0468	0.7318	1.0409	0.7193

72	1.0618	0.7293	1.0561	0.7171
73	1.0764	0.7268	1.0711	0.7150
74	1.0908	0.7244	1.0857	0.7130
75	1.1048	0.7221	1.1000	0.7110
76	1.1185	0.7199	1.1139	0.7091
77	1.1320	0.7177	1.1276	0.7073
78	1.1451	0.7156	1.1410	0.7055
79	1.1579	0.7135	1.1541	0.7038
80	1.1704	0.7115	1.1668	0.7021
81	1.1827	0.7096	1.1793	0.7004
82	1.1946	0.7077	1.1915	0.6988
83	1.2063	0.7058	1.2034	0.6973
84	1.2177	0.7040	1.2151	0.6958
85	1.2289	0.7023	1.2265	0.6943
86	1.2398	0.7006	1.2376	0.6929
87	1.2504	0.6990	1.2484	0.6915
88	1.2607	0.6974	1.2590	0.6902
89	1.2708	0.6959	1.2694	0.6889
90	1.2807	0.6944	1.2795	0.6876
91	1.2903	0.6929	1.2893	0.6864
92	1.2997	0.6915	1.2989	0.6852
93	1.3089	0.6901	1.3083	0.6840
94	1.3179	0.6888	1.3175	0.6828
95	1.3266	0.6875	1.3265	0.6817
96	1.3351	0.6862	1.3352	0.6806
97	1.3434	0.6850	1.3437	0.6796
98	1.3515	0.6838	1.3520	0.6785
99	1.3594	0.6826	1.3601	0.6775
100	1.3671	0.6815	1.3680	0.6765
120	1.4866	0.6640	1.4911	0.6609
150	1.5823	0.6494	1.5896	0.6466
200	1.6378	0.6382	1.6443	0.6343
300	1.6286	0.6296	1.6286	0.6262
400	1.5860	0.6262	1.5820	0.6256
500	1.5418	0.6253	1.5366	0.6272
600	1.5013	0.6262	1.4967	0.6293
700	1.4654	0.6284	1.4622	0.6315
800	1.4335	0.6315	1.4321	0.6334
900	1.4050	0.6353	1.4056	0.6351
1 000	1.3795	0.6396	1.3822	0.6365

REFERENCES

- [1] Ojo J. S., Ajewole M. O. and Sarkar S. K. "Rain Rate and Rain Attenuation Prediction for Satellite Communication in Ku and Ka Bands over Nigeria" Progress In Electromagnetics Research B, Vol. 5, 207–223, 2008.
- [2] Chebil J. and Rahman T.A., "Development of 1 min rain rate contour maps for microwave applications in Malaysian Peninsula", Electronics Letters 30th September 1999 Vol. 35 No. 20, pp.1172-1174.
- [3] Pozar, David M. (1993). Microwave Engineering Addison-Wesley Publishing Company. ISBN 0-201-50418-9.
- [4] ONG, J.T., and ZHU, C.N.: 'Rain rate measurements by rain gauge network in Singapore', Electron. Lett.. 1997, 33, (3), pp. 240-242.
- [5] Raytheon's Silent Guardian millimeter wave weapon
- [6] M.M.J.L. van de Kamp; "Short-term prediction of rain attenuation using two samples", Electronic Letters, vol. 38, no. 23, pp. 1476-1477, 7th November 2002
- [7] ITU-R P.1623-1, "Prediction method of fade dynamics on Earth-space paths", ITU, Geneva, 2005
- [8] JPL D-27879. Estimation of Microwave Power Margin, Losses Due to Earth's Atmosphere and. Weather in the Frequency Range of 3–30 GHz...
descanso.jpl.nasa.gov/Propagation/Ka_Band/JPL_D27879.pdf
- [9] Rain Attenuation Measurements in Amritsar over terrestrial microwave link at 19.4 & 28.75 GHz ASHOK KUMAR, I. S. HUDIARA, SARITA SHARMA and VIBHU SHARMA Department of Electronics Technology Guru Nanak Dev University Amritsar-143005, Punjab INDIA
- [10] Department of Electrical Engineering, College of Engineering. University of North Texas. Attenuation Of Microwave Signal And Its Impacts.
- [11] ITU-R P383-3, "Specific attenuation model for rain for use in prediction methods" ITU, Geneva, Switzerland, 2005.
- [12] Moupfouma, F., and Martin, L.: 'Modelling of the rainfall rate cumulative distribution for the design of satellite and terrestrial communication systems', Int. J. Sat. Commun., 1995, 13, pp. 105- 115.
- [13] Chebil J. and Rahman T.A., 'Rain rate statistical conversion for the prediction of rain attenuation in Malaysia', Electron. Lett., 1999, 35, (12), pp. 1019-1021.

- [14] ITU-R P.530-11, "Propagation data and prediction methods required for the design of terrestrial line-of-sight systems" ITU, Geneva, Switzerland, 2001 - 2005.
- [15] www.cis.ohio-state.edu/~jain/cis788-97/satellite_nets/index.htm
- [16] John S. Baras, ATM in Hybrid Networks, Center for Satellite and Hybrid Communication Networks, 1996
- [17] Dennis Roddy, "Satellite Communications", McGraw Hill Text, 1995
- [18] www.wikipedia.org/wiki/Fading
- [19] www.bsatellite.com/Bsatellite_Rainfade.pdf, Patrick Gannon, President of Business Satellite Solutions, LLC.
- [20] www.spacecom.com/customer_tools/html/body_rain_fade.htm
- [21] www.atcourses.com/sampler/Rain_Affect_Communicatons_Link.pdf
- [22] AJST, Vol. 6, No. 2: December, 2005. African Journal of Science and Technology (AJST), Science and Engineering Series Vol.6, No.2, pp.84-93
- [23] Segal, B., "The influence of rain gauge integration time on measured rainfall-intensity distribution functions," J. of Atmospheric and Oceanic Tech., Vol. 3, 662–671, 1986.
- [24] Watson, P. A., V. Sathiaselan, and B. Potter, "Development of a climatic map of rainfall attenuation for Europe," No. 300, 134, Post Graduate School of Electrical and Electronic Engineering, University of Bradford, U. K, Rep., 1981.
- [25] Rice, P. and N. Holmberg, "Cumulative time statistics of surface point rainfall rates," IEEE Trans. Commun., Vol. 21, 1131–1136, 1973.
- [26] Dutton, E. J. and H. T. Dougherty, "Year-to-year variability of rainfall for microwave applications in the USA," IEEE Trans. Commun., Vol. 28, 829–832, 1979.
- [27] Salonen, E. T. and J. P. V. Poiaries-Baptista, "A new global rainfall rate model," Proceedings of the 10th International Conf. on Ant. and Propag. (Pub N 14-176-436), 182–185, 1997.
- [28] Crane, R. K., "Prediction of attenuation by rain," IEEE. Trans. Commun., Vol. 28, No. 6, 1717–1733, 1980.
- [29] Crane, R. K., "A two-component rain model for the prediction of attenuation statistics," Radio Sci., Vol. 17, No. 6, 1371–1387, 1982.

- [30] Crane, R. K., "Evaluation of global and CCIR models for estimation of rain rate statistics," *Radio Sci.*, Vol. 20, No. 4, 865– 879, 1985.
- [31] Restrepo, J., L. D. Emiliani, and C. Fradique-Mendez, "Rain attenuation prediction in tropical zones: Theoretical analysis, measurement campaigns and model comparisons," 20th ICSSC, Montreal, Canada, 2002.
- [32] Rahman, A.A., Saleemul Huq, Raana Haider, Eirik G. Jansen, 1994, *Environment and Development in Bangladesh*, The University Press Limited, Dhaka, Bangladesh.
- [33] A.K.M.H. Rahman, "Data and Internet Service: BTTB Scenario".
- [34] Mandeep Singh Jit Singh, Hassan,S.I.S, Ain,M.F, Ghani, F, Kiyoshi Igarashi, Kenji Tanaka and Mitsuyoshi Iida "Earth-To-Space Improved Model for Rain Attenuation Prediction at Ku-Band" *American Journal of Applied Sciences* 3 (8): 1967-1969, 2006, ISSN 1546-9239. © 2006 Science Publications
- [35] Pontes M.S., Miranda E.C. de, Silva Mello L.A.R. da, Souza R.S.L. de and Almeida M.P.C. de "Rainfall-induced satellite beacon attenuation in tropical and equatorial regions" *ELECTRONICS LETTERS* 29th May 2003 Vol. 39 No. 11
- [36] M. R. Ul Islam, T. A. Rahman, S. K. A. Rahim, K. F. Al-tabatabaie and A. Y. Abdulrahman "Fade Margins Prediction For Broadband Fixed Wireless Access (BFWA) from Measurements In Tropics." *Progress in Electromagnetics Research C*, Vol. 11, 199-212, 2009.
- [37] Joko Suryana Utoro S, Kenji Tanaka Kiyoshi Igarashi and Mitsuyoshi Iida "Study of Prediction Models Compared with the Measurement Results of Rainfall Rate and Ku-band Rain Attenuation at Indonesian Tropical Cities." F2A.4, 0-7803-9282-5/05/ ICICS ©2005 IEEE.